Scientific and Validation Report for the Precipitation Product Processors of the NWC/GEO

NWC/CDOP4/MTG/AEMET/SCI/VR/Precipitation, Issue 1, Rev. 0.1
30 May 2025

Applicable to

GEO-PC-v2.0 (NWC-020)
GEO-CRR-v5.0 (NWC-025)
GEO-PCPh-v4.0 (NWC-079)
GEO-CRRPh-v4.0 (NWC-083)

Prepared by AEMET

REPORT SIGNATURE TABLE

Function	Name	Signature	Date
Prepared by	José Alberto Lahuerta (AEMET) and Ainoa Pascual (AEMET)		*30 May 2025*
Reviewed by	Pilar Ripodas		*30 May 2025*
Authorised by	Pilar Rípodas NWC SAF Project Manager		*30 May 2025*

DOCUMENT CHANGE RECORD

Version	Date	Pages	CHANGE(S)
1.0.0	31 March 2025		First version of precipitation products validation for NWC SAF SW Package v2025 ORR2.
1.0.1	30 May 2025		Version that implements the modifications established by the reviewers at the ORR2.

LIST OF TABLES AND FIGURES

1. INTRODUCTION

The EUMETSAT "Satellite Application Facilities" (SAF) are dedicated centres of excellence for processing satellite data, and form an integral part of the distributed EUMETSAT Application Ground Segment (http://www.eumetsat.int). This documentation is provided by the SAF on Support to Nowcasting and Very Short Range Forecasting, NWC SAF. The main objective of NWC SAF is to provide, further develop and maintain software packages to be used for Nowcasting applications of operational meteorological satellite data by National Meteorological Services. More information can be found at the NWC SAF webpage, http://www.nwcsaf.org. This document is applicable to the NWC SAF processing package for geostationary meteorological satellites, NWC/GEO.

1.1 SCOPE OF THE DOCUMENT

This document is the Validation Report (VR) for the precipitation GEO products Precipitating Clouds (PC), Convective Rainfall Rate (CRR) and Precipitation products from Cloud Physical Properties (PPh) of the NWC/GEO software package. PPh generates two different products: Precipitating Clouds from Cloud Physical Properties (PCPh) and Convective Rainfall rate from Cloud Physical Properties (CRRPh).
This document compares the accuracies of the GEO precipitation products to the threshold accuracies for CDOP4 listed in the "NCWSAF product requirements document" [AD 4]. In this version of the document, the results for MTG are presented. Though they are not the main issue in the document, the results for MSG corresponding to v2021 have also been included for reference.

1.2 SOFTWARE VERSION IDENTIFICATION

This document describes the algorithms implemented in the 2021 NWC-GEO software package release (GEO-PC v1.5.4, GEO-CRR v4.0.2, GEO-PCPh v3.0 and GEO-CRRPh v3.0).

1.3 IMPROVEMENT FROM PREVIOUS VERSIONS

- ✓ New CRRPh and PCPh algorithms based on a Principal Component Analysis. There is only one algorithm for each CRRPh and PCPh that includes both day and night conditions.
- ✓ The CRR product has been recalibrated using the OPERA radar network. It's algorithm remains the same, though the coefficients have changed for MTG.
- ✓ Microphysical properties are simulated at night time and used in the algorithm.
- ✓ More information is extracted from the SEVIRI channels.
- ✓ CRRPh incorporates a Cloud Water Path enhancement correction factor, a stability correction factor and a lightning module.
- ✓ Adaptation to Himawari9 and GOES17. This adaptation is purely technical in order to use Himawari9 and GOES17 channels, but no objective validation has been performed for these satellites.

Note:
PC stays the same from previous 2018.1 version

1.4 DEFINITIONS, ACRONYMS AND ABBREVIATIONS

AEMET	Agencia Estatal de Meteorología
ATBD	Algorithm Theoretical Basis Document
BALTRAD	Baltic Radar Network
CAPPI	Constant Altitude Plan Position Indicator
COT	Cloud Optical Thickness
CRRPh	Convective Rainfall Rate from Cloud Physical Properties
CRR	Convective Rainfall Rate
CSI	Critical Success Index
CT	Cloud Type
CWP	Cloud Water Path
NCAR EOL	Earth Observing Laboratory
ET	Echotop
EUMETSAT	European Organisation for the Exploitation of Meteorological Satellites
FAR	False Alarm Ratio
HRIT	High Rate Information Transmission
ICD	Interface Control Document
ICP	Illumination Conditions Parameter
IQF	Illumination Quality Flag
IR	Infrared
MAE	Mean Absolute Error
CTMP	Cloud Top Microphysical Properties
ME	Mean Error
MRV	Maximum Reflectivity in the Vertical
MSG	Meteosat Second Generation
NIR	Near Infrared
NWCLIB	Nowcasting SAF Library
NWC SAF	Satellite Application Facility for Nowcasting
OPERA	Operational Programme for the Exchange of weather Radar information
PC	Precipitating Clouds
PC	Percentage of Corrects
PCPh	Precipitating Clouds from Cloud Physical Properties
PGE	Product Generation Element
POD	Probability of Detection
PoP	Probability of Precipitation
PPh	Precipitation from Cloud Physical Properties
PPI	Plan Position Indicator
PWRH	Moisture Correction Factor
R_{eff}	Effective Radius
RLR	Rainfall-Lightning Ratio
RMSE	Root Mean Square Error
RR	Rain Rate
SAF	Satellite Application Facility
SEVIRI	Spinning Enhanced Visible and Infrared Imager
SW	Software

USA United States of America
VIS Visible
VIS-N Normalized Visible
WV Water Vapour

1.5 REFERENCES

1.5.1 Applicable Documents

The following documents, of the exact issue shown, form part of this document to the extent specified herein. Applicable documents are those referenced in the Contract or approved by the Approval Authority. They are referenced in this document in the form [AD.X].

For dated references, subsequent amendments to, or revisions of, any of these publications do not apply. For undated references, the current edition of the document referred applies.

Current documentation can be found at the NWC SAF Helpdesk web: http://www.nwcsaf.org

Reference	Title	Code	Vers	Date
[AD. 1]	Proposal for the Fourth Continuous Development and Operations Phase (CDOP 4) March 2022 – February 2027	/NWC/SAF/AEMET/MGT/CDOP4Proposal	1.0	12/03/21
[AD 2]	NWCSAF Project Plan for the NWCSAF CDOP4 phase	NWC/CDOP4/SAF/AEMET/MGT/PP	3.0.0	21/10/24
[AD 3]	Configuration Management Plan for the NWC SAF	NWC/CDOP4/SAF/AEMET/MGT/CMP	1.2.0	29/03/24
[AD 4]	NWCSAF Product Requirements Document	NWC/CDOP4/SAF/AEMET/MGT/PRD	3.0.0	21/10/24
[AD 5]	NWCSAF CDOP4 Service Specifications	NWC/CDOP4/SAF/ AEMET/MGT/SSD	1.0.0	31/10/22
[AD 6]	The Nowcasting SAF glossary	NWC/CDOP4/SAF/AEMET/MGT/GLO	1.0.0	31/10/23
Reference	Title	Code	Vers	Date
[AD. 5]	Proposal for the Fourth Continuous Development and Operations Phase (CDOP 4) March 2022 – February 2027	/NWC/SAF/AEMET/MGT/CDOP4 Proposal	1.0	12/03/21
[AD 6]	NWCSAF Project Plan for the NWCSAF CDOP4 phase	NWC/CDOP4/SAF/AEMET/MGT/PP	3.0.0	21/10/24
[AD 7]	Configuration Management Plan for the NWC SAF	NWC/CDOP4/SAF/AEMET/MGT/CMP	1.2.0	29/03/24
[AD 8]	NWCSAF Product Requirements Document	NWC/CDOP4/SAF/AEMET/MGT/PRD	3.0.0	21/10/24
[AD 5]	NWCSAF CDOP4 Service Specifications	NWC/CDOP4/SAF/ AEMET/MGT/SSD	1.0.0	31/10/22
[AD 6]	The Nowcasting SAF glossary	NWC/CDOP4/SAF/AEMET/MGT/GLO	1.0.0	31/10/23

Table 1. List of Applicable Documents

1.5.2 Reference Documents

The reference documents contain useful information related to the subject of the project. These reference documents complement the applicable ones, and can be looked up to enhance the information included in this document if it is desired. They are referenced in this document in the form [RD.X].

For dated references, subsequent amendments to, or revisions of, any of these publications do not apply. For undated references, the current edition of the document referred applies.

Current documentation can be found at the NWC SAF Helpdesk web: http://www.nwcsaf.org

Reference	Title	Code	Vers	Date
[RD 1]	Interface Control Document for Internal and External Interfaces of the NWC/GEO	NWC/CDOP3/GEO/AEMET/SW/ICD/1	2.0.1	28/02/22
[RD 2]	Data Output Format for the NWC/GEO MTG-I day-1	NWC/CDOP2/MTG/AEMET/SW/DOF	1.4.0	31/03/25
[RD 3]	Algorithm Theoretical Basis Document for SAFNWC/MSG “Precipitating Cloud” (PC-PGE04 v1.5)	SAF/NWC/CDOP2/SMHI/SCI/ATBD/4	1.5.4	15/07/13
[RD 4]	Algorithm Theoretical Basis Document for the Precipitation Product Processors of the NWC/GEO MTG-I day-1	NWC/CDOP2/MTG/AEMET/SCI/ATBD/Precipitation	1.2.0	31/03/25
[RD 5]	User Manual for the SAFNWC/MSG Parallax Correction Tool	GMV/SAFCDOP/VSAREP/02	1.0	02/06/08

Table 2. List of Referenced Documents

2. VALIDATION FOR PRECIPITATING CLOUDS PRODUCT

This section contains the results obtained from the validation of the PC product for MSG, which is described in the Algorithm Theoretical Basis Document for SAFNWC/MSG "Precipitating Cloud" (PC-PGE04 v1.5) [RD 3].

For the MTG satellite, this product has not been modified. However, a comparison between the product for MSG and for MTG was carried out so that users can verify that the product for both satellites is similar and it can therefore be used for MTG in the same manner as it was for MSG.This comparison is presented in section 2.3 of this document, while sections 2.1 and 2.2 refer to the validation procedures for MSG.

2.1 MSG SUBJECTIVE VALIDATION FOR PRECIPITATING CLOUDS (PC)

Many cases have been visually studied by comparing the probability of precipitation (PoP) obtained from the PC algorithm against the radar data. Since PC product estimates probability of precipitation occurrence, the most suitable product to compare with would be the one that assigns 100% PoP where it is raining and 0% otherwise. So PC product has been compared with modified PPI product radar images where pixels with rain rates higher than or equal to 0.2 mm/h are set as rainy pixels (red colour) and the others as no rainy pixels (black colour).
A selection of cases that show the general behaviour of this product can be seen below. Since satellite scanning over the Iberian Peninsula takes place about 10 minutes later than the satellite imagery nominal time, PC images have been compared to radar ones taken 10 minutes later for a better time matching.

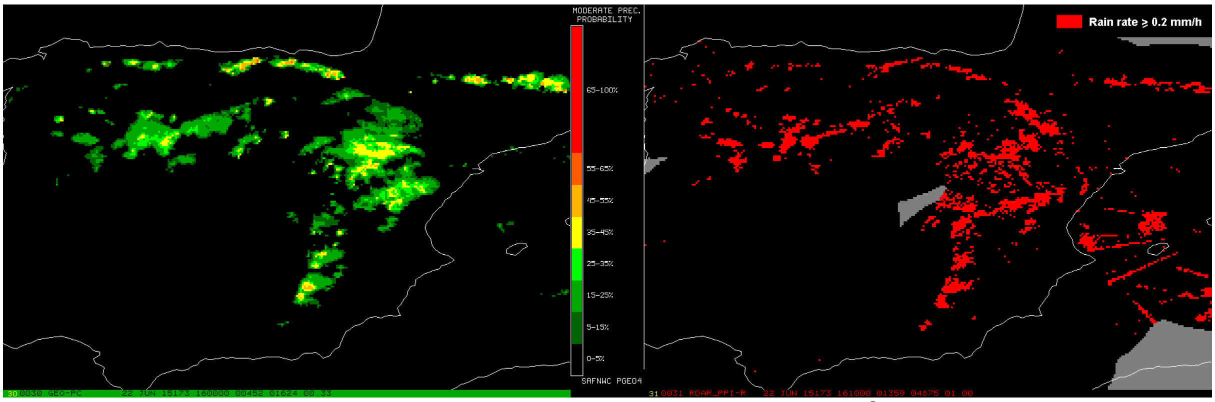

Figure 1. MSG: Comparison of PC product and radar (PPI) on 22nd June 2015 at 16:00UTC.

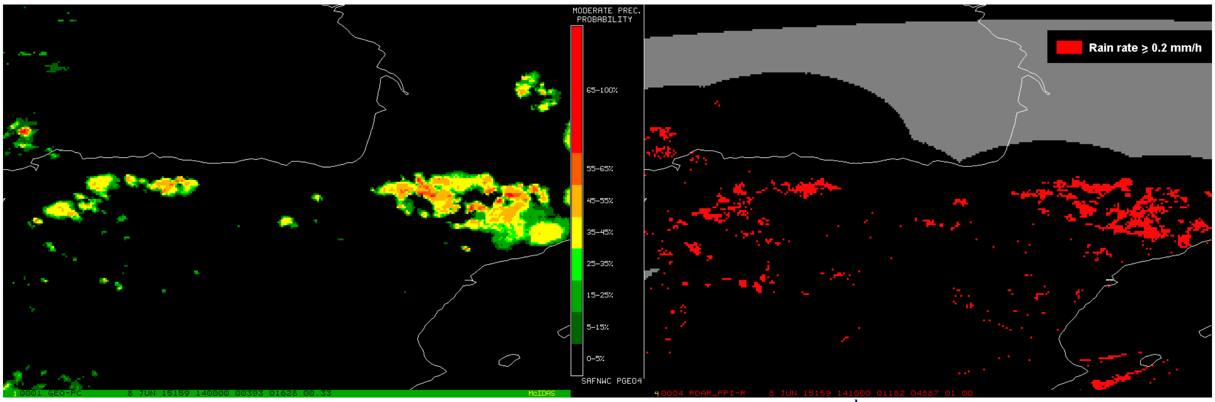

Figure 2. MSG: Comparison of PC product and radar (PPI) on 8th June 2015 at 14:00UTC.

Both Figure 1 and Figure 2 show day-time PC algorithm estimations where the overall precipitation areas are well depicted. However, PoP assigned are not so high, above all in the case of Figure 1, where few pixels take values of PoP higher than 50%. This fact could be explained by the time of the scanning of the satellite imagery used to compute the product. The set of satellite channels used by day-time PC algorithm includes some solar channels with valuable information for precipitation detection. The poorer are the illumination conditions, the lower is the confidence of the algorithm to assign higher PoPs.

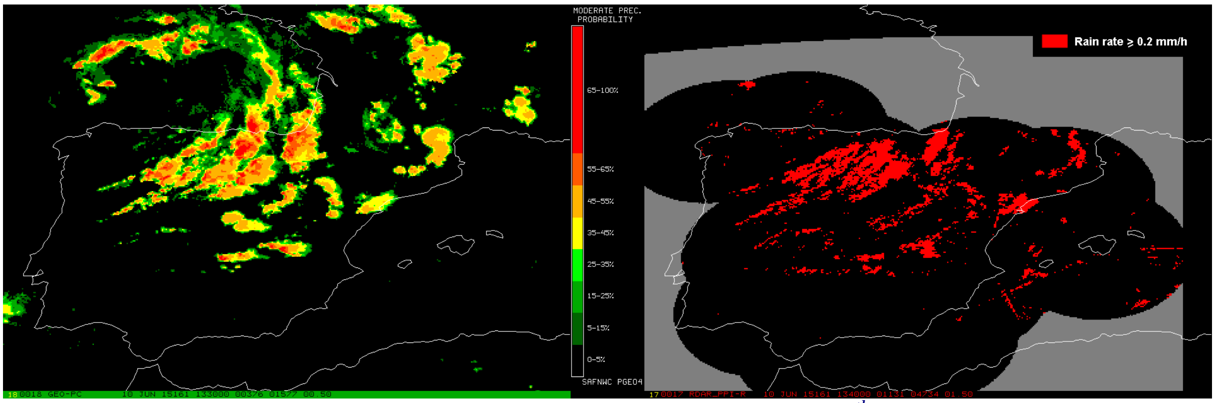

Figure 3. MSG: Comparison of PC product and radar (PPI) on 10th June 2015 at 13:30UTC.

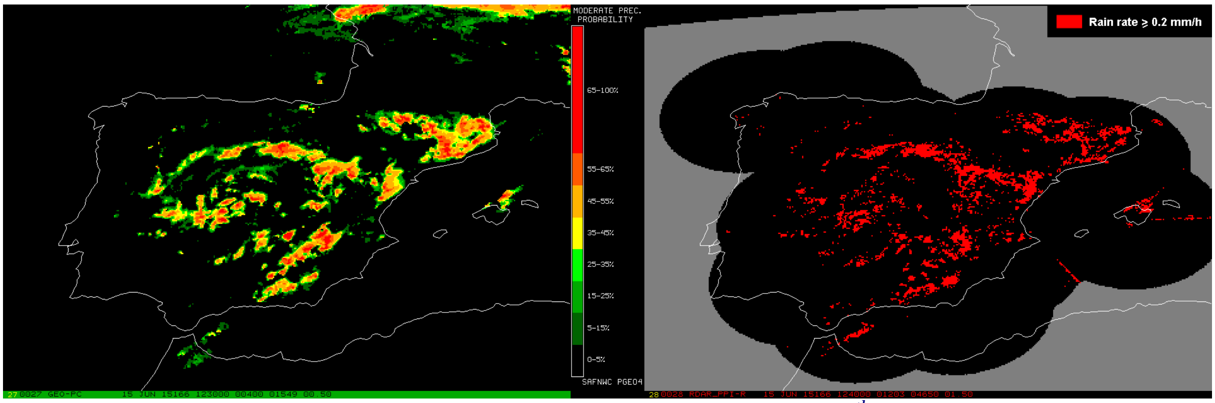

Figure 4. MSG: Comparison of PC product and radar (PPI) on 15th June 2015 at 12:30UTC.

Figure 3 and Figure 4 show day-time PC algorithm estimations with better illumination conditions than Figure 1 and Figure 2. In these cases it can be observed that the estimated precipitation areas are in good agreement with the radar ones and also that higher PoPs have been assigned.

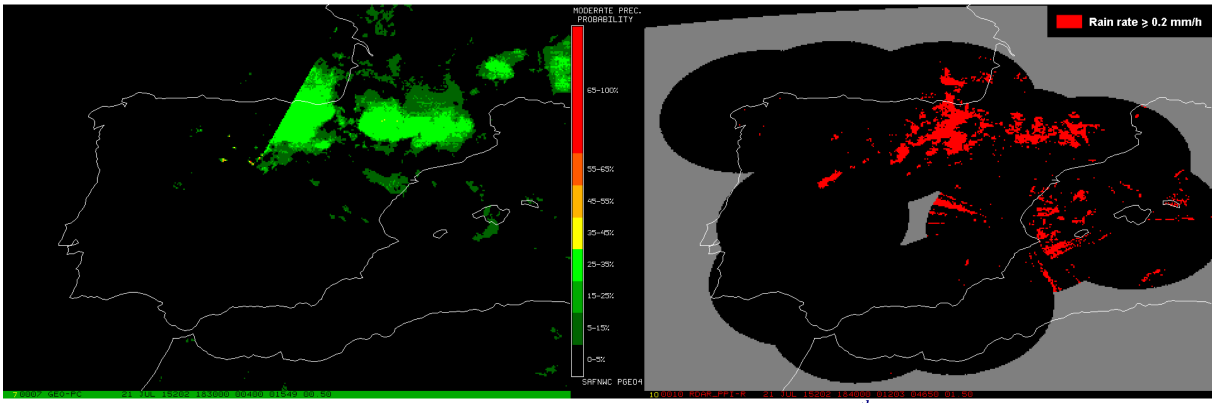

Figure 5. MSG: Comparison of PC product and radar (PPI) on 21th June 2015 at 18:30UTC

Figure 5 shows a scene with a day-night transition of PC algorithms. The day-time algorithm is displayed on the right side of the abrupt precipitation product transition. The night-time algorithm is displayed on the left side of this feature. At this time PC day-time algorithm is computed under poor illumination conditions, and so, there is a low confidence in the assignment of PoP. On the other hand night-time algorithm, which also shows a low confidence in the assignment of PoP, estimates bigger precipitation areas with more false alarms.

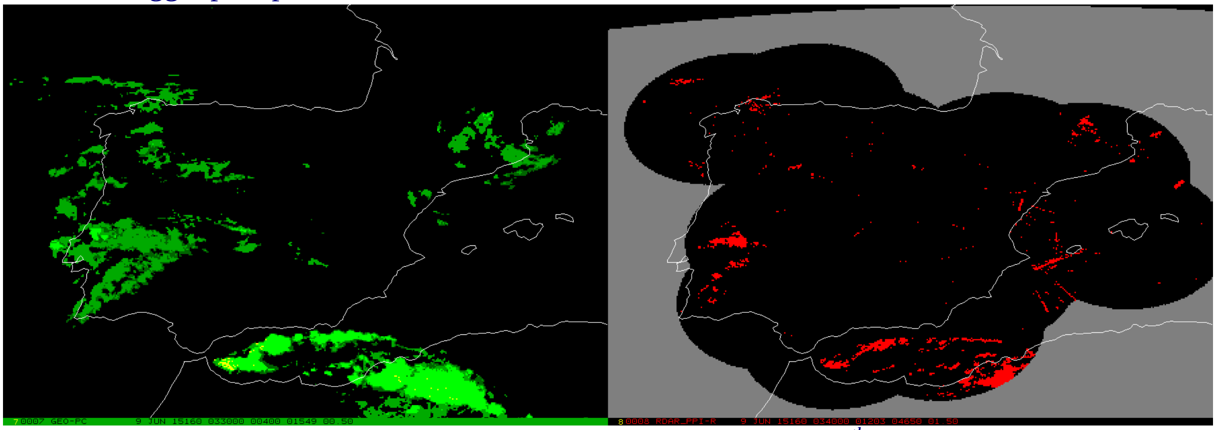

Figure 6. MSG: Comparison of PC product and radar (PPI) on 9th June 2015 at 03:30UTC

Figure 6 shows a nighttime scene where almost all precipitation areas depicted in the radar image are detected by PC product. However, since less information is contained in the night-time algorithm than in the daytime one, the confidence of PoP is lower. Also, the precipitation areas are overestimated providing a higher number of false alarms.

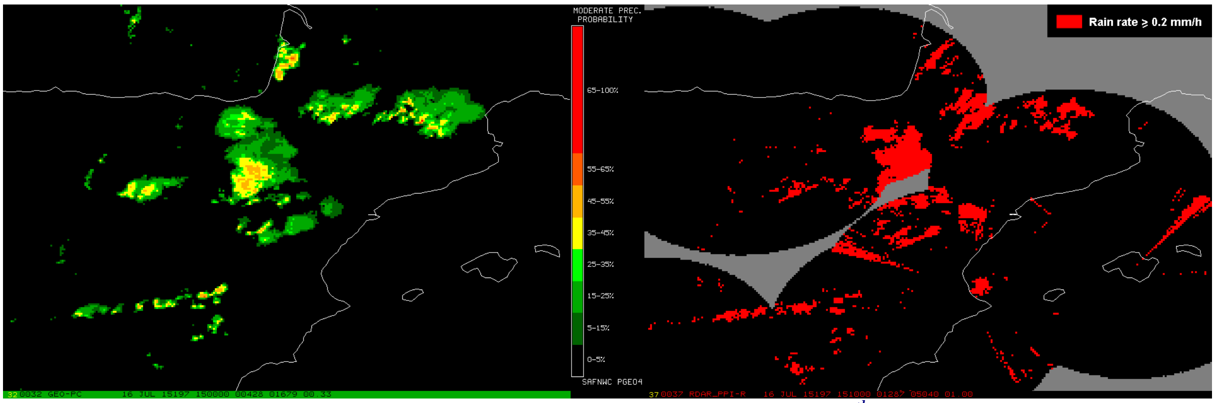

Figure 7. MSG: Comparison of PC product and radar (PPI) on 16th June 2015 at 15:00UTC.

Figure 7 shows a scene where there is a lack of several radars to compute a radar mosaic, and so there is no information over some areas. Here the usefulness of the PC product is shown. It is in agreement with the radar covered areas and complements its information over the rest of the image.

2.2 MSG OBJECTIVE VALIDATION FOR PRECIPITATING CLOUDS (PC)

2.2.1 Validation Procedure

An objective validation for the PC algorithm against Spanish composite radar data has been done. The dataset used for this validation contains 103 rainy days throughout 2008.

Both day-time and night-time algorithms have been validated. Day-time algorithm has been used for those cases with sun zenith angles lower than 80º and night-time algorithm has been used for the rest of the cases.

The original radar data is in Lambert projection, for a better matching, it has been customary reprojected to the MSG projection using a bi-linear interpolation scheme. The NWCSAF parallax tool *[RD 5]* has been applied to the PC product. A comparison against radar data in 3x3 MSG pixels boxes in a yes/no way has been done. The horizontal resolution of the pixels are 3kms at the sub-satellite point. It ranges from 6.88x3.51km at minimum resolution to 3.80x3.1km to the maximum resolution. As detection of very light rain rates using GEO satellite data is not possible, the threshold to consider a radar pixel as rainy has been fixed at 0.2 mm/h.

Ground echoes in PPI scenes have been removed. To do that, a filter image, available as a radar product, has been used in order to remove ground echoes (wind mills,…). Ground echoes, like anomalous propagation echoes, have been removed through the 10.8IR scene. To do that, a rain image has been obtained from the 10.8IR data using the basic AUTOESTIMATOR algorithm (Vicente et al., 1998). A pixel with significant radar echo is considered to be a ground echo and set to zero if no significant value is found in a 15x15 centred box in the AUTOESTIMATOR image.

Although satellite data have been used for decluttering the radar data, since this information has been used in a non-aggressive way, datasets are still independent enough for statistical comparison in the validation.

In order to avoid a high number of correct negative comparisons that can contaminate the computation of validation scores, the validation area has been restricted to 15x15 pixel boxes around radar pixels with at least 0.2 mm/h. As some PC rainy pixels can appear out of the previous validation area, those pixels have been added to the final validation area in order to include all the possible false alarms.

Due to the temporal resolution of the SEVIRI data in the normal mode, there are four PC outputs available every hour. The Spanish radar network generates a set of instantaneous products every 10 minutes. The MSG scanning over Spain is done over 10 minutes after the time of the slot. The only way to match temporally PC and radar scenes is choosing 0 and 30 minutes PC images corresponding to 10 and 40 minutes radar images respectively. As 15 and 45 minutes PC images don't match temporally with the radar ones, those images haven't been used in the validation process.

A smoothing in 3x3 MSG pixels boxes has been applied in order to reduce the radar and satellite estimations spatial mismatching. One every three ordered pixels of the smoothed fields have been taken into account.

2.2.2 The verification metric computed for this validation is described in ANNEX 1: .

Since this is a yes/no validation only categorical scores have been computed.

Probability of precipitation intervals validation:

Eight PoP intervals have been validated. These intervals have been chosen in line with the colour scale delivered with the product:

- 0-5%: 0% < PoP ≤ 5%
- 5-15%: 5% < PoP ≤ 15%
- 15-25%: 15% < PoP ≤ 25%
- 25-35%: 25% < PoP ≤ 35%
- 35-45%: 35% < PoP ≤ 45%
- 45-55%: 45% < PoP ≤ 55%
- 55-65%: 55% < PoP ≤ 65%
- 65-100%: 65% < PoP ≤ 100%

For each probability interval only the rainy area with the selected probability has been taken into account. According to this, POD will always be 100%. Attention should be focused on FAR. A region with the probability of precipitation interval (A-B] should have 100-B ≤ FAR < 100-A. For a better understanding of this, see Figure 8.Imagine a precipitation probability pattern estimated like the one in the left part of the image. And imagine that the 25-35% probability interval is going to be validated. In this case only the green area in the central part of the image would be taken into account for validation, for both observation and estimation. In this case, the entire green area would be a rainy area according to the estimation, and so, a probability of detection of 100% would be assigned to this area. This assumption is represented at the right part of the image. To check whether this area has in effect a 25-35% precipitation probability, attention should be focused on false alarms. So, if the precipitation probability is 25-35%, then, false alarm ratio should be 65-75%.

Figure 8. Drawing example of probability of precipitation intervals validation for MSG

The categorical scores obtained are showed in Table 3.

Probability interval (%)	N (Day algorithm)	FAR (%) (Day algorithm)	N (Night algorithm)	FAR (%) (Night algorithm)
0-5	580028	87	487349	88
5-15	874949	80	1238899	85
15-25	573867	67	1286422	73
25-35	331008	55	1100344	61
35-45	327523	48	191587	51
45-55	281118	38	1719	41
55-65	114062	28	527	9
65-100	24139	20	91	5

Table 3. Categorical scores for PC algorithm probability of precipitation intervals for MSG

It can be observed that PC algorithm provides FAR scores lower than expected, most of all for the highest probability intervals. It should be noted that the highest probability intervals include lower number of cases, most of all in the case of the night-time algorithm that assigns PoP with lower confidences, which is in agreement with the results observed during the subjective validation. The FAR for PoPs higher than 50% are even lower with respect to the FARs from the PoPs lower than 50%.

It can be also observed that the higher quality of the day-time algorithm obtained due to the valuable information provided by the solar channels, leads into lower FAR values for each probability interval.

2.2.3 Probability of precipitation thresholds validation:

Seven probability of precipitation thresholds have been validated. These thresholds are: 5%, 15%, 25% , 35% , 45% , 55% and 65% probability of precipitation.

For this kind of validation, the whole validation area has been taken into account and only pixels with a probability of precipitation higher than the specified threshold have been taken as satellite rainy pixels, all the other pixels are taken as non-rainy.

Probability of precipitation threshold (%)	N	FAR (%)	POD (%)	CSI (%)	PC (%)
5	5254532	62	87	36	68
15	5254532	52	71	40	78
25	5254532	44	54	38	81
35	5254532	40	41	32	82
45	5254532	34	25	22	82
55	5254532	26	9	9	80
65	5254532	20	2	0	1

Table 4. Categorical scores for PC day-time algorithm taking as rainy pixels those with probability of precipitation higher than the threshold for MSG

Probability of precipitation threshold (%)	N	FAR (%)	POD (%)	CSI (%)	PC (%)
5	6179225	72	90	27	53
15	6179225	66	74	30	68
25	6179225	59	45	27	77
35	6179225	51	8	8	81
45	6179225	33	0	0	81
55	6179225	9	0	0	81
65	6179225	5	0	0	81

Table 5. Categorical scores for PC night-time algorithm taking as rainy pixels those with probability of precipitation higher than the threshold for MSG

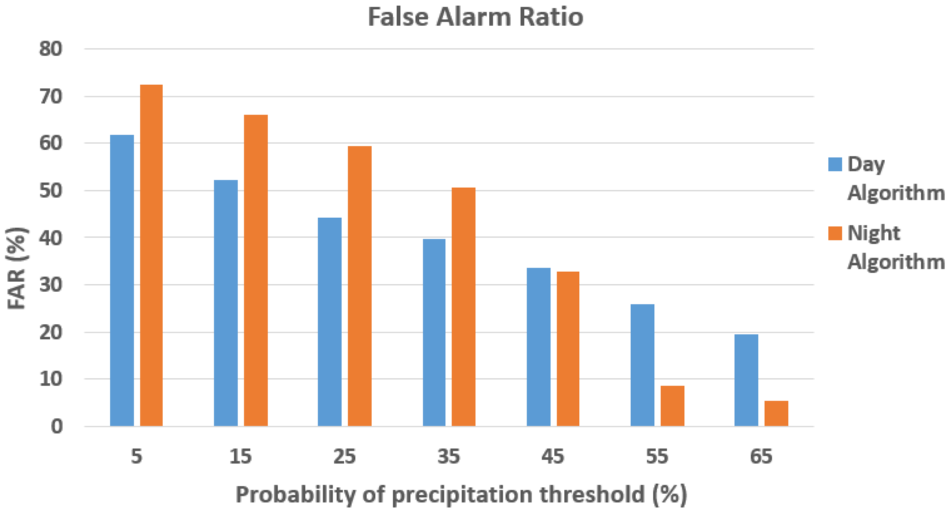

Figure 9. Comparison of day-time and night-time algorithms false alarm ratio for MSG

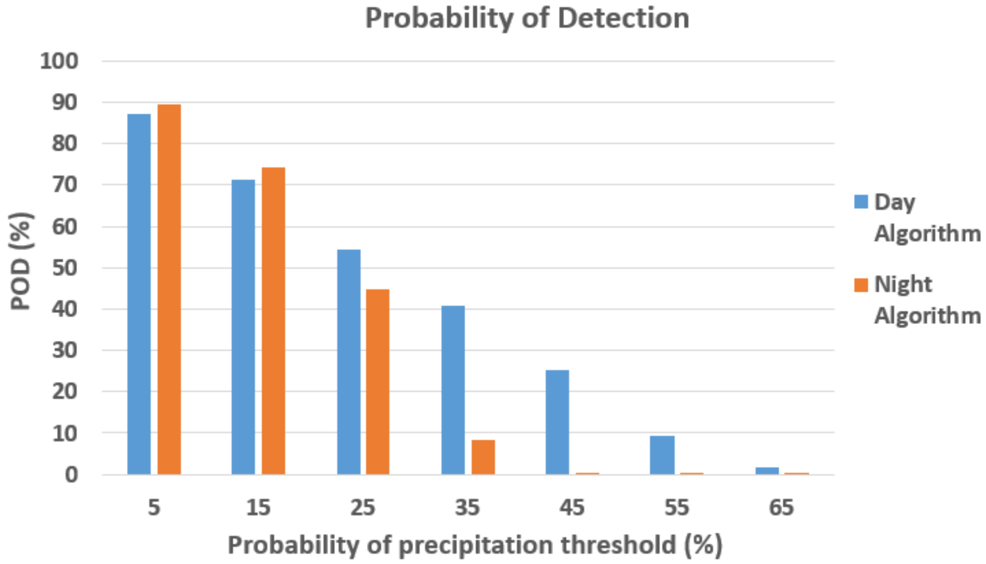

Figure 10. Comparison of day-time and night-time algorithms probability of detection for MSG

A clear better performance of the day-time algorithm over the night-time one can be observed in the graphs. Both lower FAR and higher POD have been obtained for the day-time algorithm for all the PoP thresholds. For 35% PoP and lower thresholds, POD is higher than FAR for the day-time algorithm. In the case of the night-time algorithm, this happens for 15% PoP threshold and the lower ones. For the higher PoP thresholds, scores get worse due to the low number of cases that reach these thresholds.

2.2.4 Conclusion

PC product catches most of the precipitation areas; however, the probability of precipitation assigned, in a high number of cases, is underestimated. For this reason, although precipitation is detected, most of the time, it is located in areas with PoPs lower than 55% for the day-time algorithm and lower than 45% in the case of the night-time one. PoPs higher than 65% are assigned few times in the case of the day-time algorithm and almost never in the case of the night-time one. Because of this, it is clear that the day-time algorithm provides better results than the night-time one due to the influence of the solar channels.

2.3 RESULTS OF THE COMPARISON OF THE PC PRODUCT FOR MSG AND FOR MTG

The algorithm for the Precipitating Clouds product has not been modified for the MTG satellite, and an objective validation process was not carried out. However, the results of the product for both MSG and MTG were compared to verify that the product for the new satellite maintains the same characteristics than the product for the previous one and give the users an understanding of the product for the new satellite.

It should be noted that the PC product is not operational nor critical for the users. Moreover, the plans to develop this product further are non-existent. These are the main reasons that justify that a deeper analysis was not carried out, and the following results have only an informative purpose so that the users can know what to expect when looking at the PC product for MTG.

For the study comparing the behaviour of the product with MSG and MTG, a sample of 21 days of data was used, using eight slots per day, namely the time slots: 00h, 03h, 06h, 09h, 12h, 15h, 18h and 21h. This was done so that the data was homogeneously distributed throughout the day- and night-time and throughout the sample.

It can be seen that the distribution of the PC values according to the 10 classes is similar for MSG and for MTG. This is shown in the following histograms:

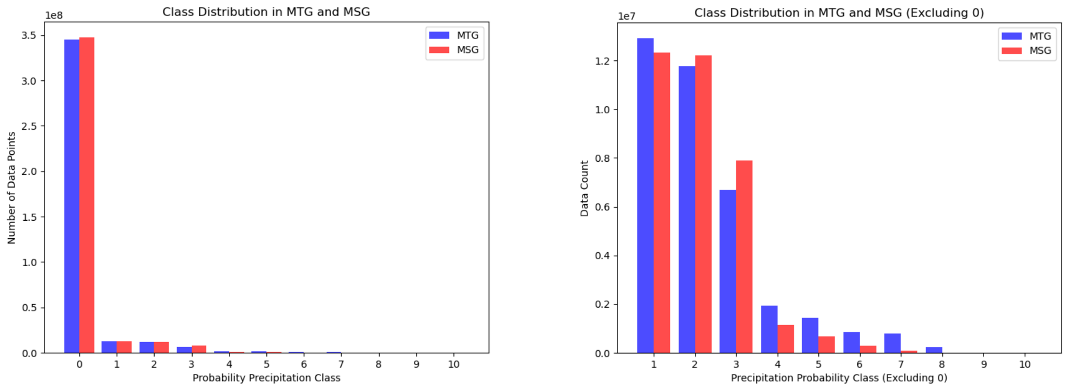

Figure 11. Comparison of the PC values distribution for MSG and MTG.

The image on the left shows the distribution of the PC values for MTG (blue) and MSG (red). Because of the great difference in the amount of values corresponding to class 0 and the rest, the histogram on the right shows the distribution for classes 1 to 10 in more detail, in order to see that they remain similar, though not identical. In fact, it can be easily appreciated that MSG (red) shows less values than MTG (blue) in the higher classes (4 to 8). This behaviour means that, in general, it can be expected when looking at the images of the product that the values for MTG will provide higher precipitation probabilities compared to those of MSG for the same time slot and date.

A quantitative analysis of how similar these distributions are was also carried out to get a better understanding of the difference in the distribution of the values between MSG and MTG. For that a matching matrix was calculated and it is shown in Figure 12.

Since MSG and MTG have different resolutions, the first thing that was done in order to obtain these quantitative results consisted of interpolating the older satellite data to the resolution of the new one. This option was chosen with the purpose of preserving all the information that the higher resolution of MTG provides, though with the drawback that the values of the MSG product had to be interpolated to the new resolution. For that, a linear method of interpolation was used, and then the results were rounded to convert them into the PC classes, which are integer numbers. This method was preferred with respect to the nearest-neighbor method because, while the PC variable consists of integer classes, these represent an underlying ordinal scale of precipitation probability. As such, the variable, though discretized for practical use, has an inherent continuity that justifies this type of interpolation. Moreover, the linear interpolation method is widely used in geoscientific applications—even with classed or thresholded data—when the underlying physical quantity can be assumed to vary smoothly in space.

While linear interpolation from the coarser MSG grid to the finer MTG grid was chosen in order to retain the full spatial detail of the MTG product, it is acknowledged that an alternative approach—such as aggregating MTG to the MSG resolution or reprojecting both products to a common coarser grid—could have reduced the risk of introducing artefacts or artificial gradients due to interpolation. This is particularly relevant when working with classed data, where interpolation may yield intermediate values not originally present in the source product. However, we do not expect this methodological choice to have a significant impact on the results of the comparison.

The comparison of both products, now with the same resolution, can be seen in the following matching matrix:

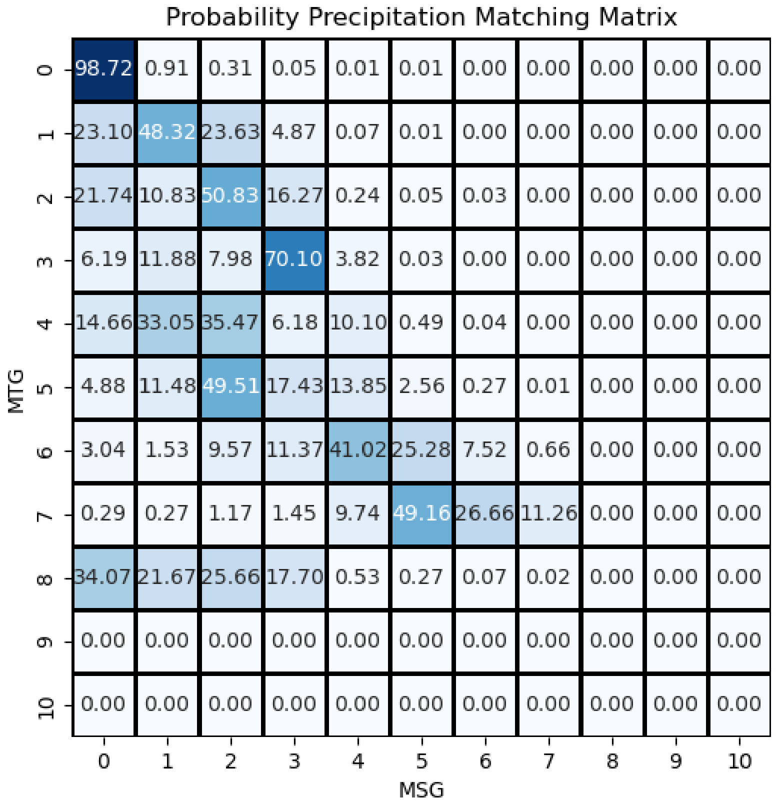

Figure 12. Probability of precipitation matching matrix

The overall accuracy parameter for this matrix has a value of:

OA = 0,9378

Because a high percentage of the values of the sample belong to the class 0, and therefore have the most weight when calculating this estimator, the value for the rest of the classes (namely, classes 1 to 10) alone was also calculated:

OA(class 1 to 10) = 0,5723

The Overall Accuracy measures the number of coincidences between the two samples of data with respect to the total number of cases compared. A high value of the OA means that there is a high level of coincidence, being 1 the indicator for a perfect match between the two sets of data.

As can be seen from the values obtained, the OA for the whole matrix is very close to one, and the OA that doesn't take into account the class 0 data is roughly 0,6. Then, it can be concluded that the main patterns of agreement, especially in the identification of non-precipitating areas (class 0), remain robust, though some notable differences should not be disregarded. These differences observed in higher classes may be due to the fact that the two satellites carry different instruments and some of the satellite channels have changed from the older satellite to the newer. This instrumental discrepancies could very well be the reason why the algorithm, wich was not modified, provides different results for the same product. Nevertheless, it is worth noting that the reprojection from MSG to MTG may also contribute to some of the discrepancies observed between the two products.

In addition, it strikes that the biggest difference is seen in class 8. Not only MSG shows no values with such high values, but it also strikes that, out of the pixels belonging to class 8 in MTG, most of them correspond to classes 0 to 3 in MSG. A visual analysis of several PC images show that this may be because, during the daytime, green areas in MSG (which is the colour corresponding to the lower classes) appear in red in MSG (the colour indicating classes equal to or greater than 7), and a bigger area is covered in MTG. The following images show this discrepancy:

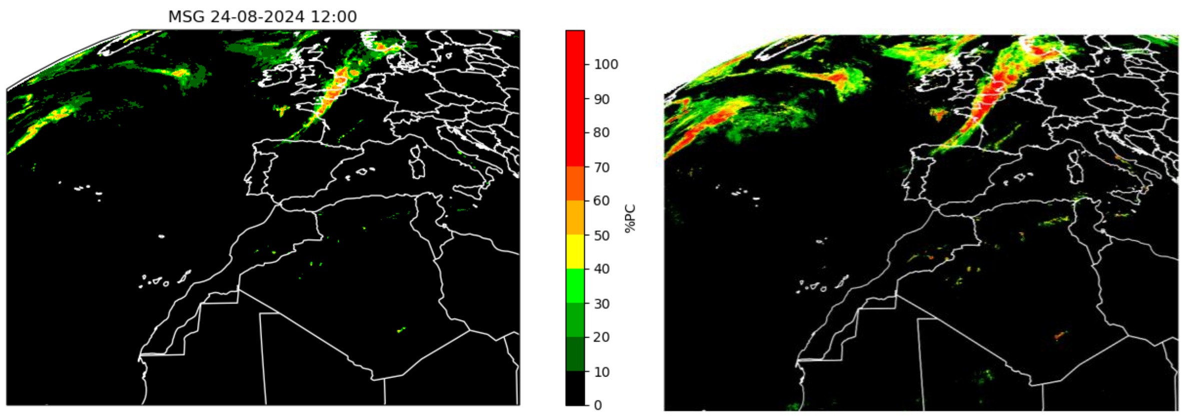

Figure 13. MTG PC 24-08-2024 12:00 for MSG (left) and MTG (right)

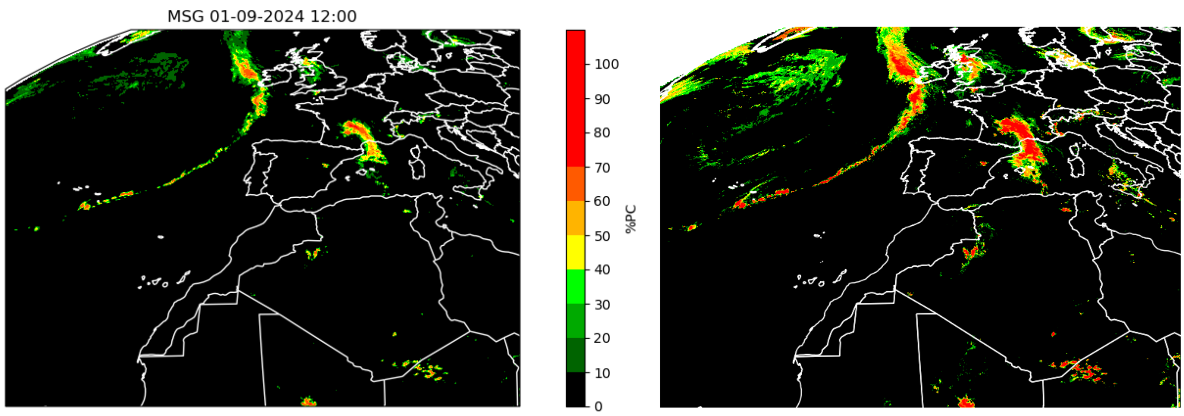

Figure 14. MTG PC 01-09-2024 12:00 for MSG (left) and MTG (right)

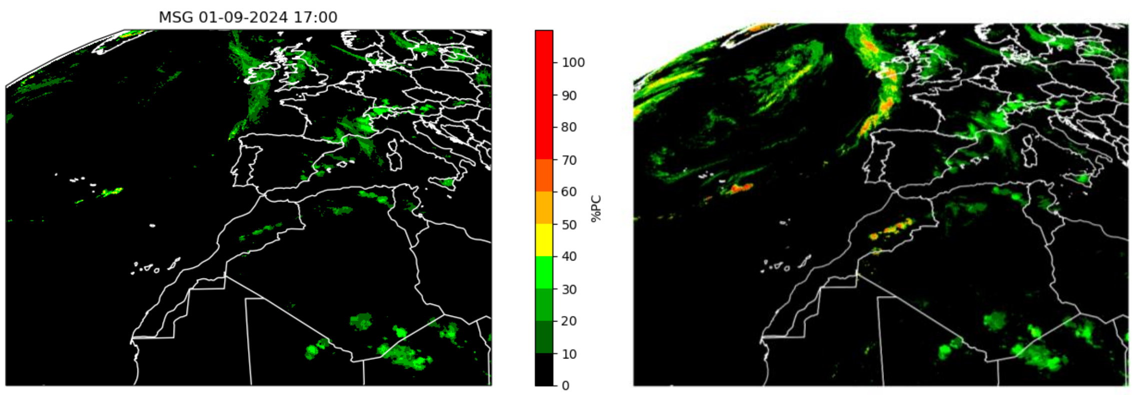

Figure 15. MTG PC 01-09-2024 17:00 for MSG (left) and MTG (right)

As can be seen in the images above, the PC for MTG shows higher values and bigger areas, which can lead to the discrepancies seen in the matching matrix for classes higher than 4. However, given that it is considered that this product, for MSG, underestimates the probability of precipitation, it is not necessarily a bad thing that for MTG the values of the product are higher and wider, though a deeper study would be required to ensure that this is actually the case for MTG.

During the nighttime, as can be seen in the images below, results for both satellites are more similar than the ones for the daytime. However, it should be noted that the areas shown in MTG are still slightly bigger than those shown in MSG, in agreement with what can be seen in the matching matrix: some of the pixels corresponding to classes 1 to 4 in MTG belong to classes 0 or 1 in MSG.

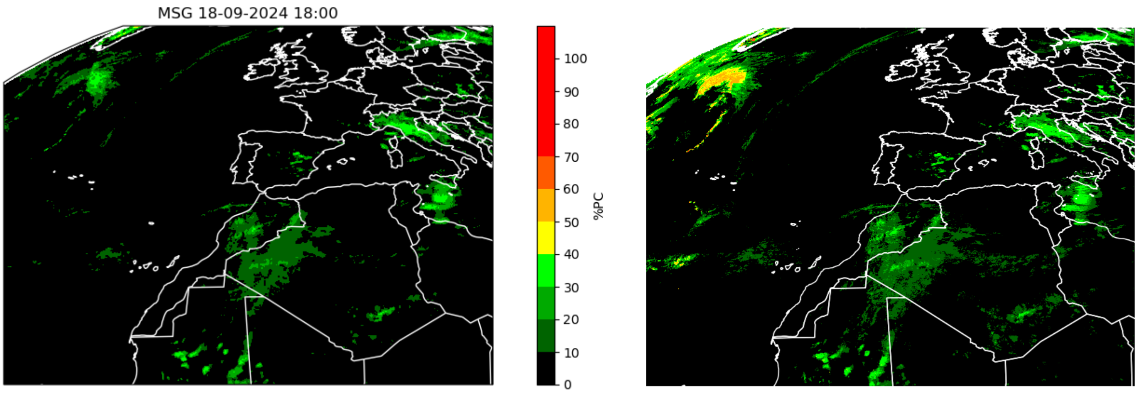

Figure 16. MTG PC 018-09-2024 18:00 for MSG (left) and MTG (right)

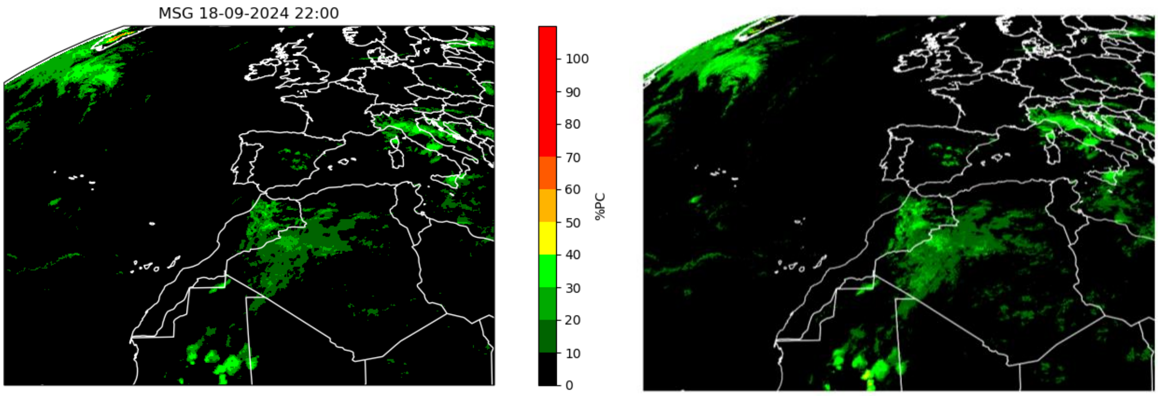

Figure 17. MTG PC 018-09-2024 22:00 for MSG (left) and MTG (right)

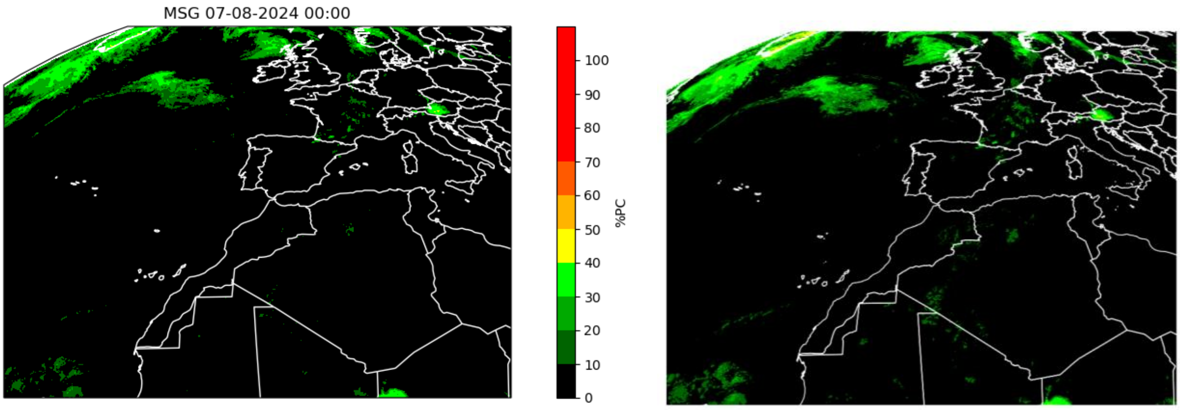

Figure 18. MTG PC 07-08-2024 00:00 for MSG (left) and MTG (right)

2.3.1 Conclusion

As stated previously, an objective validation for the PC product using MTG data was not carried out, nor was it recalibrated for the new satellite channels. The algorithm of the product was not changed either, while the instrumentation on the MTG satellite is different than the one on the MSG satellite, thus introducing modifications on some of the channels.

However, the PC product is not operational nor critical for the user, and there are no plans for further developing this product in the future. The efforts will be focused on the PCPh instead. Because of all this, only a comparison of the performance of the PC for MSG and for MTG was carried out. This study has only informative value and was performed in order to provide the users some insight on the results this product returns for the new satellite compared to those for MSG.

From this first analysis of the PC product, it can be concluded that its performance using the MTG satellite is similar to the one the product has had until now with MSG, though the differences presented are not negligible and must be taken into account. During the night time, the product for MTG shows wider areas than for MSG, but the values correspond to the lower classes of precipitation probability. The main discrepancy, however, happens during the day time, when not only the areas are wider –more so than during the night time–, but also the product returns much higher values for MTG than for MSG for the same coordinates. These differences can be seen quantitatively in the matching matrix.

It is considered that the product for MSG underestimates de probability of precipitation, so it could be assumed that the fact that MTG provides higher values is not necessarily an inconvenience or a setback. Nonetheless, in order to get a better understanding of these behaviour of the product, a deeper study would be necessary to stablish whether the PC for MTG is closer to reality than the PC for MSG. As previously established, the need for this is not considered relevant given that the PC product is not operational nor critical for the users, and the only purpose of this study is informative.

3. VALIDATION FOR CONVECTIVE RAINFALL RATE PRODUCT

This section contains the results obtained from the validation of the CRR product which is described in the “Algorithm Theoretical Basis Document for the Precipitation Product Processors of the NWC/GEO of the NWC/GEO MTG-I day-1” *[RD 4]*. The validation was performed for the MTG software version v2025. However, in line with the scope defined in this document, the results obtained for MSG with version v2021 are also included for reference purposes.

3.1 SUBJECTIVE VALIDATION FOR CONVECTIVE RAINFALL RATE (CRR)

The monitoring of the precipitation pattern as well as its evolution is valuable information for the forecaster. In order to show the valuable information that the CRR product can provide, a set of examples of CRR have been selected and compared to the radar estimations.

Subjective validation for Convective Rainfall Rate (CRR) for MSG

3.1.1

Next colour rain rate palate (mm/h) applies to figures to all precipitaton figures:

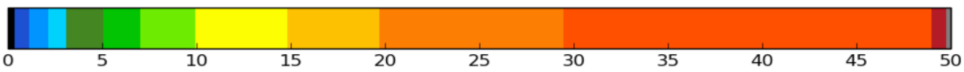

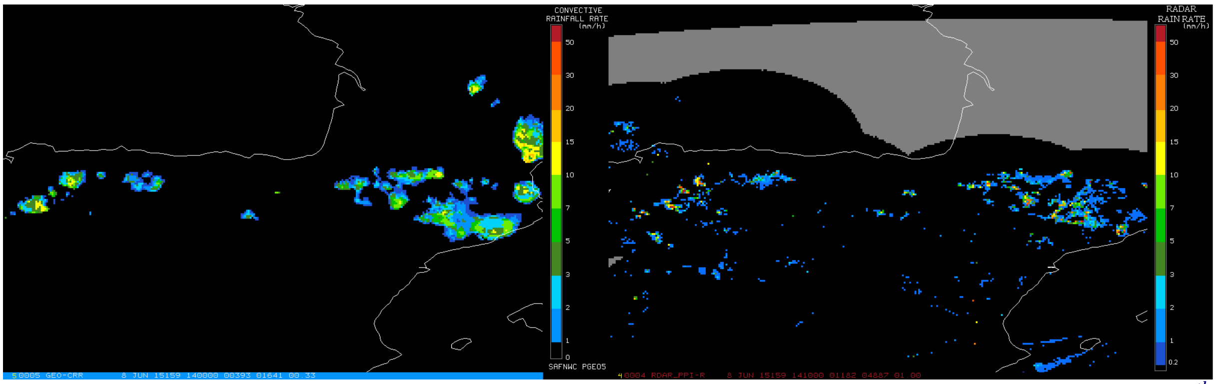

Figure 19. Comparison of CRR instantaneous rates product for MSG and radar rainfall rate on 8th June 2015 at 10:00UTC

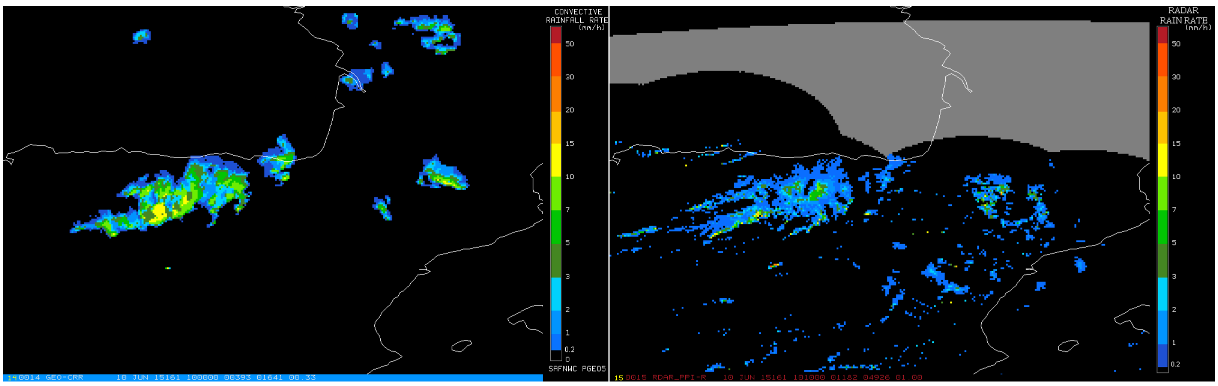

Figure 20. Comparison of CRR instantaneous rates product for MSG and radar rainfall rate on 10th June 2015 at 10:00UTC

Figure 19 and Figure 20 show a couple of comparisons of CRR instantaneous rain rates with radar PPI product where most of the precipitation areas have been detected by CRR. Although the CRR precipitation pattern is quite similar to the radar one and the maxima of precipitation match well in location, maximum CRR rain rates are in general lower than the radar ones.

It is well known that for this kind of product directly based on cloud top radiances it is very difficult to detect the smallest precipitation nuclei. And it is also difficult to detect the lowest rain rates. It can be observed in the images that the rainy area is well depicted but sometimes is overestimated, being very similar to the cloud top structure. And it can also be observed a general underestimation of the highest rain rates.

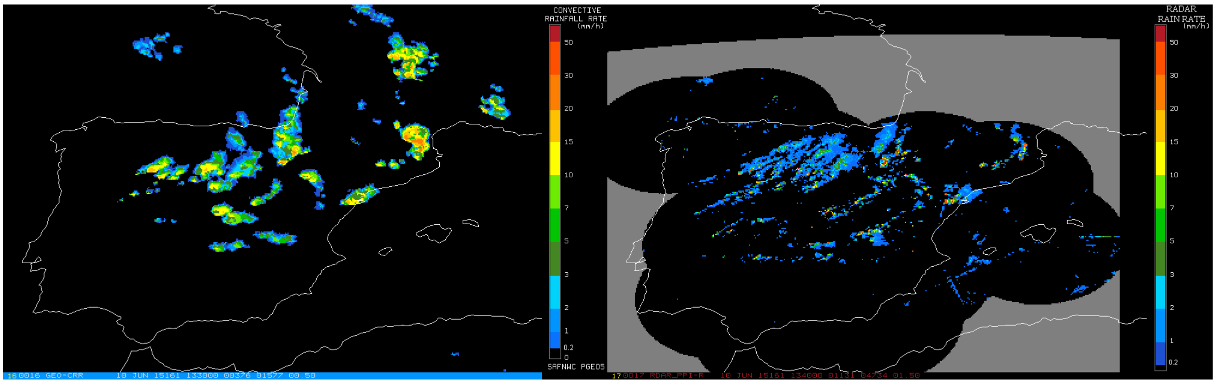

Figure 21. Comparison of CRR instantaneous rates product for MSG and radar rainfall rate on 10th June 2015 at 13:30UTC

Figure 21 shows an example of a good performance of CRR product day-time algorithm. Although the smallest rain nuclei are missed by CRR, the precipitation pattern is very similar to the radar one and the maximum rain rates are also very similar.

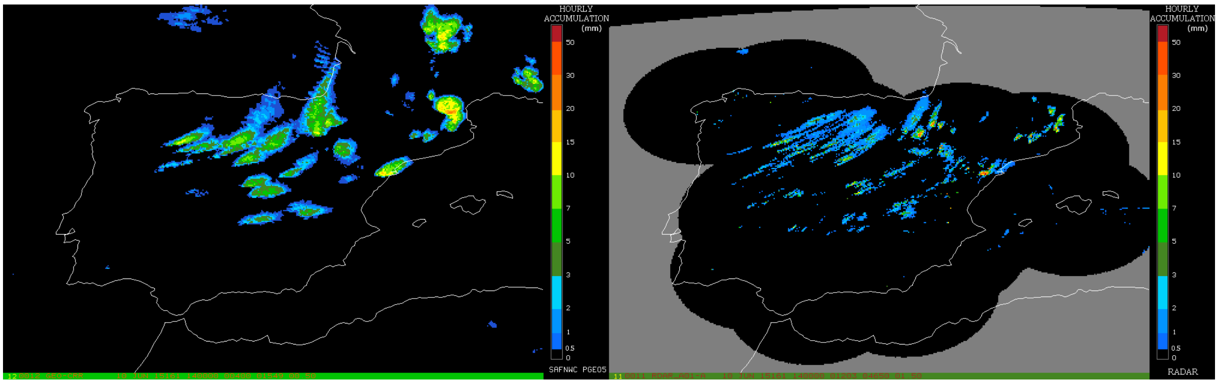

Figure 22. Comparison of CRR hourly accumulation product for MSG and radar hourly accumulation on 10th June 2015 at 14:00UTC

Figure 22 shows a comparison of hourly accumulation estimated by CRR and radar. Similar conclusions as in the case of instantaneous rain rates can be reached for hourly accumulations since hourly accumulations are obtained by using the instantaneous rain rates.

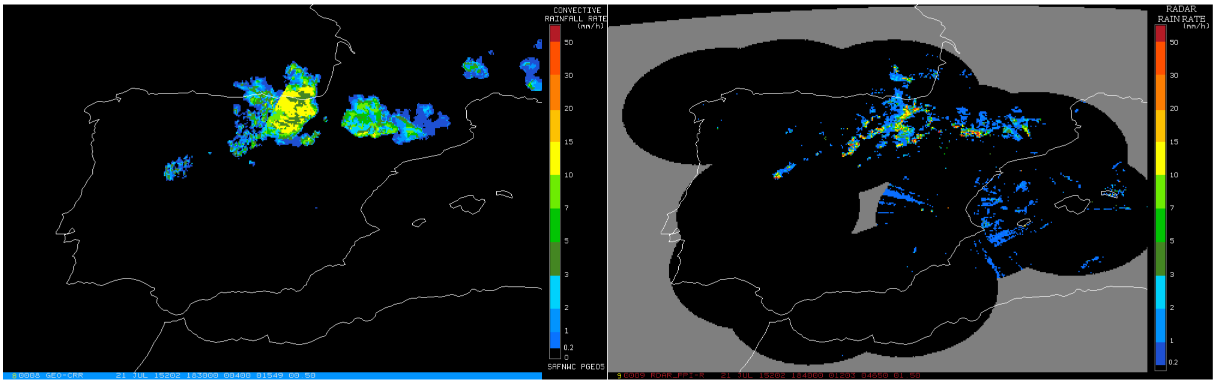

Figure 23. Comparison of CRR instantaneous rates product for MSG and radar rainfall rate on 21th June 2015 at 18:30UTC

Figure 23 shows a CRR day-night algorithm transition. The day-time algorithm is displayed on the left side of the abrupt precipitation product transition. The night-time algorithm is displayed on the right side of this feature. It is quite clear through this example the main differences between both algorithms. Day-time algorithm provides a rain pattern more adjusted to the radar one while night-time one is more similar to the cloud top, overestimating rainy areas. Day-time algorithm provides better results due to the important information included in the visible channel related to the cloud optical thickness.

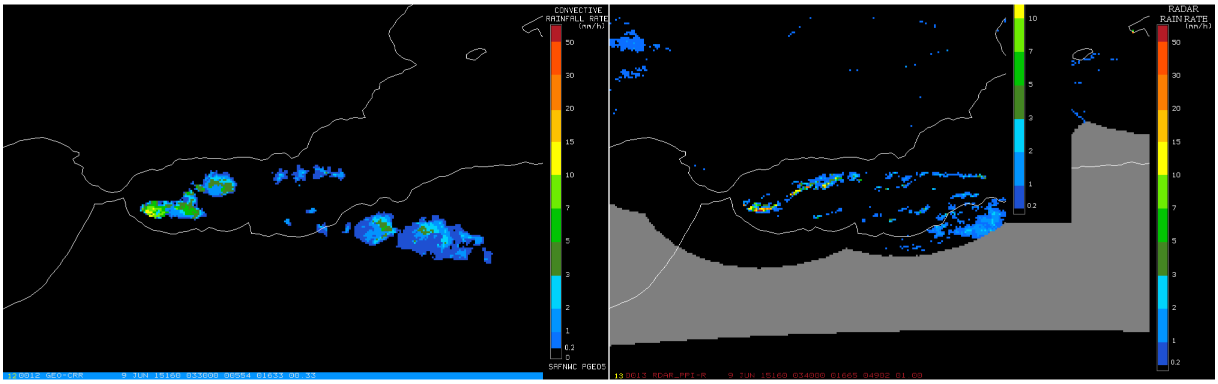

Figure 24. Comparison of CRR instantaneous rates product for MSG and radar rainfall rate on 9th June 2015 at 03:30UTC

Figure 24 shows an example of the night-time algorithm. Although quality is not as good as in the case of the day-time one, precipitation areas are very similar to the radar one, and maximum rain rates are well located.

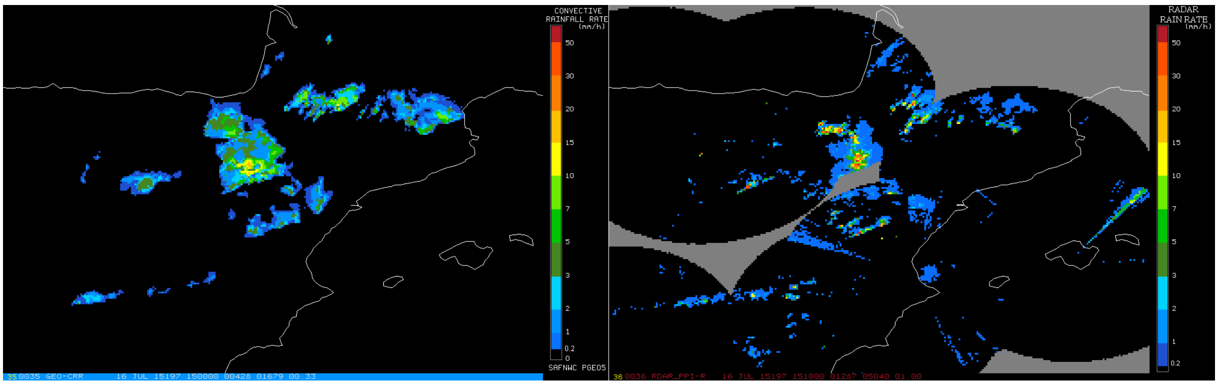

Figure 25. Comparison of CRR instantaneous rates product for MSG and radar rainfall rate on 16th June 2015 at 15:00UTC

Figure 25 shows an example of the usefulness of CRR information when radar does not totally cover the studied area. Precipitation areas in those places covered by radar are similar and complementary information can be obtained through CRR out of those areas.

Subjective validation for Convective Rainfall Rate (CRR) for MTG

3.1.23.1.2.1 *Day time*

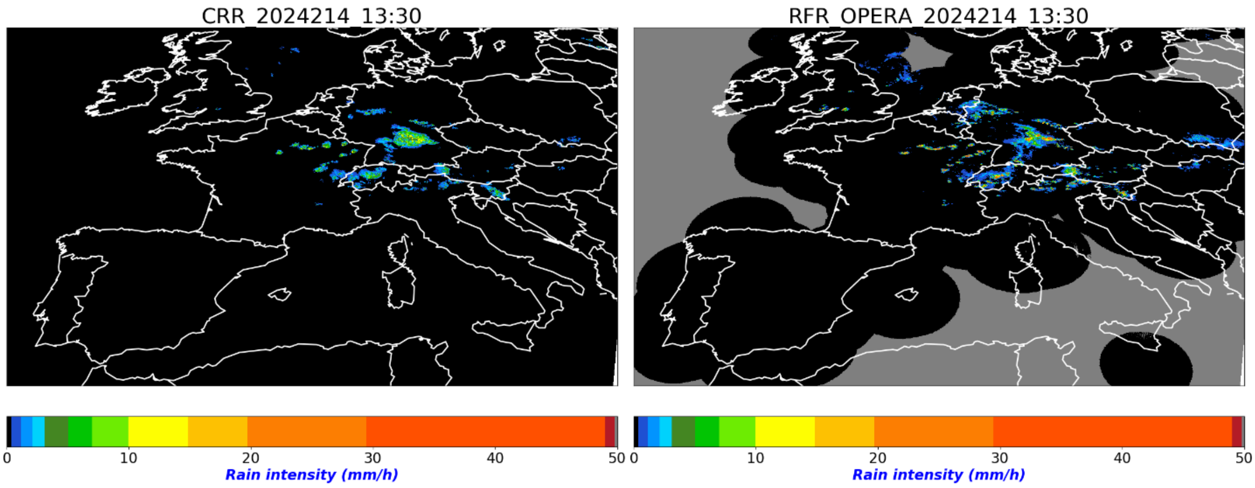

Figure 26. Comparison of CRR instantaneous rain rate for MTG and OPERA radar rainfall rate on 1th August 2024 at 13:30UTC

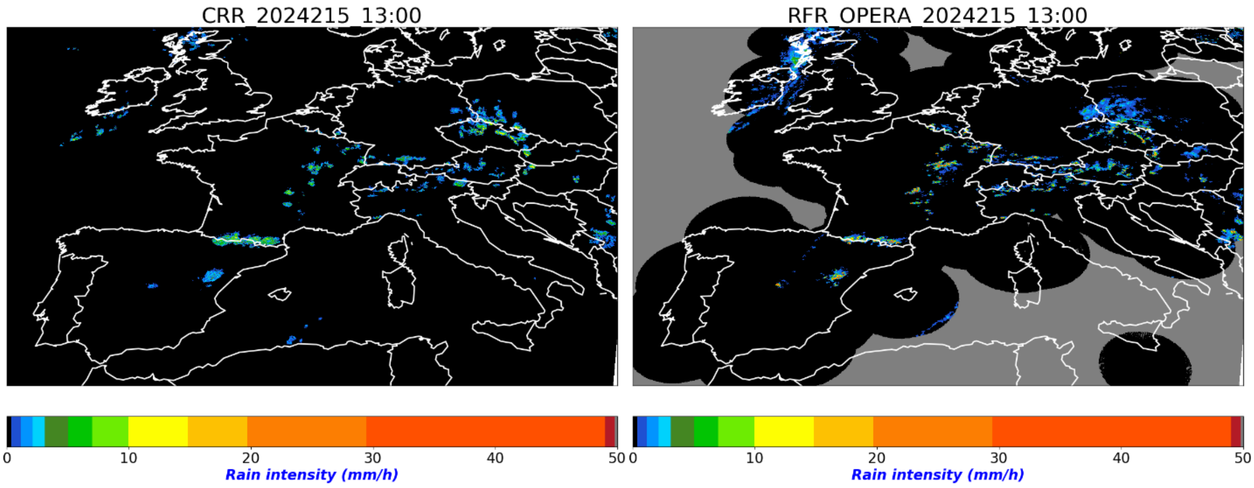

Figure 27. Comparison of CRR instantaneous rain rate for MTG and OPERA radar rainfall rate on 2th August 2024 at 13:00UTC

Figure 26 and Figure 27 show a couple of comparisons of CRR instantaneous rain rates with OPERA radar composition where most of the precipitation areas have been detected by CRR.

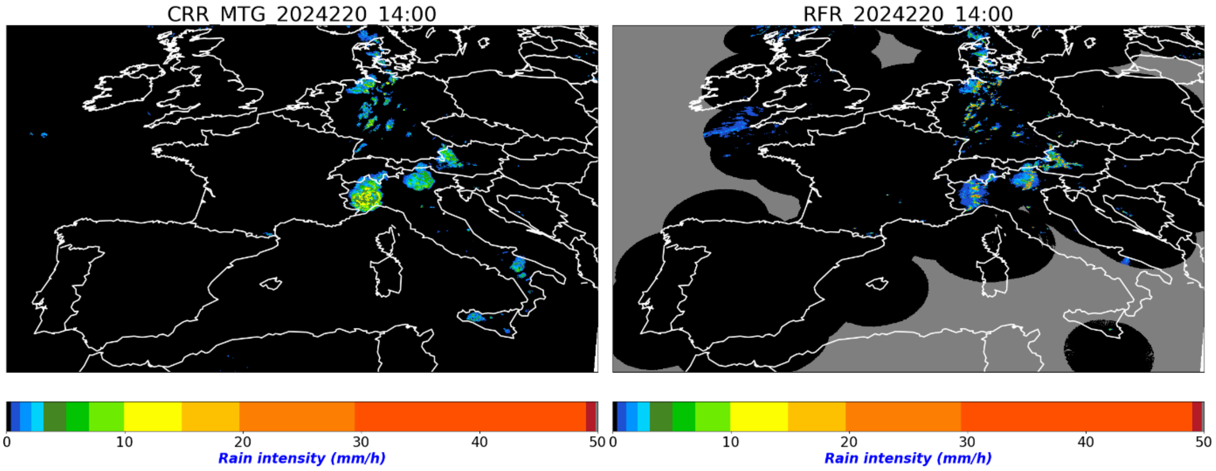

Figure 28. Comparison of CRR instantaneous rain rate for MTG and OPERA radar rainfall rate on the 7th of August, 2024 at 14:00UTC

Figure 28 is another example of a good performance of CRR day time product. In this case there is convection in Germany, Italy and the Netherlands. Precipitation cells are well detected by the CRR product. Rain intensities showed in the OPERA image are higher than the CRR output. This may be due to the fact that the lightning module has not been used by the CRR.

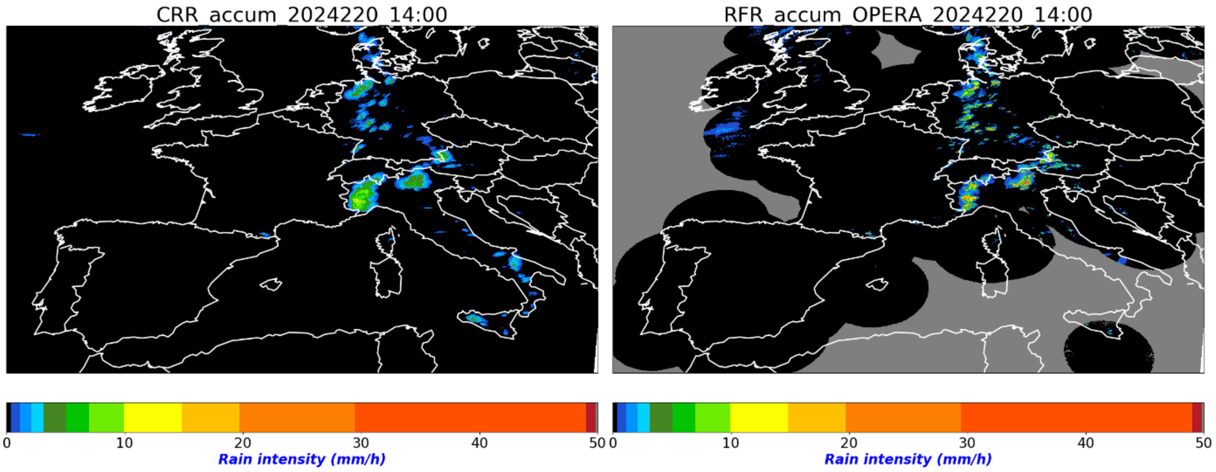

Figure 29. Comparison of CRR hourly accumulation product for MTG and OPERA radar hourly accumulation on 7th August 2024 at 14:00UTC

Figure 29 shows a comparison of hourly accumulation estimated by CRR and radar. Similar conclusions as in the case of instantaneous rain rates can be reached for hourly accumulations since hourly accumulations are obtained by using the instantaneous rain rates.

3.1.2.2 Night time

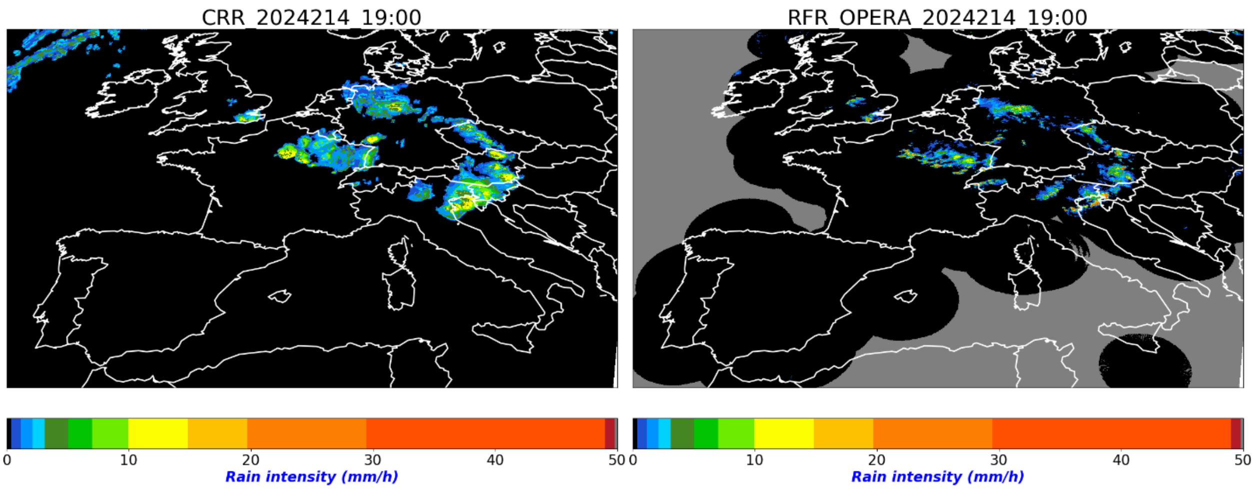

Figure 30. Comparison of CRR instantaneous rain rate for MTG and OPERA radar rainfall rate on 1th August 2024 at 19:00UTC

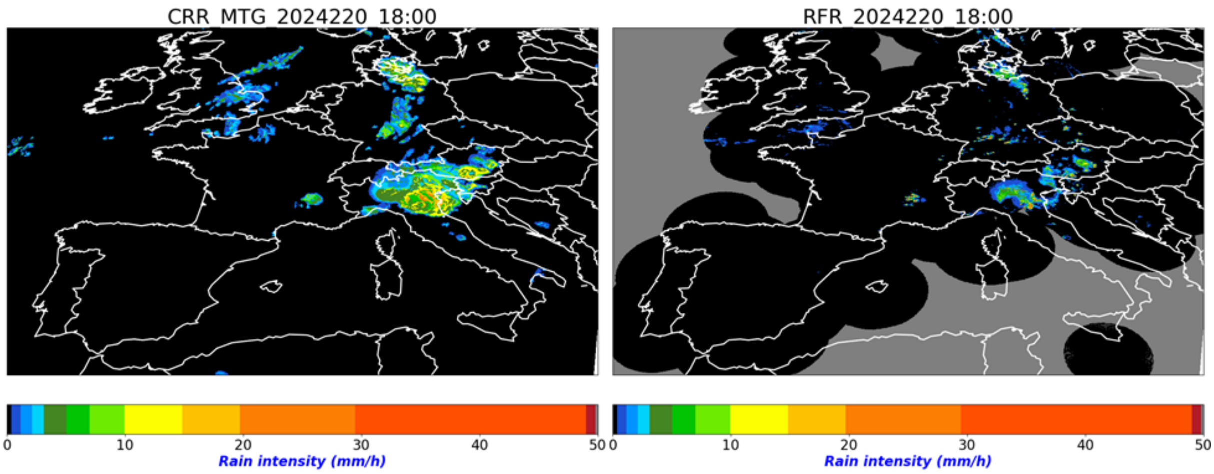

Figure 31. Comparison of CRR instantaneous rain rate for MTG and OPERA radar rainfall rate on 7th August 2024 at 18:00UTC

Figure 30 and Figure 31 are examples of the night-time algorithm. Precipitation areas are well located in general; however, overestimation in the extension of those areas is also evident. This has been noticed whenever the anvil of convective clouds spreads the product extent of the precipitation area like happens in the north of Italy. There are some missing precipitation areas in the north of France that the night product does not detect, and some false alarms over Great Britain.

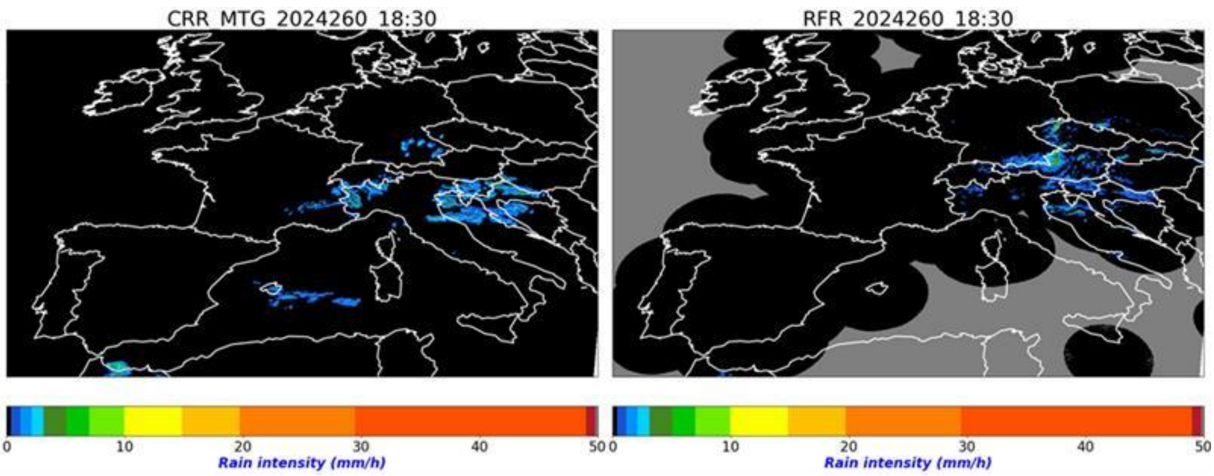

Figure 32. *Comparison of CRR instantaneous rain rate* for MTG *and OPERA radar rainfall rate on 16th September 2024 at 18:30 UTC*

CRR night output associated to Figure 32 reveals some false alarms near the Balearic islands, the Mediterranean sea and the East of France. Precipitation in central Europe is detected.

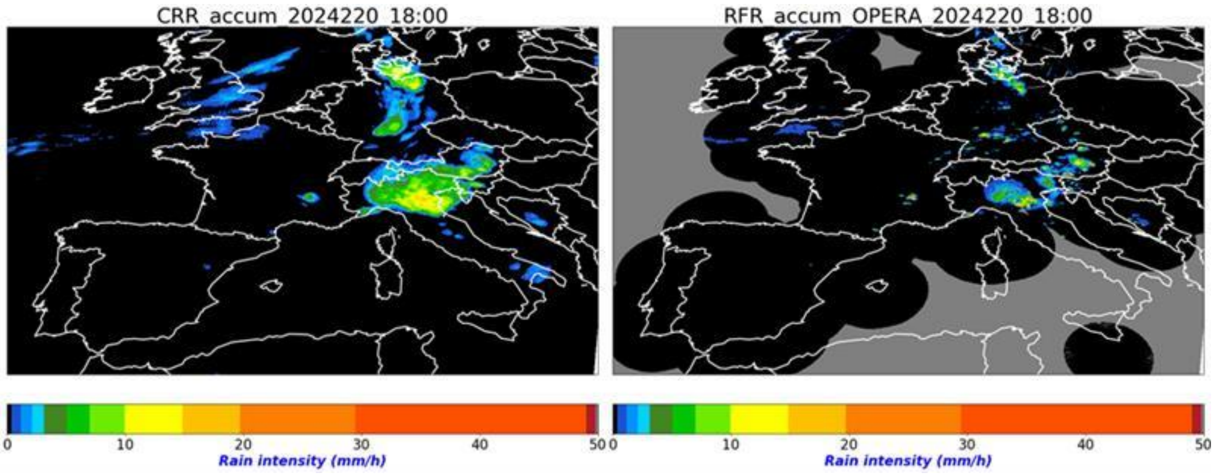

Figure 33. Comparison of CRR hourly accumulation product for MTG and OPERA radar hourly accumulation on 7th August 2024 at 18:00UTC

Figure 33 shows a comparison of hourly accumulation estimated by CRR and the OPERA radar composite. Since precipitation areas are slighty overestimated in the intantaneuos rain rate that behaviour is transferred to the hourly accumulations.

3.2 Objective Validation for Convective Rainfall Rate (CRR)

3.2.1 Validation Procedure (MSG)

The objective instantaneous rain rates validation has been done against instantaneous rates taken from Spanish radar PPI data and the hourly accumulations have been done against radar hourly accumulations obtained from the 500m Pseudo-CAPPI. The original data in Lambert projection has been customary reprojected on the MSG projection using a bi-linear interpolation scheme.

Ground echoes in PPI scenes have been removed. To do that, a filter image, available as a radar product, has been used in order to remove ground echoes (windmills, …). For instantaneous products there exists the possibility to remove ground echoes, like anomalous propagation echoes, through the 10.8IR scene. A rain image has been obtained from the 10.8IR data using the basic AUTOESTIMATOR algorithm (Vicente et al., 1998). A pixel with significant radar echo is considered to be a ground echo and set to zero if no significant value is found in a 15x15 centred box in the AUTOESTIMATOR image.

Although satellite data have been used for decluttering the radar data, since this information has been used in a non-aggressive way, datasets are still independent enough for statistical comparison.

In the instantaneous cases, since CRR product addresses convective situations, only images with convective echoes should be validated. In order to select those images, when in the ECHOTOP image the ratio between the number of pixels with ECHOTOP higher than 6 Km and the number of pixels with ECHOTOP higher than 0 Km is lower than 15%, the radar images have been rejected. This procedure tends to discard non-convective precipitation.

Images with convective situations can also include non-convective echoes. In order to validate only the convective ones, a validation area has been selected taking into account the convective area that has been calculated in each image. To do that, PPI and ECHOTOP images have been used. The convective area in the instantaneous images has been made up of 15x15 pixels boxes centred on pixels that reach a top of 6 km and a rainfall rate of 3 mm/h simultaneously. In the hourly accumulations, the validation area has been chosen adding the validation areas in the corresponding instantaneous images. As some CRR rainy pixels can appear out of the convective area, these pixels have been added to the validation area in order to include all the possible false alarms.

The perfect matching between images will never be reached so a smoothing process in a 3x3 pixels base has been done. The horizontal resolution of the pixels are 3kms at the sub-satellite point. Pixel resolution ranges from 6.88x3.51km at the north of the Spanish Península to 3.8x3.1km at the south. Then a pixel by pixel (every three pixels) comparison has been carried out. The definition of the statistics computed can be checked at ANNEX 1: .

The CRR values have been obtained applying all the corrections with the default values *[RD 4]*. The fields for the moisture, parallax and orographic corrections have been extracted from ECMWF at 0.5 x 0.5 degree spatial resolution, every 3h.

The dataset used for the validation of both algorithms contains 78 days with convective events along 2008. Accuracy and categorical statistics described in ANNEX 1: have been computed for instantaneous rain rates and for hourly accumulations.

3.2.1.1 Instantaneous Rain Rates

According to the procedure described above, the statistical accuracy measurements are shown in the following table:

Algorithm	N	Mean (mm/h)	ME (mm/h)	MAE (mm/h)	RMSE (mm/h)
Day time	832614	0,58	0,54	1,19	2,97
Night time	877299	0,62	0,82	1,55	3,18

Table 6. Accuracy measurements for instantaneous rates for MSG

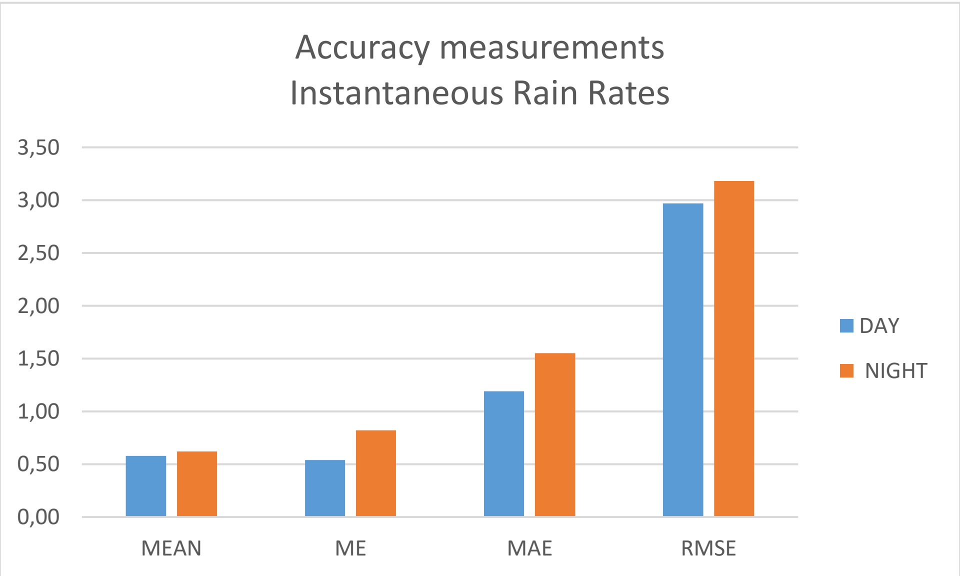

Figure 34: Accuracy measurements for CRR instantaneous rates for MSG

Although both day-time and night-time algorithms provide similar results, it can be observed a slight better performance in the day-time algorithm according to the results showed in Figure 34. This can be explained, as seen during the subjective validation, because day-time algorithm adjust better precipitation areas reducing error with respect to the night-time ones.

Categorical scores for CRR can be obtained assuming that values higher than or equal to 0.2 mm/h for instantaneous rates are considered rainy. Results are shown in Table 14.

Algorithm	FAR (%)	POD (%)	CSI (%)	PC (%)
Day time	34	63	48	65
Night time	46	54	37	55

Table 7. Categorical scores for CRR instantaneous rates for MSG

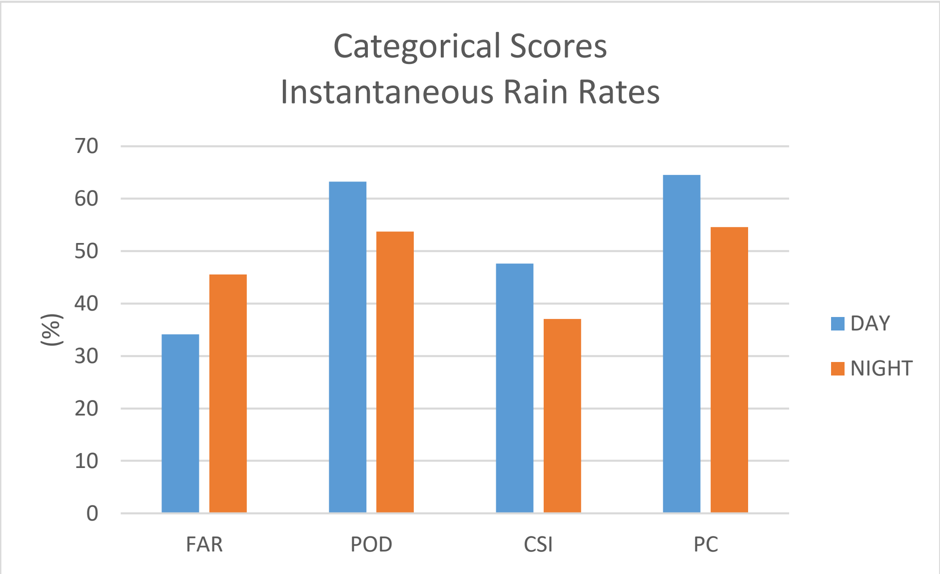

Figure 35. Categorical scores for CRR instantaneous rates for MSG

Figure 35 also brings to light the better estimations of the day-time algorithm that provides lower FAR and higher POD than the night-time one. These results, showed also in Table 14, fulfil the FAR and POD target values defined in the "NWCSAF Product Requirements document" [AD 4].

3.2.1.2 Hourly accumulations

Accuracy measurements, obtained statistically as explained above, for hourly precipitation accumulations are shown in Table 8 .

Algorithm	N	Mean (mm/h)	ME (mm/h)	MAE (mm/h)	RMSE (mm/h)
Day time	465555	0,37	0,43	0,80	1,96
Night time	598562	0,40	0,57	0,99	2,19

Table 8. Accuracy measurements for CRR hourly accumulations for MSG

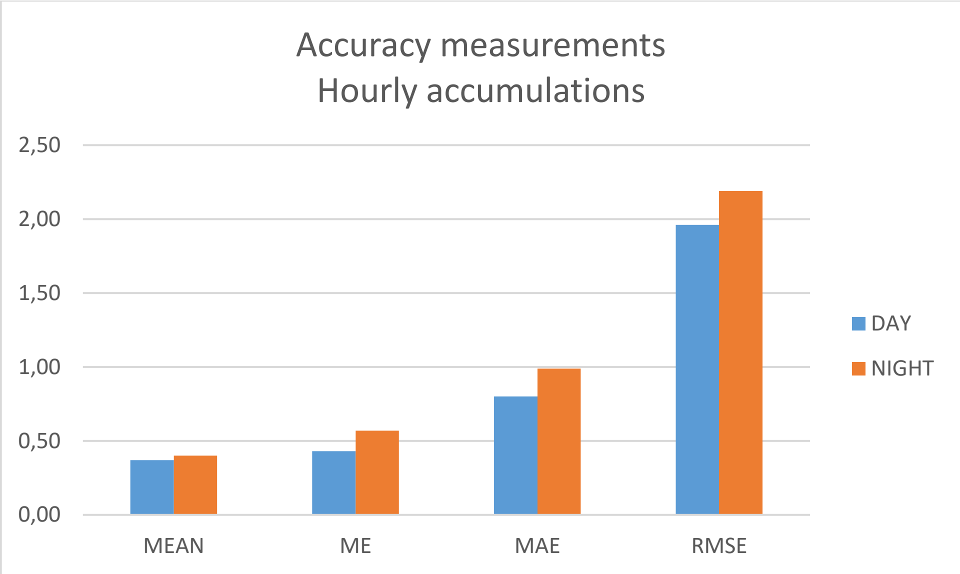

Figure 36. Accuracy measurements for CRR hourly accumulations for MSG

Since hourly accumulations have as a base the instantaneous rain rates, similar results are expected. Figure 36 show that accuracy measurements take lower values for hourly accumulations than for instantaneous rain rates. This happens because hourly accumulations fields are smoother than instantaneous rain rates ones. Better performance of the day-time algorithm with respect to the night-time one can be seen.

Categorical scores can be obtained assuming that values higher than or equal to 0.2 mm/h for hourly precipitation accumulations are considered rainy. Results are shown in Table 15.

Algorithm	FAR (%)	POD (%)	CSI (%)	PC (%)
Day time	51	65	39	63
Night time	58	56	32	56

Table 9. Categorical scores for CRR hourly accumulations for MSG

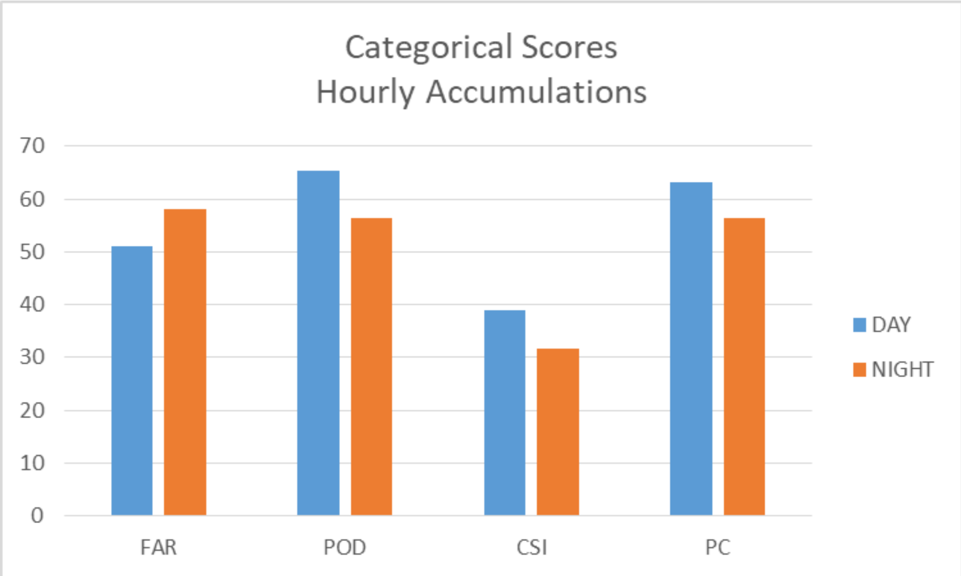

Figure 37. Categorical scores for CRR hourly accumulations for MSG

As for categorical scores, Figure 39 shows also the better estimations provided by the day-time algorithm and results from Table 15 fulfil the FAR and POD target values defined in the "NWCSAF Product Requirements document" [AD 4].

3.2.1.3 Conclusion

Algorithm	Threshold Accuracy FAR (%)	Target Accuracy FAR (%)	Optimal Accuracy FAR (%)	FAR (%)
3 - Variables	<60	<40	<38	34
2 - Variables	<65	<50	<44	46

Table 10. Comparison of CRR instantaneous rates FAR scores and FAR accuracy values defined in the NWCSAF Product Requirement table for MSG

Algorithm	Threshold Accuracy POD (%)	Target Accuracy POD (%)	Optimal Accuracy POD (%)	POD (%)
3 - Variables	>40	>53	>87	63
2 - Variables	>35	>47	>85	54

Table 11. Comparison of CRR instantaneous rates POD scores and POD accuracy values defined in the NWCSAF Product Requirement table for MSG

Algorithm	Threshold Accuracy FAR (%)	Target Accuracy FAR (%)	Optimal Accuracy FAR (%)	FAR (%)
3 - Variables	<65	<55	<45	51
2 - Variables	<70	<60	<50	58

Table 12. Comparison of CRR hourly accumulations FAR scores and FAR accuracy values defined in the NWCSAF Product Requirement table for MSG

Algorithm	Threshold Accuracy POD (%)	Target Accuracy POD (%)	Optimal Accuracy POD (%)	POD (%)
3 - Variables	>45	>58	>95	65
2 - Variables	>37	>50	>90	56

Table 13. Comparison of CRR hourly accumulations POD scores and POD accuracy values defined in the NWCSAF Product Requirement table for MSG

3.2.2 Validation Procedure (MTG)

Instantaneus CRR rain rates and CRR hourly accumulations have been validated against the European Operational Program for Exchange of Weather Radar information (OPERA)

The OPERA NIMBUS production generates and disseminates pan-European instantaneous surface rain rate (in mm/h) and 1-hour rainfall accumulation (in mm) composites, both at 15-minute intervals, with a spatial resolution of 2 km .

For the rain rate composite (RR), the value of each composite rain rate pixel is calculated by selecting the lowest radar pixels relative to sea level and applying the Marshall Palmer Z–R relationship ($Z=aR^b$, with coefficients a=200 and b=1.6) to convert the reflectivity factor value (dBZ in linear units) into rainfall intensity (mm/h). The hour rainfall accumulation composite (ACC) is the sum of the previous four 15-minute RR composites.

The spatial coverage over a the European region is defined with the corner coordinates approximately: (70 N 30 W), (70N 50E), (32N 15W), (32 N 30E) with the horizontal resolution grid size of 2 km by 2 km. The image size is therefore 2200 by 1900 pixels. The composites cover almost the whole of Europe in a Lambert Equal Area projection. Temporal coverage is the 15-minute interval inside which are start and end date-time of each scan, and it is updated every 15 minutes or 96 times per day. For the NIMBUS 15-minute composites, the data time widow is - 12 minutes before and + 7 minutes after the nominal times of HH:00, HH:15, HH:30, and HH:45. Note that Nimbus takes the input data that is closest to the nominal time for production of the composites

MTG satellite derived precipitation products have a 10 minutes temporal resolution and 2x2 horizontal resolution (subsatellite point). OPERA radar data have been converted into MTG projection using Nearest Neighbor interpolation. For the instantaneous validation 2 slots per hour have been selected at 00 and 30 minutes of FCI time. To temporally match the satellite with the radar product, rainfall rates have been taken at 15 and 45 minutes. This is to account for the delay in the satellite signal, which is around 8 minutes at the Southern latitudes considered in the validation (larger at higher latitudes). Once OPERA radar have been reprojected into MTG projection, both CRR, that has been created over the northerm hemisphere, and OPERA data have been cropped to the same European region where it has been finally validated. The image size of the validation area is 814x1414 pixels with corner coordinates approximately: (64N,29W),(66N,46E),(34N,14W), (34N,19E).

“No data" OPERA data, that refers to pixels that are out of range or in a blanked sector, were discarded, along with "undetect" OPERA data, that indicates that the received radar signal is at or below the noise level (this is generally associated with dry weather). Low quality satellite data have been also removed. Satellite pixels with bad "crr_quality" were excluded from calculations. Error filtering is also done by the OPERA team. Several techniques are applied to radar data, such as the anomaly-removal module (bropo) (Peura, 2002), the hit accumulation clutter filter (Scovell et al., 2013), the beam blockage correction (beamb) (Henja and Michelson, 2012) and the satfilter (Marcos and Rodríguez, 2017). The NIMBUS quality index follows the total QI function of BALTRAD (Szturc et. al., 2011), which sets the QI to the minimum of the three quality indicators of the BALTRAD toolbox (bropo, beamb, and satfilter). If none of these filters have been applied, the quality index is set to 1. The quality index value range is between 0 (poorest quality) and 1 (best quality). Finally OPERA data with quality index QI <0.1 were excluded.

Every slot was divided in two day/night areas attending to the "crr_conditions" parameter, available in the NWC-SAF precipitation product files. The value of this parameter indicates whether the day or the night algorithm is being used. Twilight areas were discarded.

MTG calibration and validation days were composed by a list of 40 days between the July the 31th to December the 11th 2024. The 75% of these days were devoted to the recalibration process whilts the rest were used to validation process.

Convective areas have been built up selecting 25x25 boxes around those pixels that met two criteria at the same time: column maximum reflectivity > 40 dBz and surface rain intensity > 10 mm/h. 40 dBZ is the value that traditionally has been proposed as a lower limit to identify unmistakably convective precipitation in the lowest PPI level (Steiner et al, 1995) and also state of art researchers (Poelman and Delobbe, 2018).
The perfect matching between radar and satellite images will never be reached so a smoothing process in a 3x3 pixels base has been done to avoid the double penalty problem.

As far as the hourly accumulation is concerned the crr_accumulated product has been compared against the OPERA hourly accumulation product. At every hour convective boxes has been evaluated and a day-night distinction has also be done.

Then a pixel by pixel (every three pixels) comparison has been carried out. The definition of the statistics computed can be checked at ANNEX 1:
The CRR values have been obtained applying all the corrections with the default values *[RD 4]*, except for the lightning correction. The fields for the moisture, parallax and orographic corrections have been extracted from ECMWF at 0.2 x 0.2 degree spatial resolution, every 6h.
Accuracy and categorical statistics described in ANNEX 1: have been computed for instantaneous rain rates and for hourly accumulations.

3.2.2.1 Instantaneous Rain Rates

Categorical scores for CRR can be obtained assuming that values higher than or equal to 0.2 mm/h for instantaneous rates are considered rainy. Results are shown in Table 14.

Algorithm	N	POD (%)	FAR (%)	CSI (%)	PC (%)
Day time	3722185	59	18	52	77
Night time	4792714	60	28	49	69

Table 14. Categorical scores for CRR instantaneous rates in convective areas for MTG

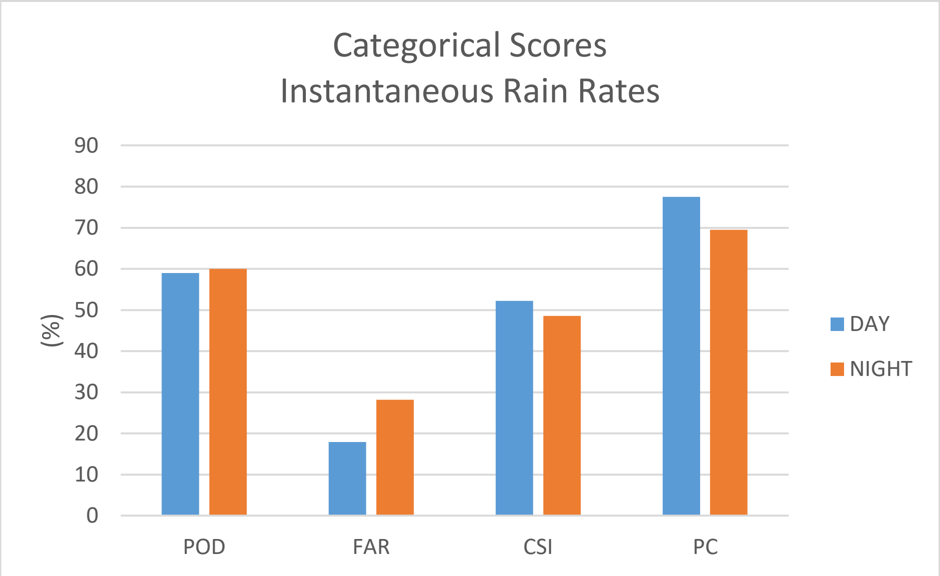

Figure 38. Categorical scores for CRR instantaneous rates for MTG

According Figure 38, day time algorithm shows similar values of POD with lower FAR. Higher values of Critical Success Index along with Percentege of correct leds to a better estimations of day time algorithm.These results, showed also in Table 14, fulfil the FAR and POD target values defined in the "NWCSAF Product Requirements document" [AD 4].

3.2.2.2 Hourly accumulations

Categorical scores can be obtained assuming that values higher than or equal to 0.2 mm/h for hourly precipitation accumulations are considered rainy. Results are shown in Table 15.
Before calculating the POD and FAR scores, correct negatives (see ANNEX 1: VERIFICATION METRIC section) have been filtered because they represent a large number of the data population, reduce the speed computing and they are not involved in the categorical scores formula of POD and FAR.

Algorithm	N	POD (%)	FAR (%)	CSI (%)	PC (%)
Day time	1140558	60	12	55	56
Night time	1810650	67	27	54	54

Table 15. Categorical scores for CRR hourly accumulations in convective areas for MTG

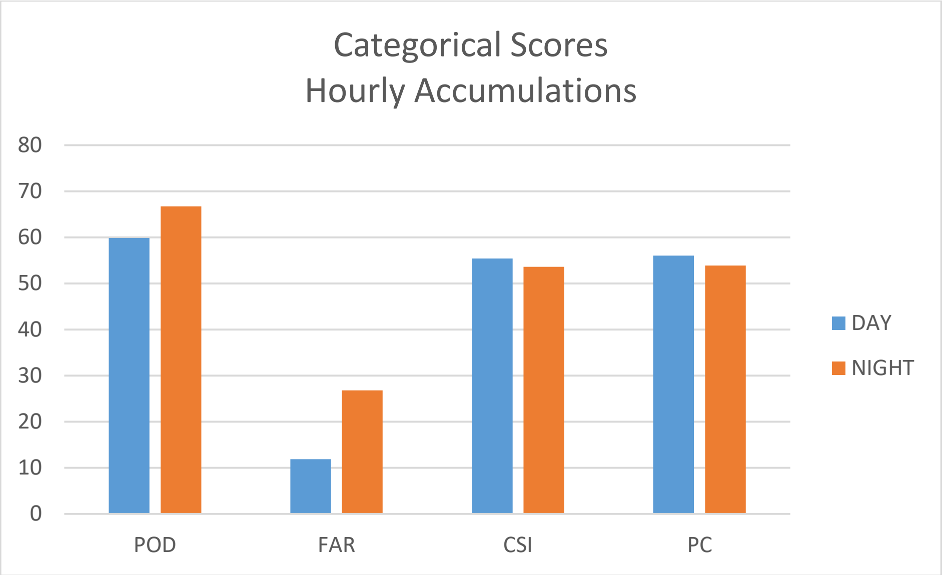

Figure 39. Categorical scores for CRR hourly accumulations for MTG

Hourly accumulation results shown in Figure 39 are consistent with those thrown by instantaneous rain rates. PC values are lower than instantaneous ones because of the exclusion of correct negatives. Slightly low POD of day algorithm against night algortith but significant lowest FAR of day time algorithm with higher CSI and PC suggest a better performance of day time algorithm.

Results from Table 15 fulfil the FAR and POD target values defined in the ”NWCSAF Product Requirements document“**¡Error! No se encuentra el origen de la referencia.**[AD 4].

3.2.2.3 Conclusion

Algorithm	Threshold Accuracy FAR (%)	Target Accuracy FAR (%)	Optimal Accuracy FAR (%)	FAR (%)
3 - Variables	<60	<40	<38	18
2 - Variables	<65	<50	<44	28

Table 16. MTG: Comparison of CRR instantaneous rates FAR scores and FAR accuracy values defined in the NWCSAF Product Requirement table

Algorithm	Threshold Accuracy POD (%)	Target Accuracy POD (%)	Optimal Accuracy POD (%)	POD (%)
3 - Variables	>40	>53	>87	59
2 - Variables	>35	>47	>85	60

Table 17. MTG: Comparison of CRR instantaneous rates POD scores and POD accuracy values defined in the NWCSAF Product Requirement table

Algorithm	Threshold Accuracy FAR (%)	Target Accuracy FAR (%)	Optimal Accuracy FAR (%)	FAR (%)

3 - Variables	**<65**	**<55**	**<45**	**12**
2 - Variables	**<70**	**<60**	**<50**	**27**

Table 18. MTG: Comparison of CRR hourly accumulations FAR scores and FAR accuracy values defined in the NWCSAF Product Requirement table

Algorithm	**Threshold Accuracy POD (%)**	**Target Accuracy POD (%)**	**Optimal Accuracy POD (%)**	**POD (%)**
3 - Variables	**>45**	**>58**	**>95**	**60**
2 - Variables	**>37**	**>50**	**>90**	**67**

Table 19. MTG: Comparison of CRR hourly accumulations POD scores and POD accuracy values defined in the NWCSAF Product Requirement table

As can be seen in Tables 16-19, the results of the CRR validation for MTG are within the established requirements, so the product is ready to be operational.

4. VALIDATION FOR PRECIPITATING CLOUDS FROM CLOUD PHYSICAL PROPERTIES PRODUCT

This section contains the results obtained from the validation of the PCPh product which is described in the "Algorithm Theoretical Basis Document for the Precipitation Product Processors of the NWC/GEO of the NWC/GEO MTG-I day-1"*[RD 4]*.

The validation procedure consists of two parts: A subjective validation and an objective validation. In the first case, a visual validation of PCPh output against the Spanish radar composite for different time slots was done for MSG satellite, and against OPERA rain rate composition was done for MTG satellite. In the second case a categorical pixel by pixel comparasion has been done against the Spanish composite radar data for the MSG satellite and against the OPERA radar network for the MTG satellite.

POD and FAR scores will be the metrics used to evaluate the product.

4.1 SUBJECTIVE VALIDATION FOR PRECIPITATING CLOUDS FROM CLOUD PHYSICAL PROPERTIES (PCPH)

In this section a visual check is possible by comparing the probability of precipitation (PoP) obtained from the PCPh algorithm against the radar data from the Spanish radar data when it comes to the MSG satellite and from the OPERA radar network when it comes to the MTG satellite.

For MSG, this subjective study has focused on rainy episodes throughout 2016, while for MTG the rainy episodes correspond to the year 2024. Different day and night time slots have been chosen to depict the PCPh general behaviour. A pair of images are shown to subjectively validate the PCPh product. PCPh product will be visually compared in Spain for MSG and in OPERA region for MTG.

4.1.1 The image on the right side corresponds with the radar rainfall rate (RFR), and the image on the left side corresponds with the PCPh output.

DAY

As far as the visualization of PCPh output is concerned, pixels with NO DATA have been plotted in grey, due to an undefined phase or No Data or corrupted data input. Black colour stands for no probability of rain.

4.1.1.1 MSG SATELLITE

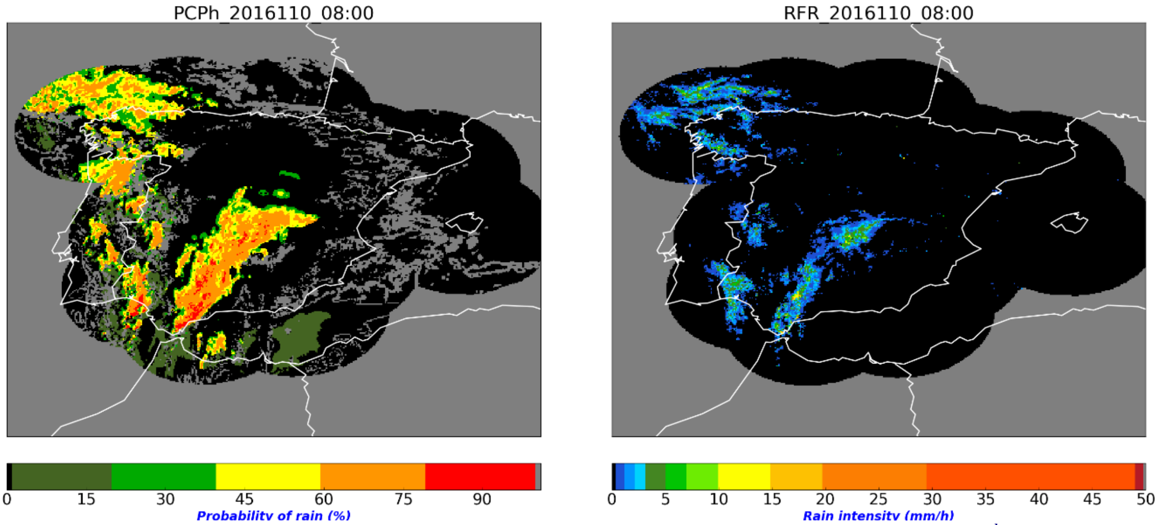

Figure 40. Comparison of PCPh day product for MSG and radar rainfall rate on 19th April 2016 at 08:00UTC

Figure 40 is an example of PCPh day algorithm. There is a general good agreement between the precipitating area provided by the Spanish radar and the probability of rain.

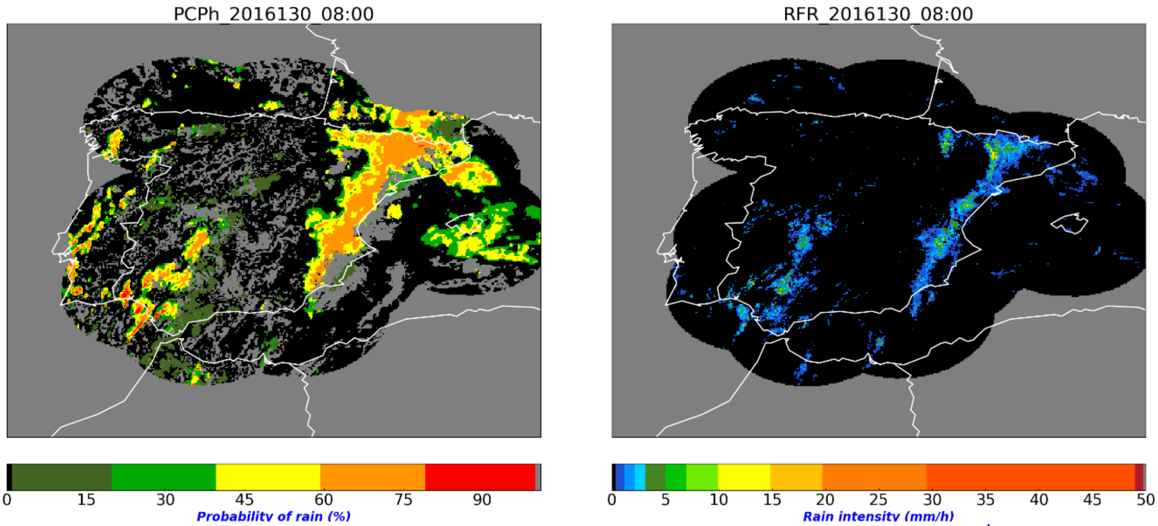

Figure 41. Comparison of PCPh day produc for MSG and radar rainfall rate on 9th May 2016 at 08:00UTC

In Figure 41, it can also be checked that the rainy areas depicted by the Spanish radar match with the higher values of the PCPh day output. In this occasion, it appear an area near the Balearic Islands where the probability of rain is higher to 30% and there are only little pixels classified as rainy in the Spanish composite radar.

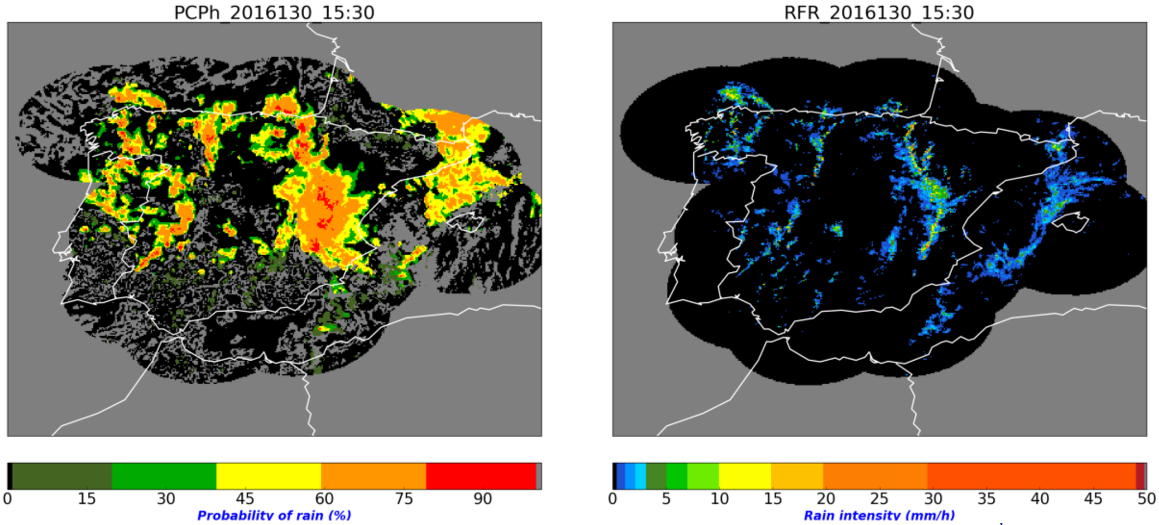

Figure 42. Comparison of PCPh day produc for MSGt and radar rainfall rate on 09th May 2016 at 15:30UTC

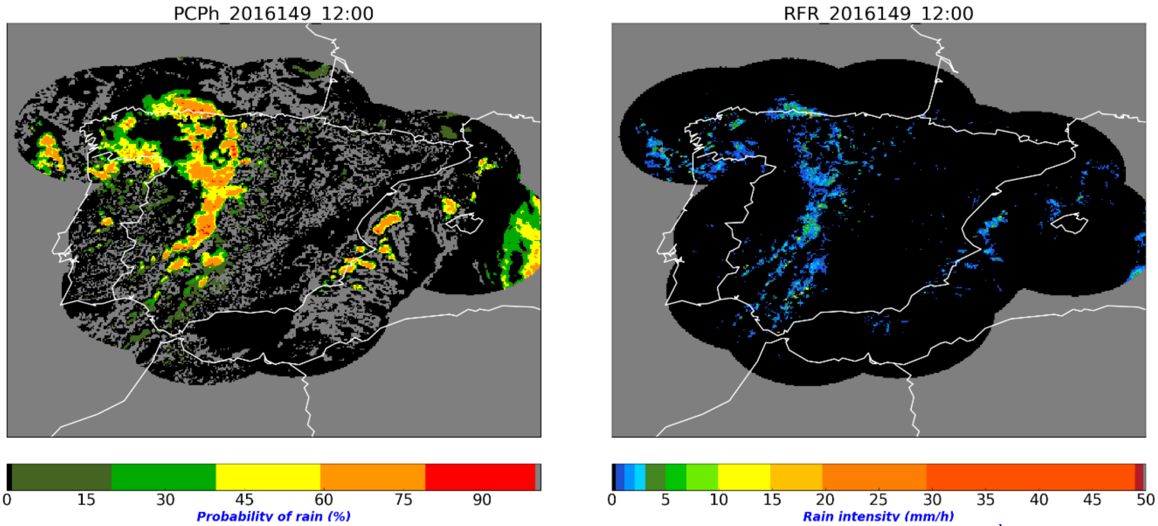

Figure 43. Comparison of PCPh day product for MSG and radar rainfall rate on 28th May 2016 at 12:00UTC

Figures 42 and 43 are good examples of a good performance of PCPh day product. Almost every area with rain represented in the Spanish composite radar has a correspondence in the probability of rain. It can also be noticed that the higher rain rates values provided by the Spanish radar correspond with the higher values in the probability of rain.

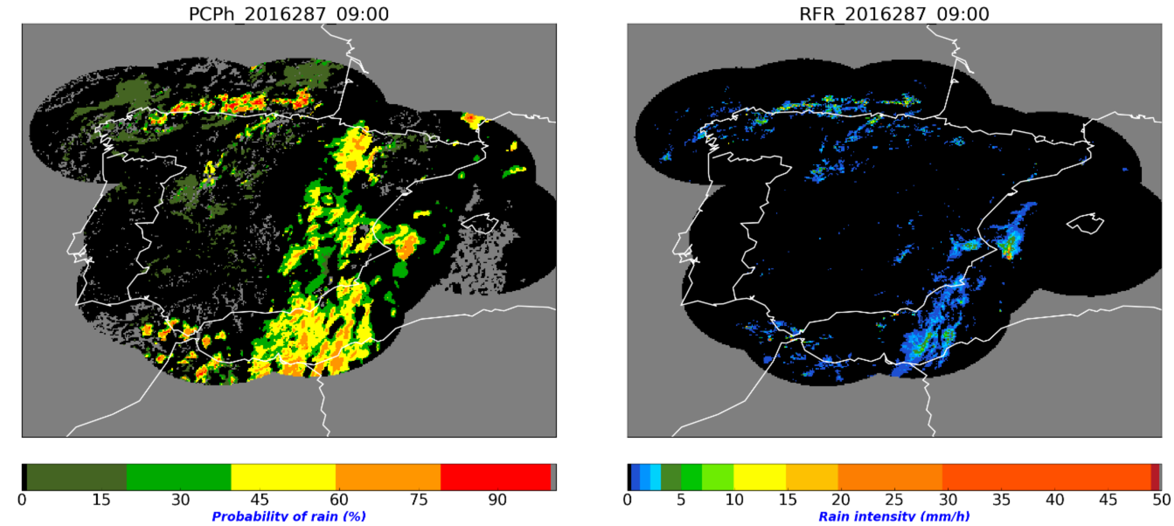

Figure 44. Comparison of PCPh day product for MSG and radar rainfall rate on 13th October 2016 at 09:00UTC

In Figure 44, it can be noticed that, in the Iberian mountain range there is black hole with the shape of a ring, just inside an area with probability of rain. It is due to the stability correction factor. This correction factor is set by default but it can be turned off. What this correction factor do is to remove areas with no probability of rain based on NWP stability indexes (Showalter, Lifted and K). That is the reason why in some occasions it appears a black whole inside a probability of rain precipitating area. More information about this correction factor can be found in the "Algorithm Theoretical Basis Document for the Precipitation Product Processors of the NWC/GEO "*[RD 4]*.

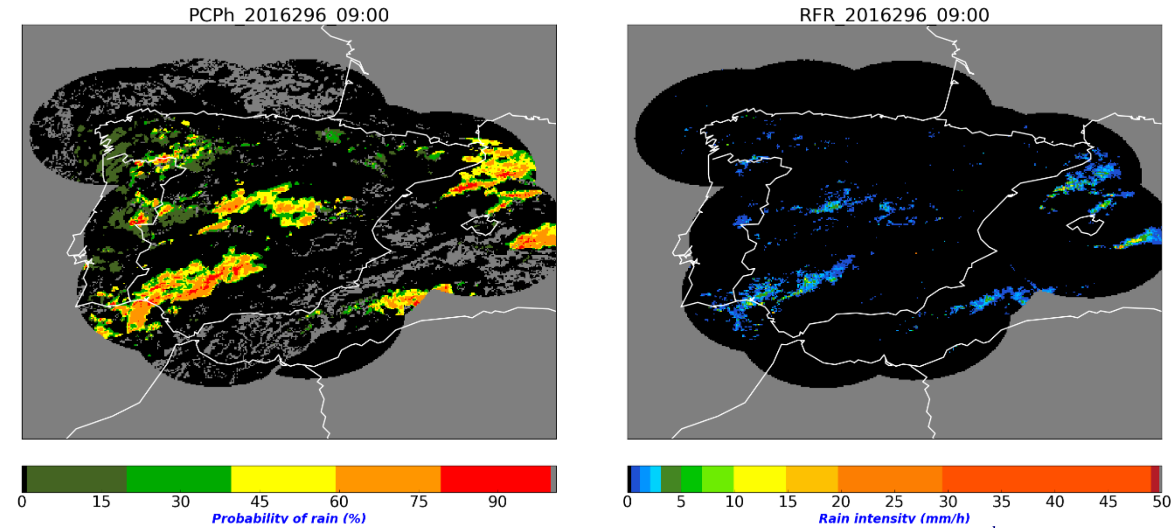

Figure 45. Comparison of PCPh day product for MSG and radar rainfall rate on 22nd October 2016 at 09:00UTC

This last example of PCPh day algorithm shows the product is able to detect little precipitation areas located in several regions of the Iberian Peninsula: in the mountains of León, south of the Pyrenees, the central part of the Iberian Peninsula and in between the Cape of Gata and the Cape of Palos, for example.

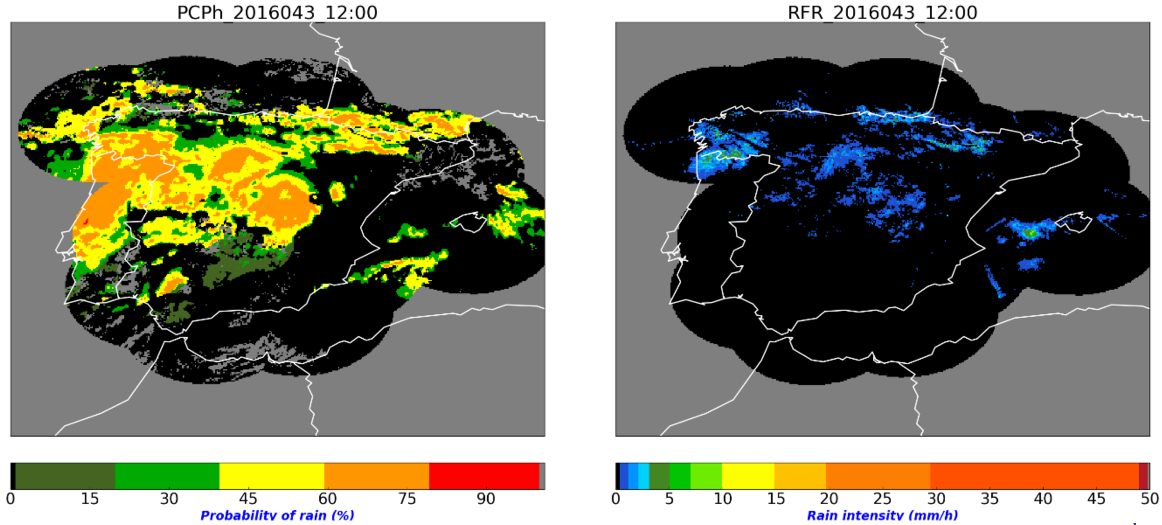

Figure 46. Comparison of PCPh day product for MSG and the Spanish radar composite on 12th February 2016 at 12:00UTC

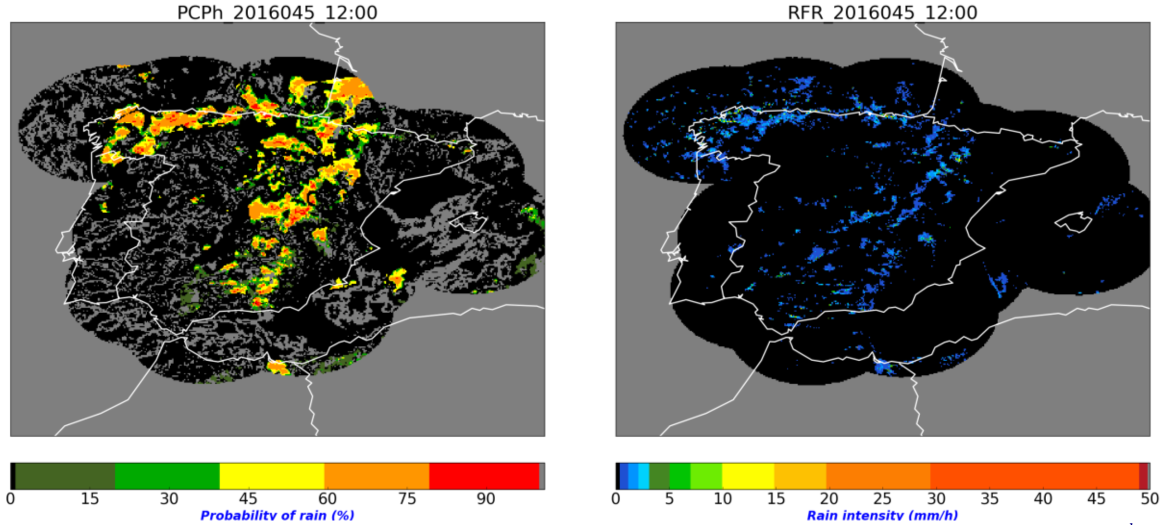

Figure 47. Comparison of PCPh day product for MSG and the Spanish radar composite on 14th February 2016 at 12:00UTC

To finish with the subjective validation of PCPh day algorithm, to more examples are displayed, corresponding with winter time (Figures 46 and 47). In Figure 46, PCPh tends to extend the PoP to a wider area, whilst in Figure 29 the visual match seems to be more accurate.

4.1.1.2 MTG SATELLITE

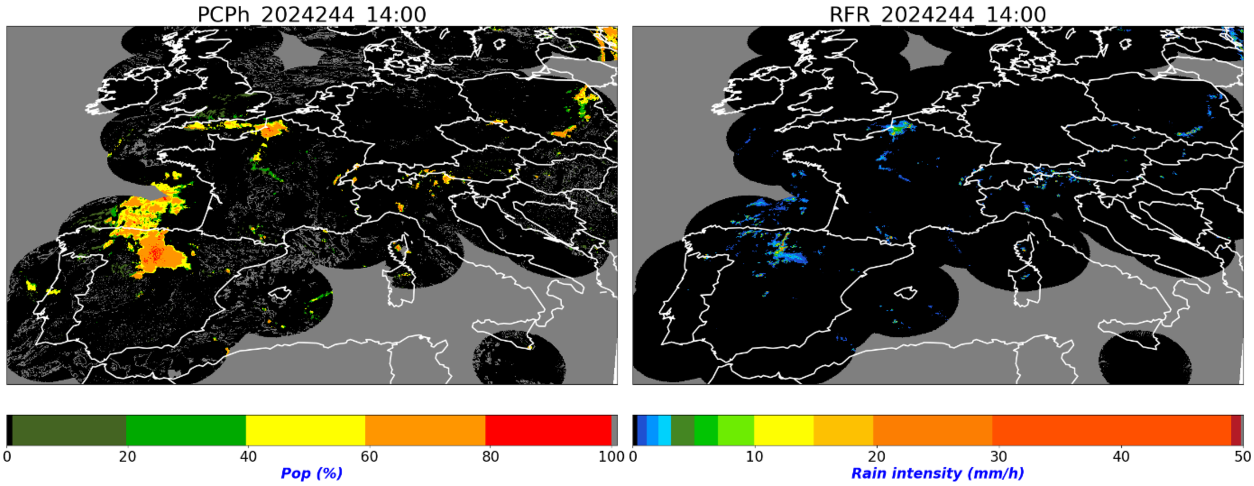

Figure 48. Comparison of PCPh day product for MTG and OPERA radar rainfall rate on 31th August 2024 at 14:00UTC

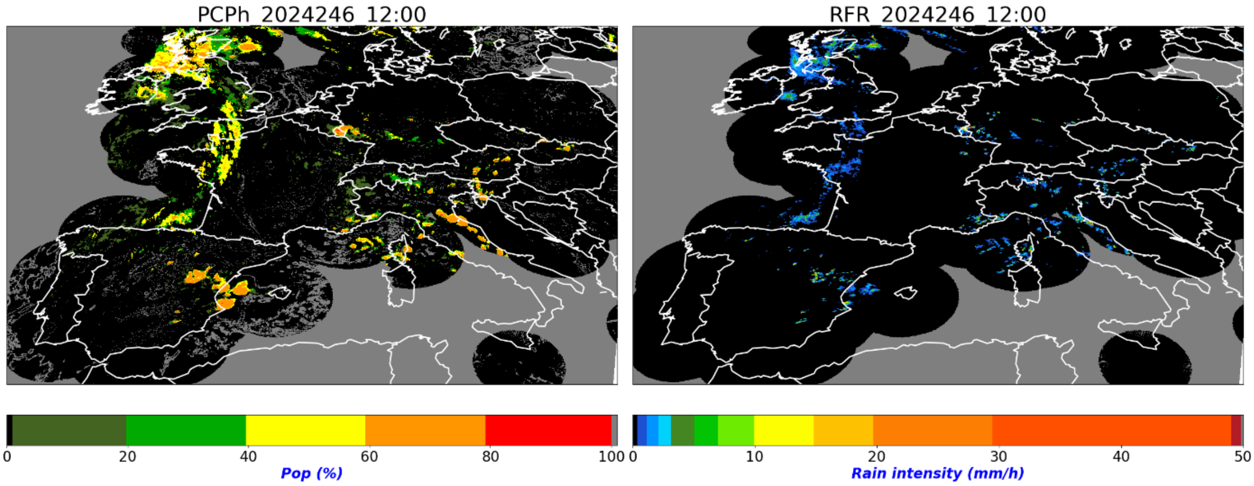

Figure 49. Comparison of PCPh day product for MTG and OPERA radar rainfall rate on 2th September 2024 at 08:00UTC

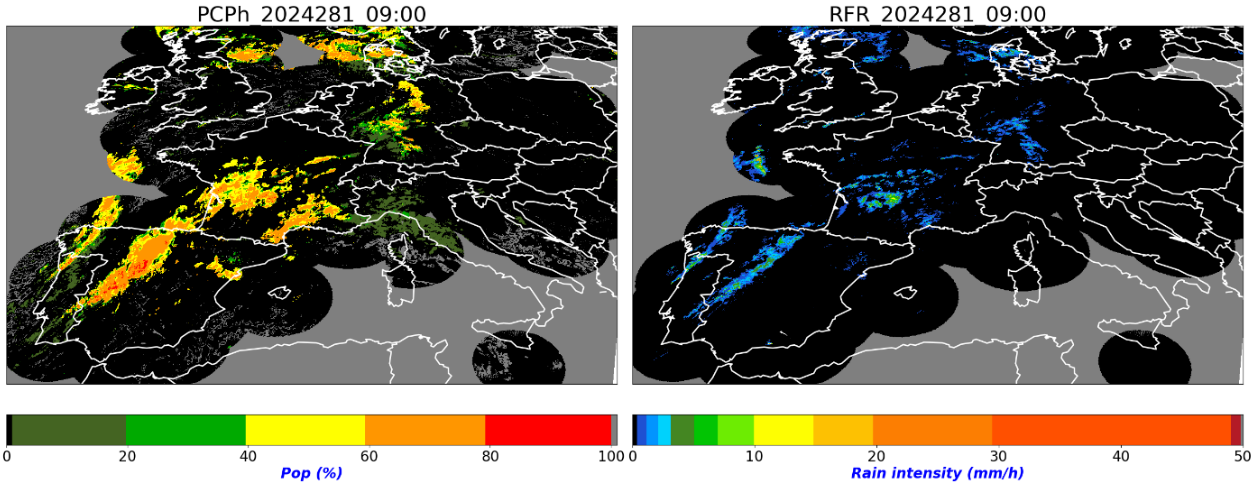

Figure 50.Comparison of PCPh day product for MTG and OPERA radar rainfall rate on 7th October 2024 at 05:00UTC

These three examples show a good performance of PCPh day algorithm in terms of depicting the precipitating area. Day time product tends to not give low values of probability of precipitation. Values higher to 80% are not very common in general.

4.1.2 NIGHT

PCPh night standards visualization are the same as for the day time. Hence, grey-colour are used for the NO DATA pixels, due to an undefined phase or No Data or corrupted data input. Black colour stands for no probability of rain.

4.1.2.1 MSG SATELLITE

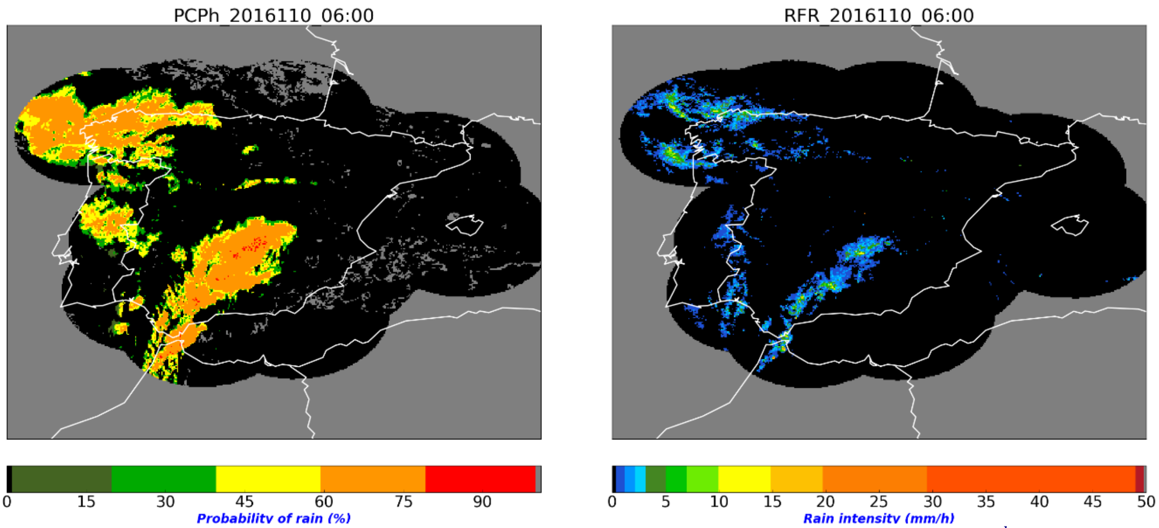

Figure 51. Comparison of PCPh night product for MSG and radar rainfall rate on 19th April 2016 at 06:00UTC

In this example of PCPh night algorithm there also exits a good agreement between the rainy areas depicted in the Spanish radar and the probability of rain. However, it seems the precipitating areas are overestimated. That will be traduced in a higher proportion of False Alarm rates.

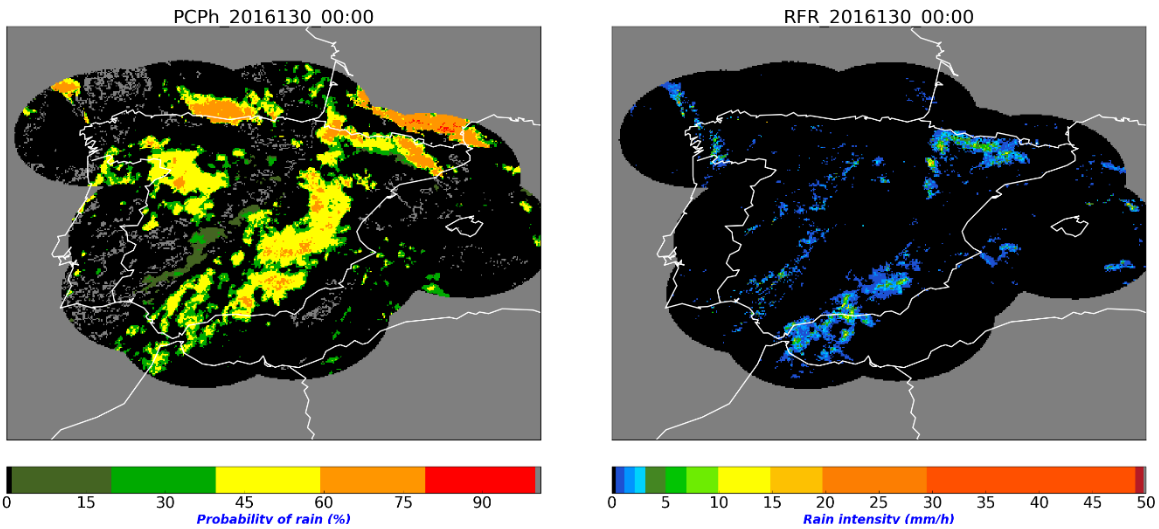

Figure 52. Comparison of PCPh night product for MSG and radar rainfall rate on 9th May 2016 at 00:00UTC.

As happened in the previous example, there is a general good performance of the PCPh night algorithm, except for the region in the North of the Iberian Peninsula covering Asturias and Cantabria where it seems it is not raining according to the Spanish radar.

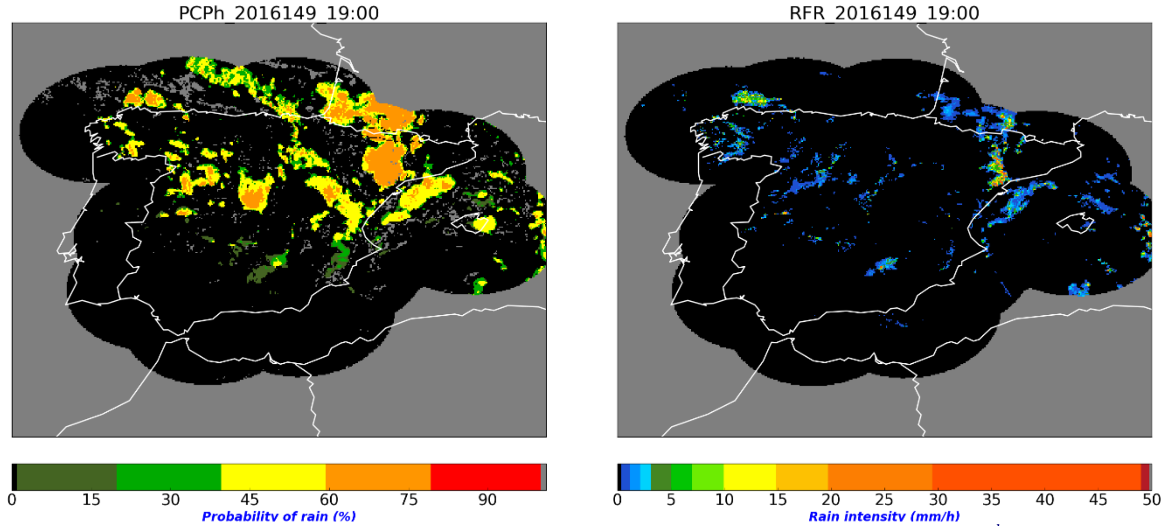

Figure 53. *Comparison of PCPh night product for MSG and radar rainfall rate on 28th May 2016 at 19:00UT*

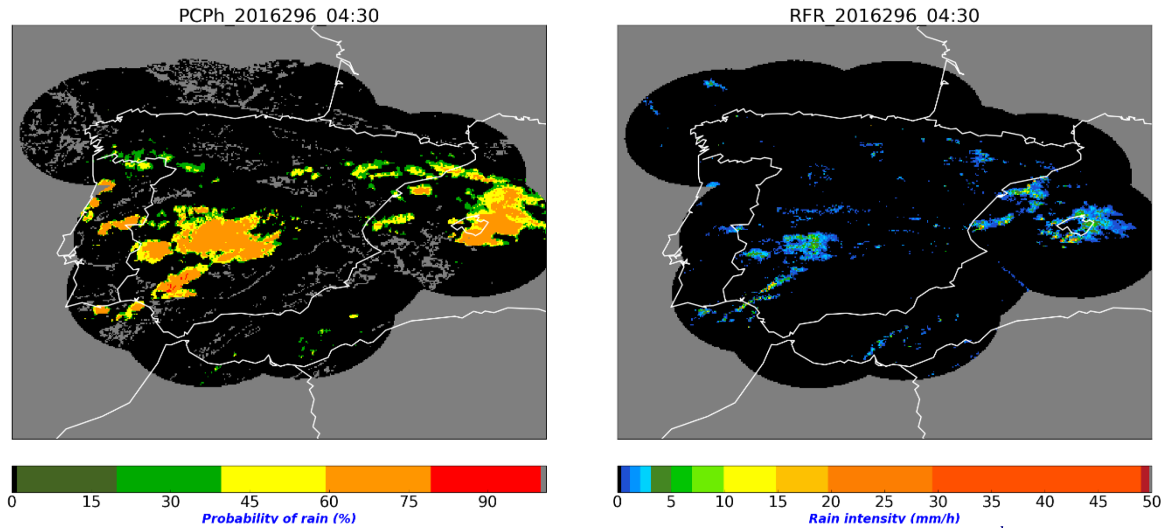

Figure 54. Comparison of PCPh night product for MSG and radar rainfall rate on 22th October 2016 at 04:30UT

Figures 53 and 54 show a night scene where, overall, almost all precipitation areas depicted in the radar image are detected by PCPh. It can be noticed that PCPh night version tends to show larger precipitation areas than the radar (False alarms increases). At night time, it can also be observed that PCPh do not reach some high values of probability of precipitation compared with day time PCPh algorithm. This can be attributed to the lack of the visible channels and the cloud microphysics. Although a simulation of the VIS0.6 and the Cloud Water Path is done at night time, this simulations are not perfect. That is possibly the reason why PCPh night algorithm tends to provide lower values. More information about PCPh day and night algorithm can be found in the

"Algorithm Theoretical Basis Document for the Precipitation Product Processors of the NWC/GEO "*[RD 4]*.

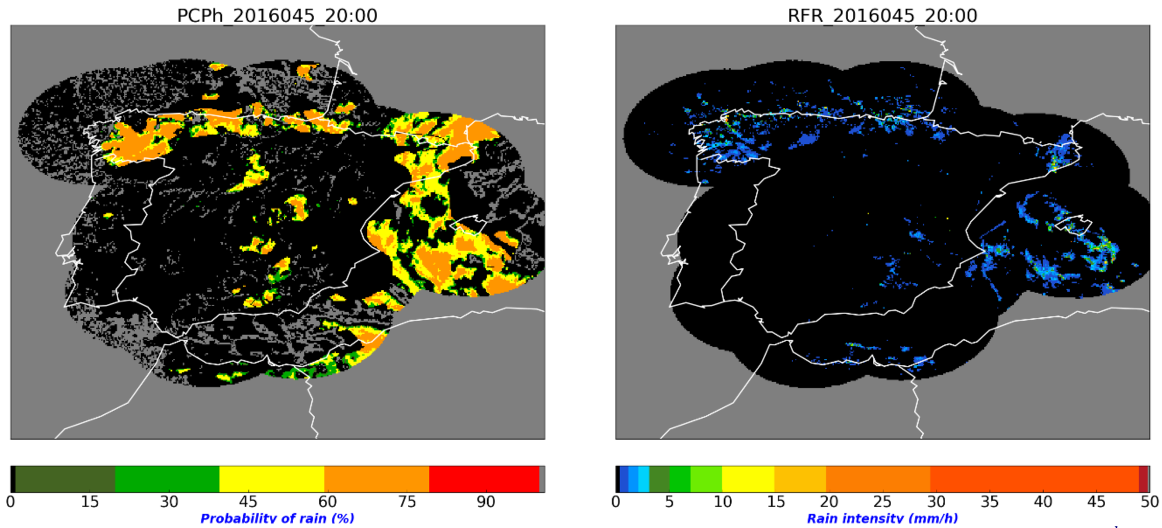

Figure 55. Comparison of PCPh night product for MSG and the Spanish radar composite on 14th Febrary 2016 at 20:00UTC.

Figure 55 corresponds with an example of PCPh night performance in winter season. At first sight it seems that most of the precipitation areas seems to be well reproduced. At the north of Spain the effects of the stability correction are noticed, reducing the number of PoP cells. Additionally, according to the national radar composite (on the right side) there are some little precipitating areas in the Alboran sea that the PCPh product does not detect.

4.1.2.2 MTG SATELLITE

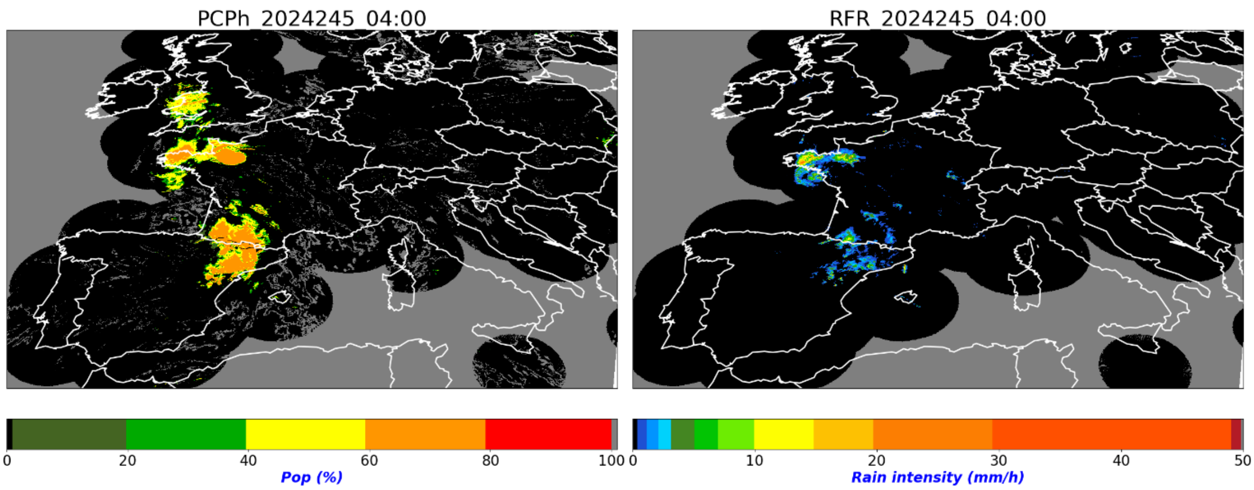

Figure 56. Comparison of PCPh night product for MTG and OPERA radar rainfall rate on 1th September 2024 at 04:00UTC

In this example of PCPh night algorithm there also exits a good agreement between the rainy areas depicted in the OPERA radar and the probability of rain. However, it seems the precipitating areas are overestimated. That will be traduced in a higher proportion of False Alarm rates.

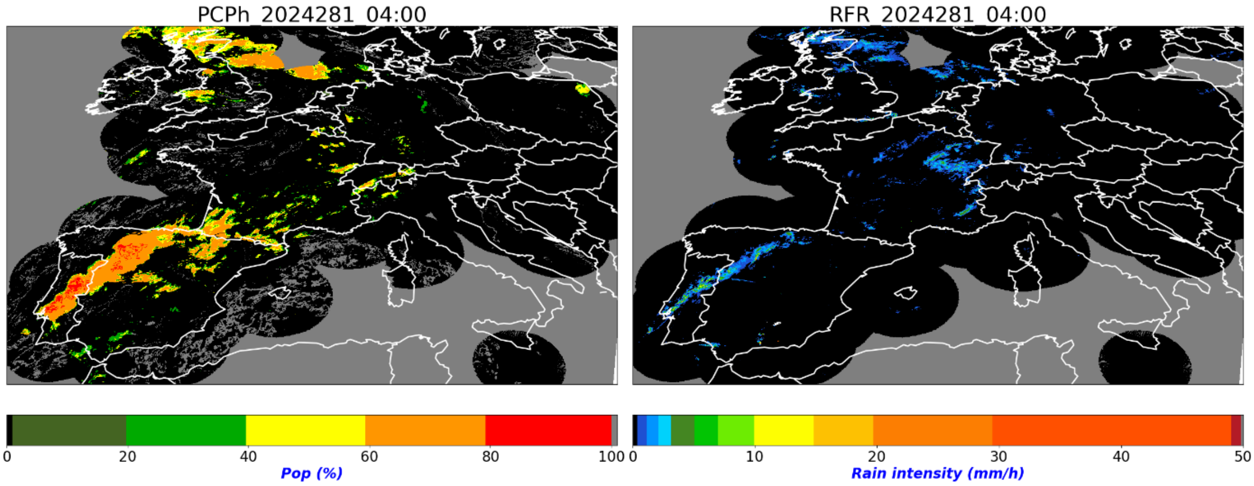

Figure 57. Comparison of PCPh night product for MTG and OPERA radar rainfall rate on 7th October 2024 at 04:00UTC.

As happened in the previous example, there is a general good performance of the PCPh night algorithm, except for some areas near the Pyrinees where false alarms are more evident.

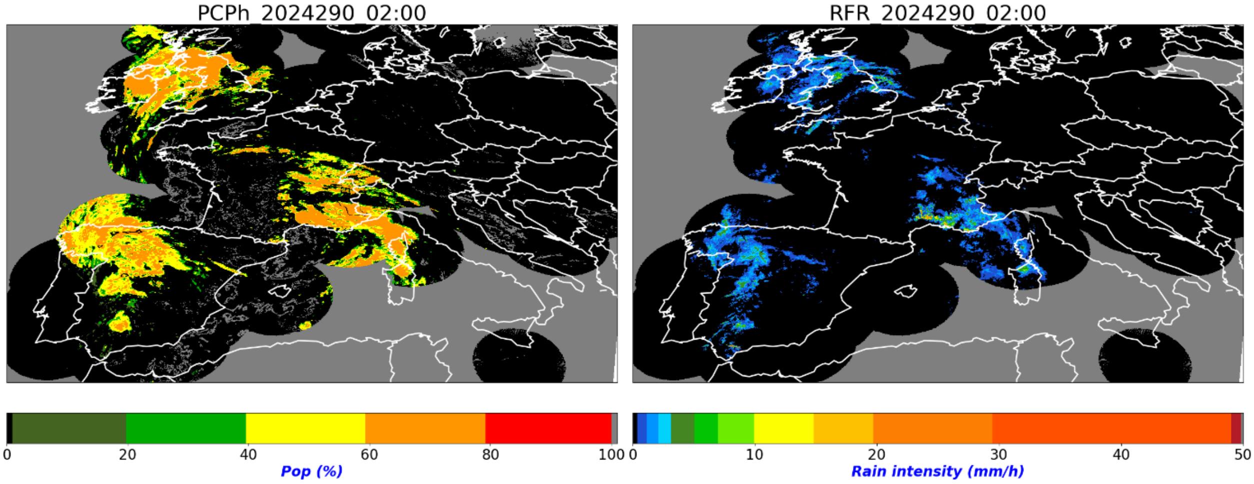

Figure 58. *Comparison of PCPh night product for MTG and OPERA radar rainfall rate on 15th October 2024 at 02:00UTC*

This last image shows an autumn example. More clouds with colder tops turns into wider probability of precipitation areas. That is the case of the northwest part of Sapin and the northeast part of France. Some artefacts are produced by the higest part montain ranges, such as near the Cantabrian mountain range. This is due to the use of the stability correction module and the the NWP data.

4.2.1

4.2 OBJECTIVE VALIDATION FOR PRECIPITATING CLOUDS FROM CLOUD PHYSICAL PROPERTIES (PCPH)

Validation Procedure

PCPh and CRRPh algorithms have been compared against the Spanish composite radar for the MSG satellite, and against the OPERA composite network radar for the MTG satellite. An objective

validation based on POD and FAR metrics has been conducted. It will be checked if the requirements included in the "NWCSAF Product Requirements Document" [AD 4] are met.
A day-night distinction has been included.

4.2.1.1 Validation Procedure for MSG: Common elements to PCPh and CRRPh

For the MSG satellite, every slot has been classified as day slot, night slot or mixed, depending on the number of day or night pixels of each image. In order to evaluate the day algorithm separately from the night algorithm, mixed slots have been discarded. This way a day or night slot only contains pixels of the same category.

Both PCPh and CRRPh products have been calibrated with a list of days throughout 2015 that accomplished at least one of two criteria. They are based on echotop (ET) and rainfall rate (RFR). Another list of days has been created throughout 2016, with the same criteria as 2015, to validate the product.

RFR in mm/h is obtained from the lowest Plan Position Indicator (PPI) of the radar using the Marshal-Palmer relation, $Z=200R^{1.6}$, where Z ($mm^6\ mm^{-3}$) is the reflectivity factor and R($mm\ h^{-1}$) is the rainfall rate. Echotop values in km. correspond with the maximum height that echoes bigger than 12dBz are able to reach.

First criterion: A particular day is included in the calibration and validation list if the percentage of pixels with ET>6km. with respects to pixels with ET>0 km exceeds the threshold of 65% at least for one slot of this day.

Second criterion: It is calculated the proportion of radar pixels with RFR>=0.2mm/h with respect to the whole image. Whenever at least one slot of a day reaches the percentage limit of 8% the day was also included in the calibration and validation list.

Since Microphysical Cloud Top parameters used by PCPh and CRRph have been computed only for sun zenith angles lower than 70º, this validation has been undertaken under the same condition.

Both PCPh and CRRPh products assign NO DATA value to those pixels with undefined phase according to the phase output of the CMIC product, which means that no information on whether the cloud consists of water or ice is available. Those pixels have been excluded in the algorithm validation.

Radar data, which are in Lambert Projection with a 1km*1km pixel resolution, have been converted into the MSG projection, using a bi-linear interpolation. The horizontal resolution of the MSG pixels are 3kms at the sub-satellite point, that in case of our area of interest, ranges from 6.9x3.5km at the north of the Spanish Península to 3.8x3.1km at the south. Parallax correction has been applied to PCPh and CRRPh. As a perfect matching between Radar and MSG images is not possible, a smoothing process in 3x3 boxes pixels has been done. The threshold to consider a pixel to rainy has been fixed at 0.2 mm/h because detection of very light rain rates using GEO satellite data is not possible.

A radar quality image has been used as a filter image to get rid of spurious echoes, such as windmill echoes. Anomalous propagation echoes have been removed through the 10.8IR scene. A rain image has been obtained from the 10.8IR data using the basic AUTOESTIMATOR algorithm (Vicente et al., 1998). A pixel with significant radar echo is considered to be a ground echo and set to zero if no significant value is found in a 15x15 box centred in the AUTOESTIMATOR image.

Due to the temporal resolution of the SEVIRI data in the normal mode, there are four satellite derived outputs available every hour. The Spanish radar network generates a set of instantaneous products every 10 minutes. The MSG scanning over Spain is done over 10 minutes after the slot hour. The only way to temporally match precipitating products (PCPh and CRRPh) with radar images is choosing 0 and 30 minutes PCPh/CRRPh images corresponding to 10 and 40 minutes radar images respectively. This way 15 and 45 minutes PCPh/CRRPh images, which do not temporally match with the radar images, have not been used in the validation process.

PCPh and CRRPh values have been obtained applying all the corrections with the default values *[RD 4]*. The fields for the stability correction have been extracted from ECMWF at 0.5 x 0.5 degree spatial resolution, every 6h.

Categorical statistic have been used to validate de product. They are explained in ANNEX 1: VERIFICATION METRIC.

ONLY TO PCPh:

PCPh has been validated in the same conditions it have been calibrated. Hence, Boxes size of 25*25 pixels centred in those radar pixels with rain rates > 0.2 mmh^{-1} have been selected. No restriction to echotops have been set.

4.2.1.2 Validation Procedure for MTG: Common elements to PCPh and CRRPh

MTG validation days consists of list of 40 days between the July the 31th to December the 11th 2024. PCPh and CRRPh have been created with all the possible corrections applied except for the lightning correction. NWP fields necessary to apply stability correction have been extracted from ECMWF at 0.2 x 0.2 degree spatial resolution, every 6h.

V2025 software version uses the stability correction only for the night time for both MTG and MSG satellites. V2021 software version used that correction for the whole day.

For the rain rate composite (RR), the value of each composite rain rate pixel is calculated by selecting the lowest radar pixels relative to sea level and applying the Marshall Palmer Z–R relationship ($Z=aR^b$, with coefficients a=200 and b=1.6) to convert the reflectivity factor value (dBZ in linear units) into rainfall intensity (mm/h).

Since Microphysical Cloud Top parameters used by PCPh and CRRph have been computed only for sun zenith angles lower than 70º, this validation has been undertaken under the same condition.

Both PCPh and CRRPh products assign NO DATA value to those pixels with undefined phase according to the phase output of the CMIC product, which means that no information on whether the cloud consists of water or ice is available. Those pixels have been excluded in the algorithm validation.

MTG satellite derived precipitation products (PCPh and CRRPh) have a 10 minutes temporal resolution and 2x2 horizontal resolution (subsatellite point). OPERA radar data have been converted into MTG projection using Nearest Neighbor interpolation. Two slots per hour have been selected at 00 and 30 minutes of FCI time. To temporally match the satellite with the radar product, rainfall rates have been taken at 15 and 45 minutes. This is to account for the delay in the satellite signal, which is around 8 minutes at the Southern latitudes considered in the validation (larger at higher latitudes). PCPh and CRRPh have been created over the Northern Hemisphere. Once OPERA radar have been reprojected into MTG projection, CRRPh,PCPh along with radar data have been cropped to the same European region where it has been finally validated. The image size of the validation area is 814x1414 pixels with corner coordinates approximately: (64N,29W),(66N,46E),(34N,14W),(34N,19E).

Parallax correction has been applied to PCPh and CRRPh. As a perfect matching between Radar and MTG images is not possible, a smoothing process in 3x3 boxes pixels has been done. The threshold to consider a pixel to rainy has been fixed at 0.2 mm/h because detection of very light rain rates using GEO satellite data is not possible.

Several techniques are applied to radar data, such as the anomaly-removal module (bropo) (Peura, 2002), the hit accumulation clutter filter (Scovell et al., 2013), the beam blockage correction (beamb) (Henja and Michelson, 2012) and the satfilter (Marcos and Rodríguez, 2017). The NIMBUS quality index follows the total QI function of BALTRAD (Szturc et. al., 2011), which sets the QI to the minimum of the three quality indicators of the BALTRAD toolbox (bropo, beamb, and satfilter). If none of these filters have been applied, the quality index is set to 1. The quality index value range is between 0 (poorest quality) and 1 (best quality). Finally OPERA data with quality index QI <0.1 were excluded.

Categorical statistic have been used to validate de product. They are explained in ANNEX 1: VERIFICATION METRIC.

ONLY TO PCPh:

PCPh has been validated in the same conditions it have been calibrated. Hence, Boxes size of 25*25 pixels centred in those radar pixels with rain rates > 0.2 mmh^{-1} have been selected. No restriction to vertical reflectivity have been set.

4.2.2 Probability of precipitation categorical thresholds validation

4.2.2.1 Probability of precipitation categorical thresholds validation for MSG

Six different probability of precipitation thresholds have been established to check the dependence of the categorical validation process with those thresholds. The chosen thresholds go from 10% to 60% in increasing steps of 10% probability of precipitation for the PCPh product.
Within all of the following PCPh categorical thresholds validation, radar rainy pixels are defined as having a rain rate of at least 0.2 mm/h

DAY:

PoP threshold (%)	N	POD (%)	FAR (%)	CSI (%)	PC (%)
10%	28839291	75	51	42	87
20%	28839291	68	47	42	88
30%	28839291	61	44	41	89
40%	28839291	51	38	39	90
50%	28839291	37	30	32	90
60%	28839291	21	21	19	89

Table 20. Categorical scores for PCPh day algorithm taking as rainy pixels those with probability of precipitation higher than the threshold.

NIGHT:

PoP threshold (%)	N	POD (%)	FAR (%)	CSI (%)	PC (%)
10%	135968389	63	67	28	84
20%	135968389	58	65	28	85
30%	135968389	54	64	27	86
40%	135968389	46	63	26	87
50%	135968389	36	61	23	88
60%	135968389	25	60	18	89

Table 21. Categorical scores for PCPh night algorithm taking as rainy pixels those with probability of precipitation higher than the threshold.

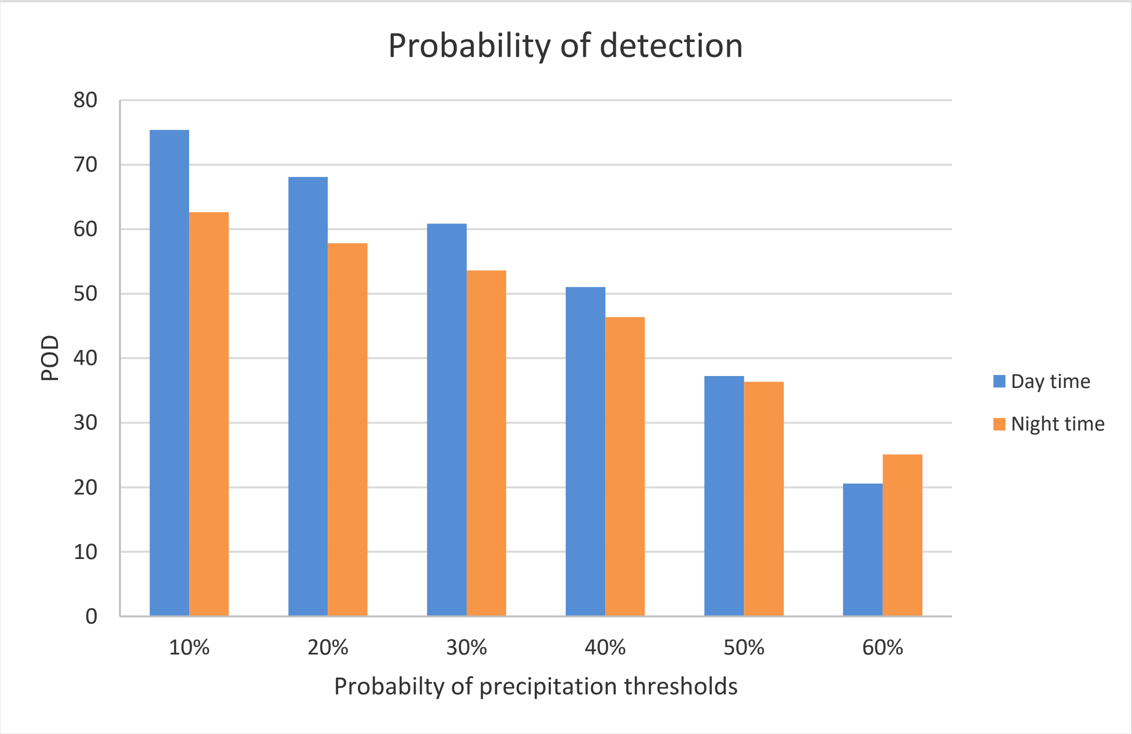

Figure 59. Probability of detection comparison between day time and night time algorithms for MSG.

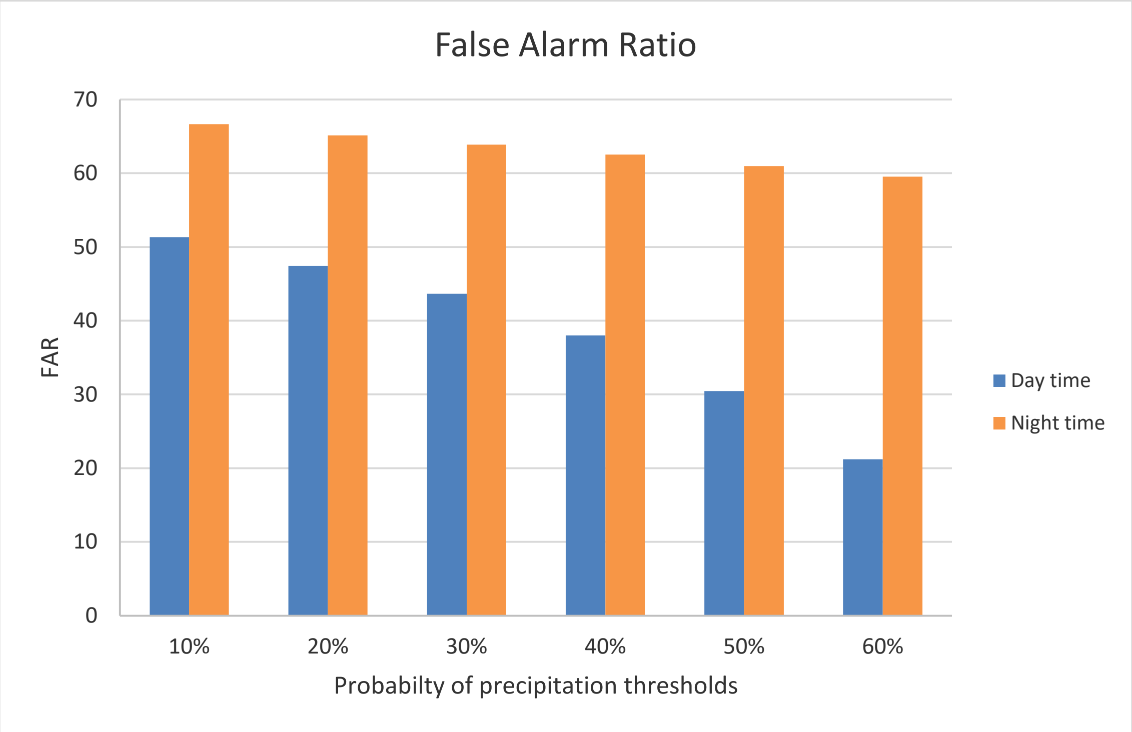

Figure 60. False alarm ratio comparison between day time and night time algorithms for MSG.

As it can be appreciated in Figure 35, the probability of detection decrease with the increase of the established thresholds. POD is always higher in day time algorithm compared with the night version, except for the last threshold (60%). POD values get worse with increasing values of the probability of precipitation thresholds. This POD reduction is expected since there are fewer PCPh points insid the higher thresholds intervals.

As regards Figure 36, FAR in day time algorithm are lower than night time cases.Like POD, there is a reduction in FAR with incresing probability of detection theresholds. This reduction is more noticeable in day time than in night time. As in previous case, FAR reduction is also logical due to the fewer PCPh points inside the higher thresholds intervals.

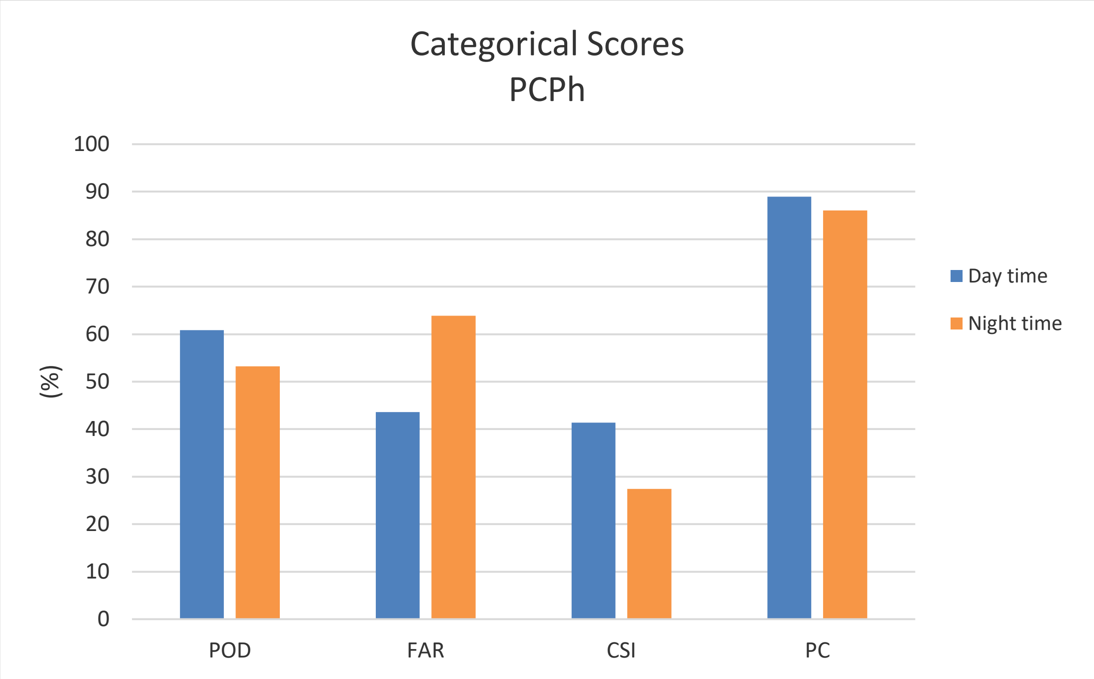

Figure 61. Categorical scores for PCPh day and night time algorithms taking as rainy pixels those with probability of precipitation higher than 30% and higher than 0.2mm/h in case of radar pixels for MSG.

A clear better performance of PCPh day time algorithm compared with PCPh night algorithm can be deduced from Figure 37. Higher values of POD, PC and CSI in day algorithm against the night version and also a lower value of False Alarm allow us infer PCPh day algorithm outplay the night version.

4.2.2.2 Probability of precipitation categorical thresholds validation for MTG

Six different probability of precipitation thresholds have been established to check the dependence of the categorical validation process with those thresholds. The chosen thresholds go from 5 % to 60 % in increasing steps of probability of precipitation for the PCPh product.
Within all of the following PCPh categorical thresholds validation, rainy pixels from the radar are fixed to at least 0.2 mm/h in every of them.
Since the population number is to high, to reduce computation calculation, it has been established a data limit of 15 million points.

DAY:

PoP threshold (%)	N	POD (%)	FAR (%)	CSI (%)	PC (%)
10%	15000000	77	43	49	96
20%	15000000	68	38	48	96
30%	15000000	61	34	46	97
40%	15000000	54	31	43	97

60%	15000000	26	20	25	96

Table 22. Categorical scores for PCPh day algorithm taking as rainy pixels those with probability of precipitation higher than the threshold.

NIGHT:

PoP threshold (%)	N	POD (%)	FAR (%)	CSI (%)	PC (%)
5%	15000000	59	55	35	94
10%	15000000	56	53	34	94
20%	15000000	51	50	34	95
30%	15000000	46	48	33	95
40%	15000000	38	45	29	95
60%	15000000	15	36	14	95

Table 23. Categorical scores for PCPh night algorithm taking as rainy pixels those with probability of precipitation higher than the threshold.

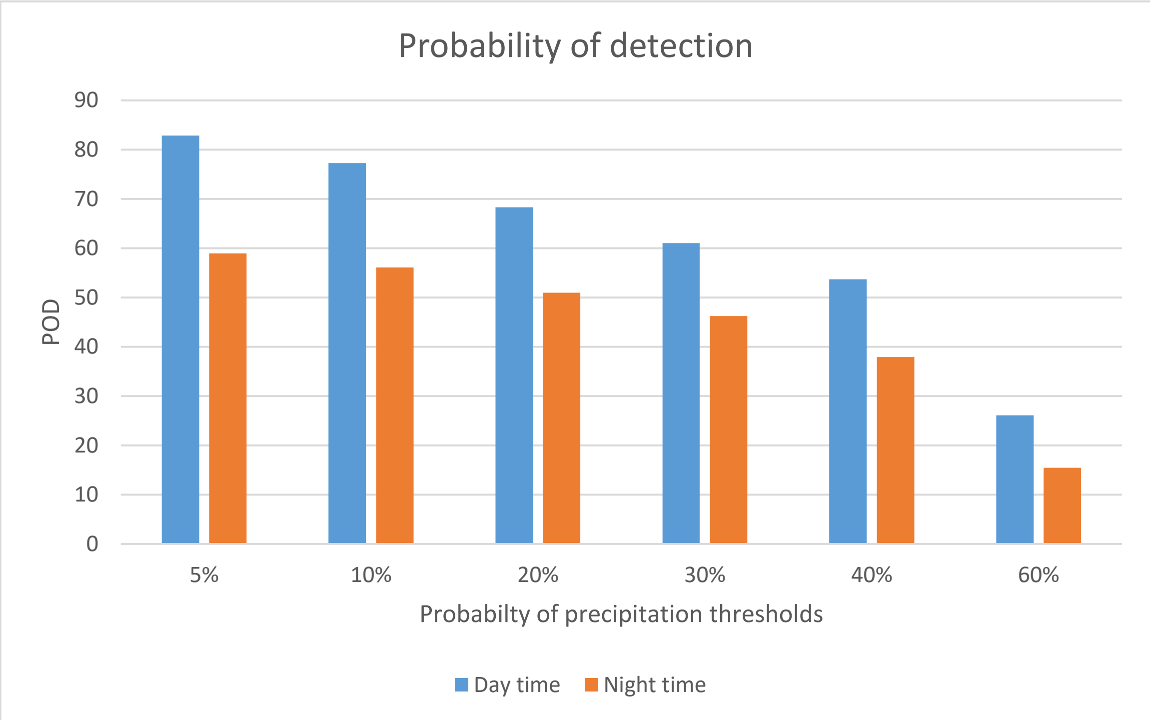

Figure 62. Probability of detection comparison between day time and night time algorithms for MTG.

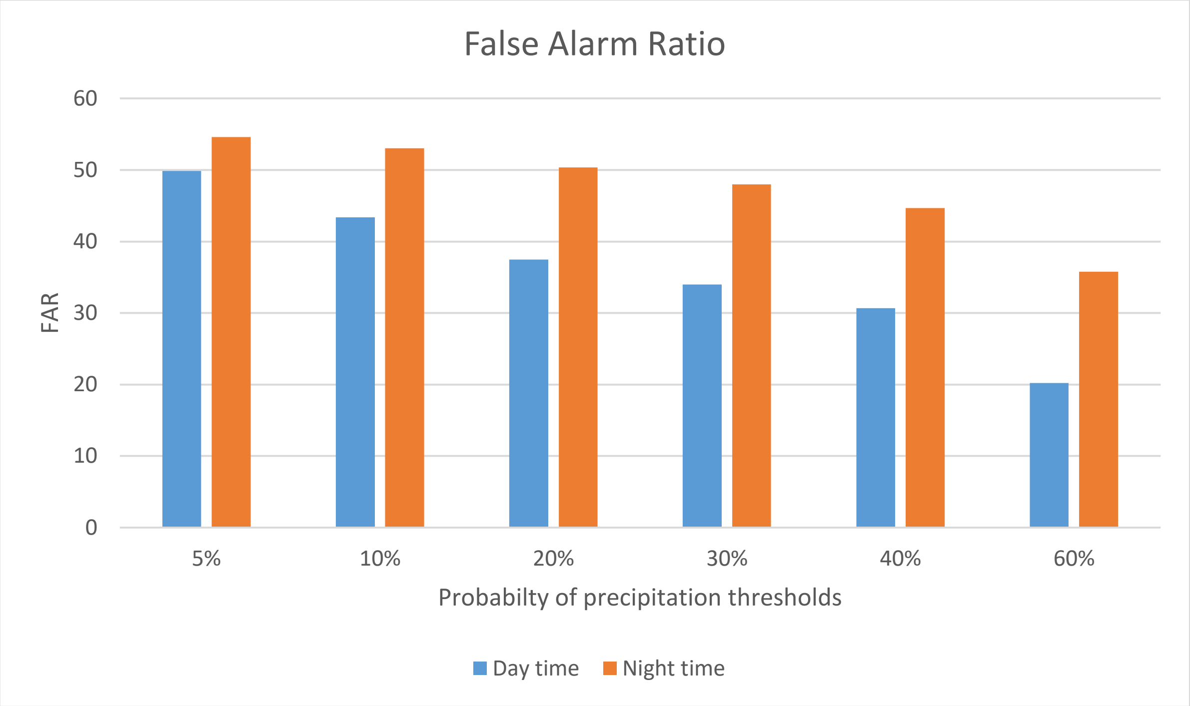

Figure 63. False alarm ratio comparison between day time and night time algorithms for MTG.

As it can be appreciated in Figure 62, the probability of detection decrease with the increase of the established thresholds. POD is always higher in day time algorithm compared with the night version.POD values get worse with increasing values of the probability of precipitation thresholds. This POD reduction is expected since there are fewer PCPh points inside the higher thresholds intervals.

As regards Figure 63, FAR values in day time algorithm are lower than night time cases.Like POD, there is a reduction in FAR with incresing probability of detection theresholds. This reduction is more noticeable in day time than in night time. As in previous case, FAR reduction is also logical due to the fewer PCPh points inside the higher thresholds intervals.

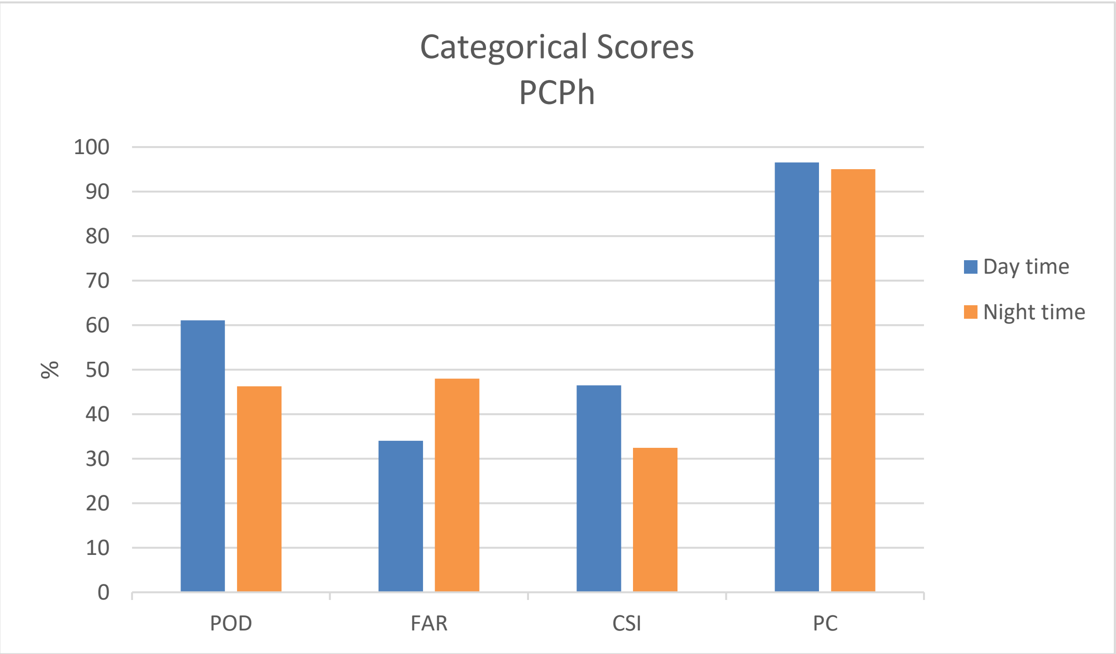

Figure 64. Categorical scores for PCPh day and night time algorithms for MTG taking as rainy pixels those with probability of precipitation higher than 30% and higher than 0.2mm/h in case of radar pixels.

A clear better performance of PCPh day time algorithm compared with PCPh night algorithm can be deduced from Figure 64. Higher values of POD, PC and CSI in day algorithm against the night version and also a lower value of False Alarm allow us infer PCPh day algorithm outplay the night version.

Conclusions

4.2.3.1 Conclusions for MSG

Validation results for the PCPh are going to be compared with those requirements included in the "NWCSAF Product Requirements Document" [AD.4]. According to this document, PCPh pixels with probability of precipitation higher than 30% are considered rainy and are compared with radar pixels with rain intensity equal or higher than 0.2 mm/h.

PCPh Algorithm	Threshold Accuracy POD(%)	Target Accuracy POD (%)	POD (%)	Threshold Accuracy FAR(%)	Target Accuracy FAR (%)	FAR (%)
Day time	>55	>65	61	<70	<65	44
Night time	>45	>50	54	<70	<60	64

Table 24. Comparison of PCPh values against POD and FAR scores defined in the NWCSAF Product Requirement table.

With the intention of showing the evolution of the product and the progress in its performance, results for the former PCPh product (version 2018) are shown below.

PCPh Algorithm	Threshold Accuracy POD(%)	Target Accuracy POD (%)	POD (%)	Threshold Accuracy FAR(%)	Target Accuracy FAR (%)	FAR (%)
Day time	>55	>65	35	<70	<65	36
Night time	>45	>50	30	<70	<60	66

Table 25. Comparison of PCPh v2018 version against POD and FAR scores defined in the NWCSAF Product Requirement table.

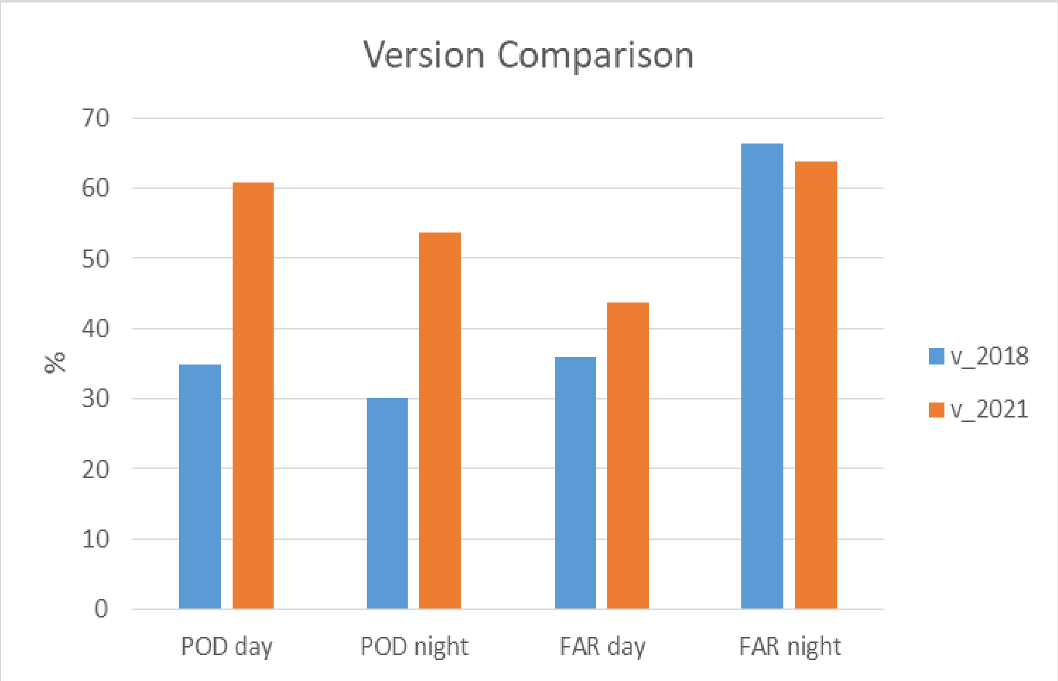

Figure 65. Comparison between 2018 and 2021 PCPh versions. Categorical scores for PCPh day and night time algorithms taking as rainy pixels those with probability of precipitation higher than 30% and higher than 0.2mm/h in case of radar pixels.

In spite of the fact 2021 PCPh version does not reach the commitments for the product only for a little it means a substantial improvement respect the previous version that had a preoperational status.

PCPh product provide us with a general good depiction of the precipitation areas. The higher values of the PCPh products are obtained at day time in correspondence with the higher radar rain rates. Night time tends to slightly overestimate the precipitation area along with no so high values.

According to the categorical validation, POD and FAR requirements are met for the “Threshold Accuracy limits” for day and night time. If we move to the “Target Accuracy”, then at day time neither POD score is reached by a little (61 vs 65 %) nor FAR score at night time (64 vs 60%).

Taking into account day and night requirements and the threshold and target limits, PCPh achieved quality is in between both of them in the Iberian Península.

As far as the visual validation is concerned, it has been visually checked that the orography may produce some unrealistic shapes. These artefacts produced by mountains are steady and it appears in the same places so it can be easily detected. Apart from that, the stability correction factor finally depends on the NWP model. If a specific meteorological pattern is wrongly reproduced, it will have an impact on the precipitation product. If the NWP model fails at detecting stable areas some holes inside precipitating areas may appear.

4.2.3.2 Conclusions for MTG

Validation results for the PCPh are going to be compared with those requirements included in the “NWCSAF Product Requirements Document” [AD.4]. According to this document, PCPh pixels with probability of precipitation higher than 30% are considered rainy and are compared with radar pixels with rain intensity equal or higher than 0.2 mm/h.

PCPh Algorithm	Threshold Accuracy POD(%)	Target Accuracy POD (%)	POD (%)	Threshold Accuracy FAR(%)	Target Accuracy FAR (%)	FAR (%)
Day time	>55	>65	61	<70	<65	34
Night time	>45	>50	46	<70	<60	48

Table 26. Comparison of PCPh values against POD and FAR scores defined in the NWCSAF Product Requirement table.

PCPh product provide us with a general good depiction of the precipitation areas. The higher values of the PCPh products are obtained at day time in correspondence with the higher radar rain rates. Night time tends to slightly overestimate the precipitation area along with no so high values.

According to the categorical validation, FAR requirements in OPERA region are met for the "Target Accuracy" and POD values are met for the "Threshold accuracy" for both day time and night time.

As far as the visual validation is concerned, it has been visually checked that the orography may produce some unrealistic shapes. These artefacts produced by mountains are steady and it appears in the same places so it can be easily detected. Apart from that, the stability correction factor finally depends on the NWP model. If a specific meteorological pattern is wrongly reproduced, it will have an impact on the precipitation product. If the NWP model fails at detecting stable areas some holes inside precipitating areas may appear.

Comparing MSG results against MTG results it has been noted a slight better performance in the case of MTG version.

5. VALIDATION FOR CONVECTIVE RAINFALL RATE FROM CLOUD PHYSICAL PROPERTIES PRODUCT

This section contains the results obtained from the validation of the CRRPh product which is described in the "Algorithm Theoretical Basis Document for the Precipitation Product Processors of the NWC/GEO" *[RD 4]*.

The validation procedure consists of a subjective validation and and objective validation.

The subjective validation compares 2 images: when it comes to MSG, the radar rainfall rate (RFR) for the Spanish composition with the CRRPh product. In the case of MTG satellite, the OPERA radar rainfall rate (RFR) for the European composition has been used and compared with the CRRPh product.

The objective validation is based on a pixel to pixel comparison between the radar data and the CRRPh product. As far as the objective validation is concerned, different categorical scores have been calculated (see Annex I at the end).

5.1 Subjective validation for Convective Rainfall rate from Cloud Physical Properties (CRRPh)

The monitoring of the precipitation pattern, as well as its evolution, is a valuable information for the forecaster. In order to check this information, visual comparisons between CRRPh and radar images have been done. A summary of these comparisons containing different study cases that represent the general behaviour of these algorithms have been selected for this purpose.

The CRRPh product includes a set of corrections that can be applied. In the case of MSG validation report the stability correction applies at day time and night time. As far as MTG the validation report has been done applying this correction only at night time.
It has been noticed that the stability correction at day time does not add significant improvements.
The results for MSG correspond to the v2021 version. In that version by default stability correction applied at both day and night.
All the images and results presented in this document include these correction factors. More information about them can be found in the "Algorithm Theoretical Basis Document for the Precipitation Product Processors of the NWC/GEO MTG-I day-I"*[RD 4]*.

Regarding CRRPh visualization, pixels with NO DATA have been plotted in grey, due to an undefined phase or No Data or corrupted data input. Black colour stands for no rain. This applies to both the day time and the night time algorithms.

5.1.1 DAY

5.1.1.1 MSG DAY

A pair of images are shown to subjectively validate the CRRPh day product: The image on the right side corresponds with the radar rainfall rate (RFR) and the image on the left side corresponds with the rain rates of the CRRPh product (see Figures 39-47).

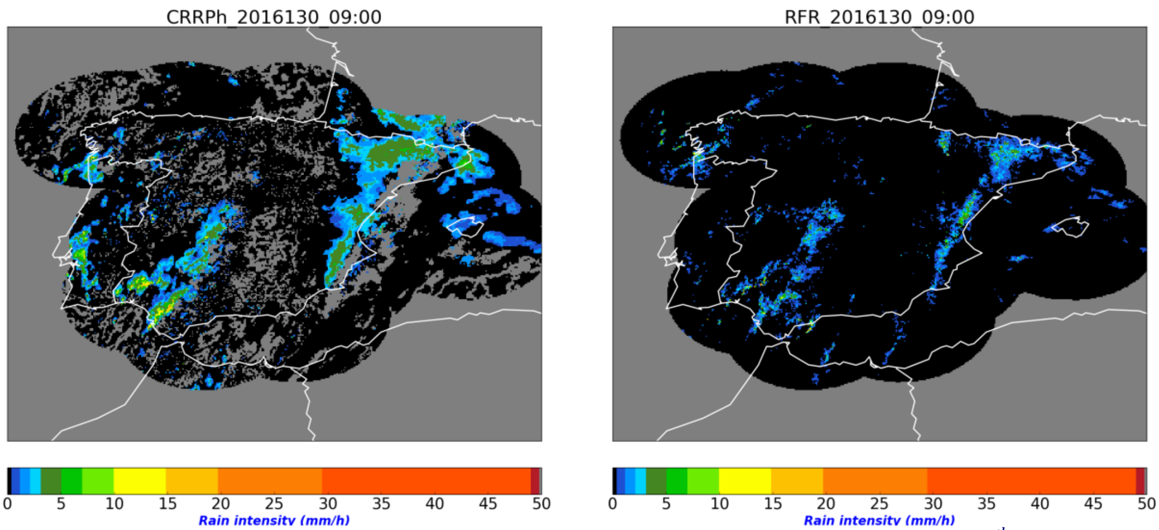

Figure 66. Comparison of CRRPh day product for MSG and radar rainfall rate on 9th May 2016 at 09:00UTC

This is a good example of the general CRRPh day time algorithm. According to the radar image that is on the right side, there is a line of precipitation coming from the northeast to the southeast of the Iberian Peninsula, close to the Mediterranean coast well detected by the product. There is another precipitation area in the centre of Spain with higher rain rates at the south.Finally, there are more little cells spread at the northwest that the product is able to detect. In this occasion is the Balearic Island the region where the product performs worse.

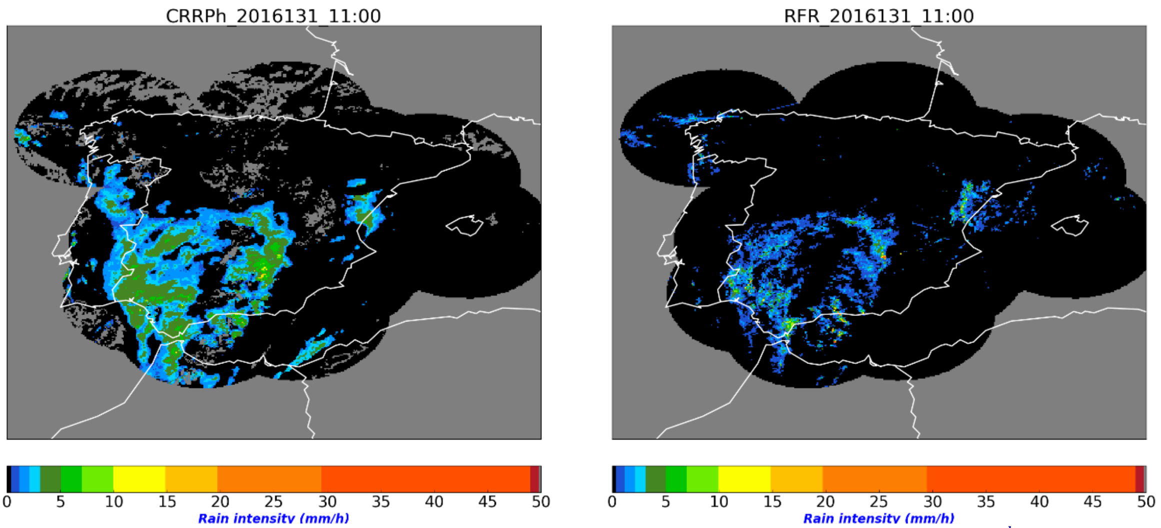

Figure 67. Comparison of CRRPh day product for MSG and radar rainfall rate on 10th May 2016 at 11:00UTC

In this second example a wide precipitation area extends all over the Centre and South of the Iberian Peninsula. The precipitation area is well represented by the product with a slight overestimation of it. At the north of Valencia and the west part of Galicia rainy areas are represented.

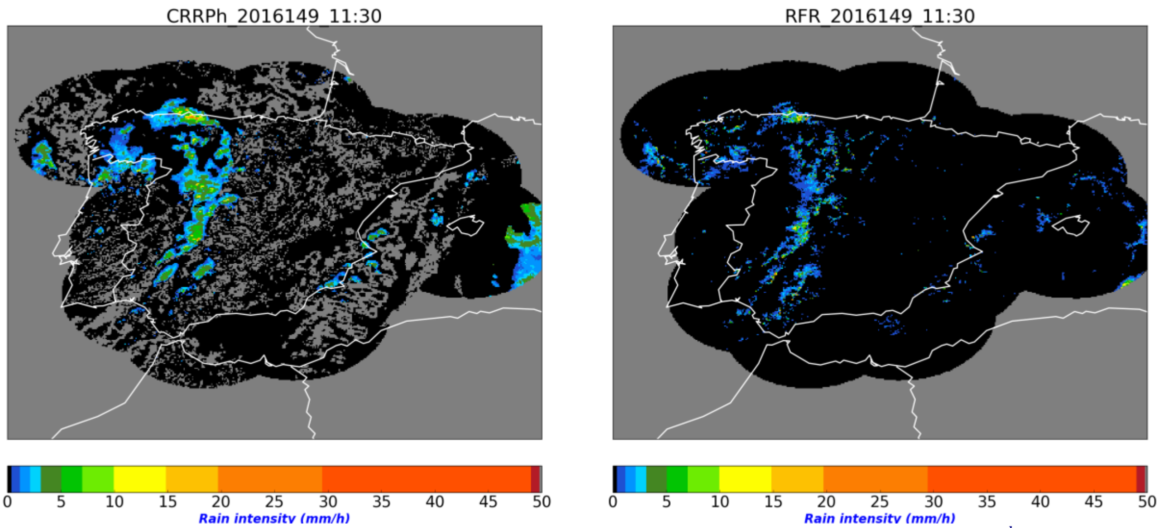

Figure 68. Comparison of CRRPh day product for MSG and radar rainfall rate on 28th May 2016 at 11:30UTC

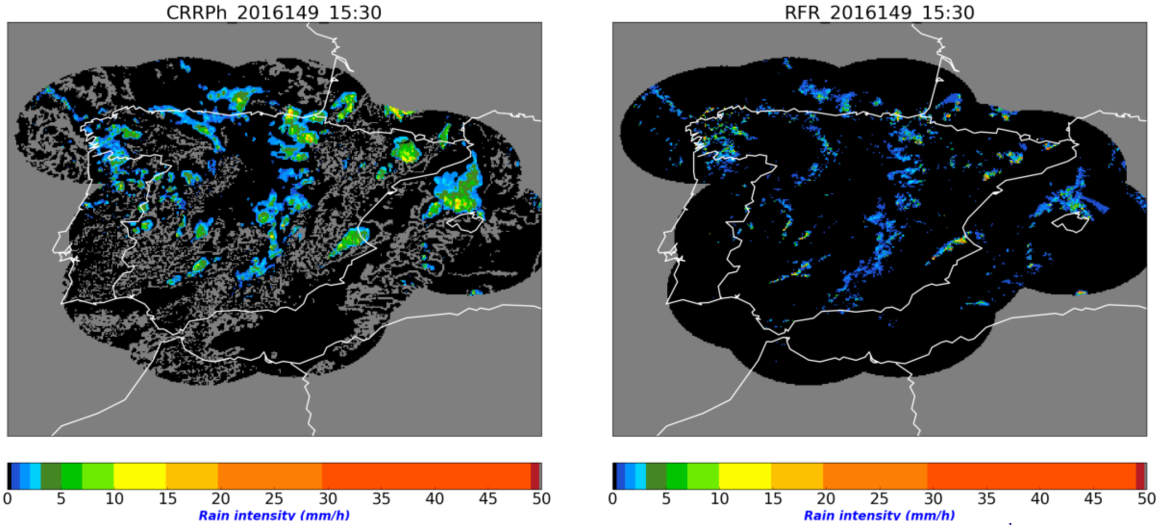

Figure 69. Comparison of CRRPh day product for MSG and radar rainfall rate on 28th May 2016 at 15:30UTC

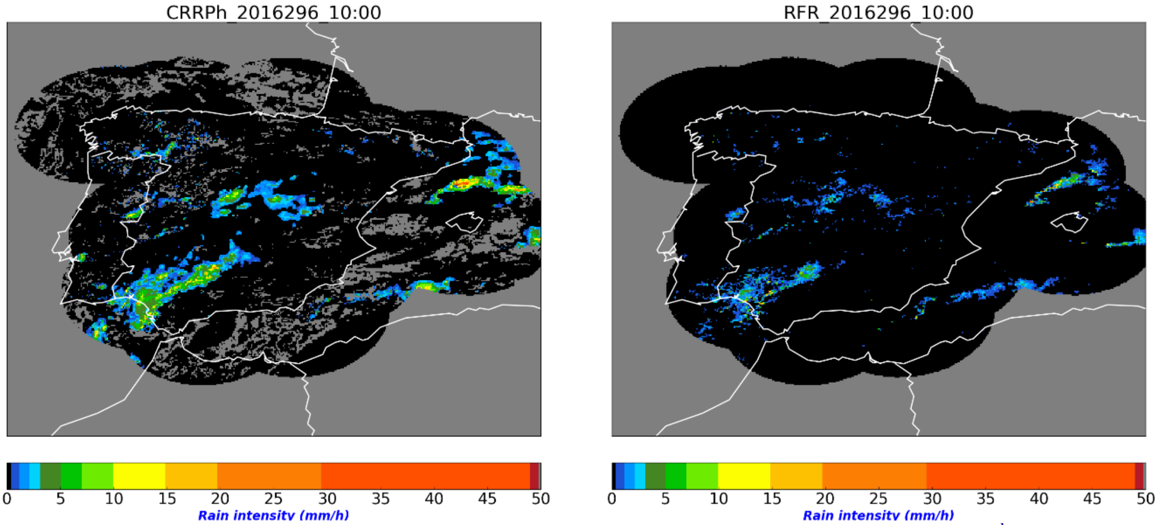

Figure 70. Comparison of CRRPh day product for MSG and radar rainfall rate on 22th October 2016 at 10:00UTC

Figures 68, 69 and 70 are good examples of the CRRPh ability to detect early stages of convective nuclei. From the point of view of a forecaster the early detection of growing cumulus that may end in active thunderstorms add valuable information.

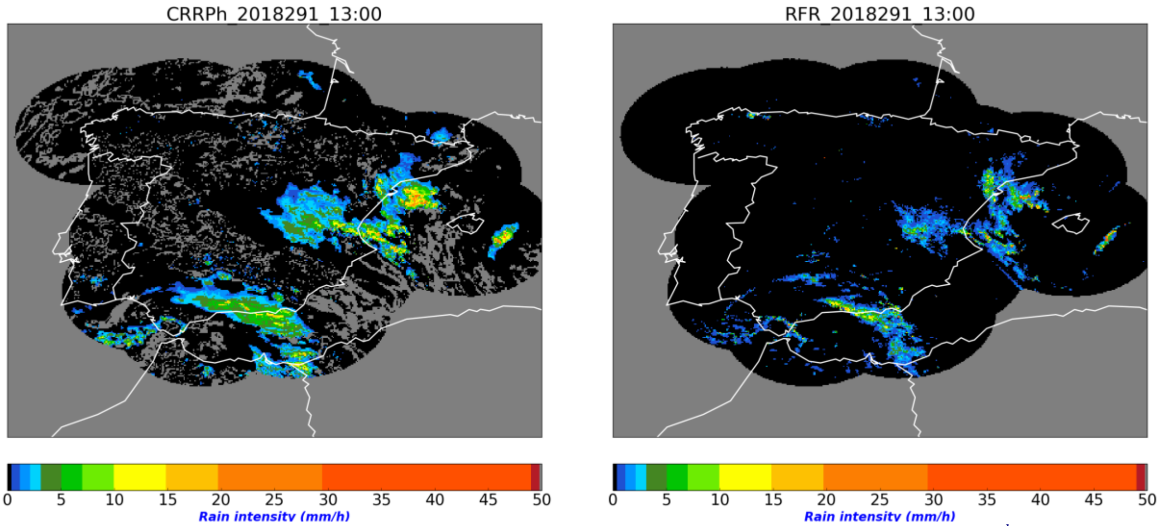

Figure 71. Comparison of CRRPh day product for MSG and radar rainfall rate on 18th October 2018 at 13:00UTC

Figure 71 is an example of active convective nuclei with high rain rates associated to them. CRRPh detect the precipitating areas and assign high rates in the same areas the Spanish radar does.

An example of the CRRPh performance out of the area the product has been calibrated is shown below. In this case, black colour stands for no precipitating areas and NO DATA input values due to an undefined phase or No data or corrupted data input.

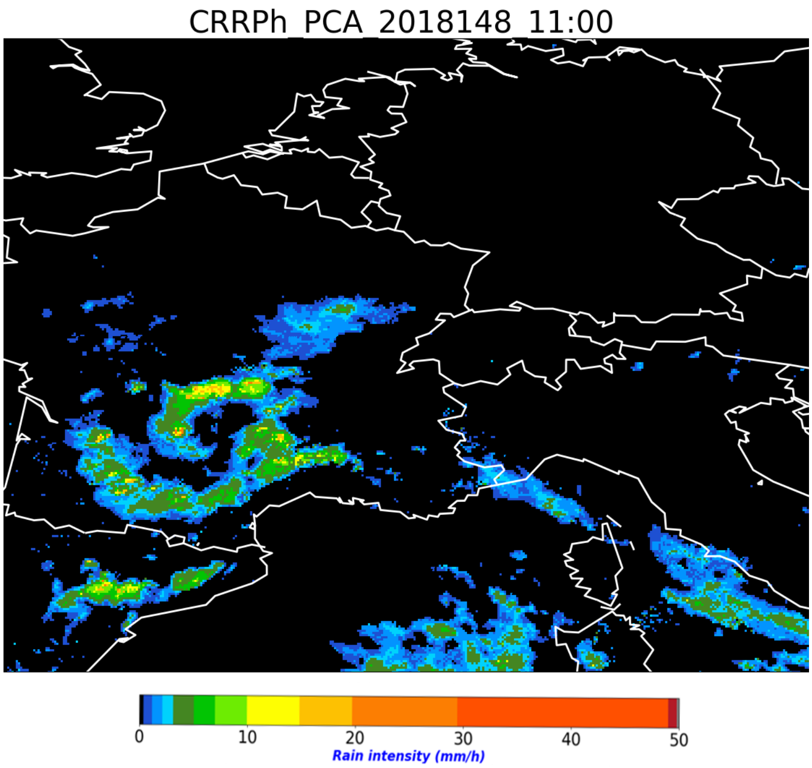

Figure 72. CRRPh day product for MSG on 28th May 2018 at 11:00UTC

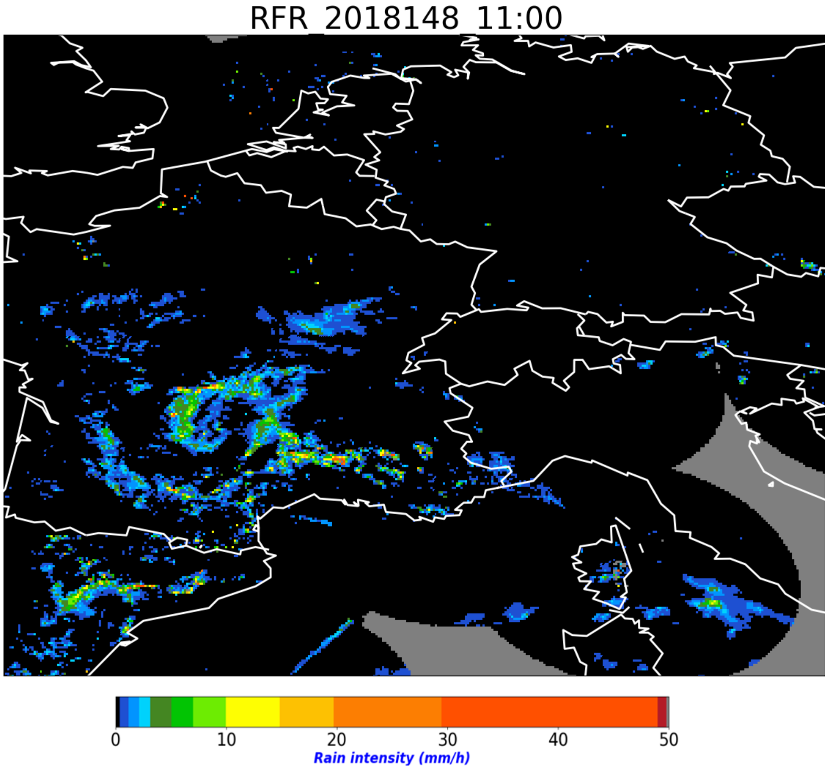

Figure 73. OPERA radar composite the 28th May 2018 at 11:00

In this event there was significant convection activity throughout all the day in France, middle Europe and also in Spain. At first sight it can be noticed a big extension of precipitation at the south of France that CRRPh detected with good detail. There were many convective nuclei that CRRPh was able to depict. This is another example of the CRRPh ability to detect not only the more developed convective nuclei but also the first stages of growing thunderstorms.

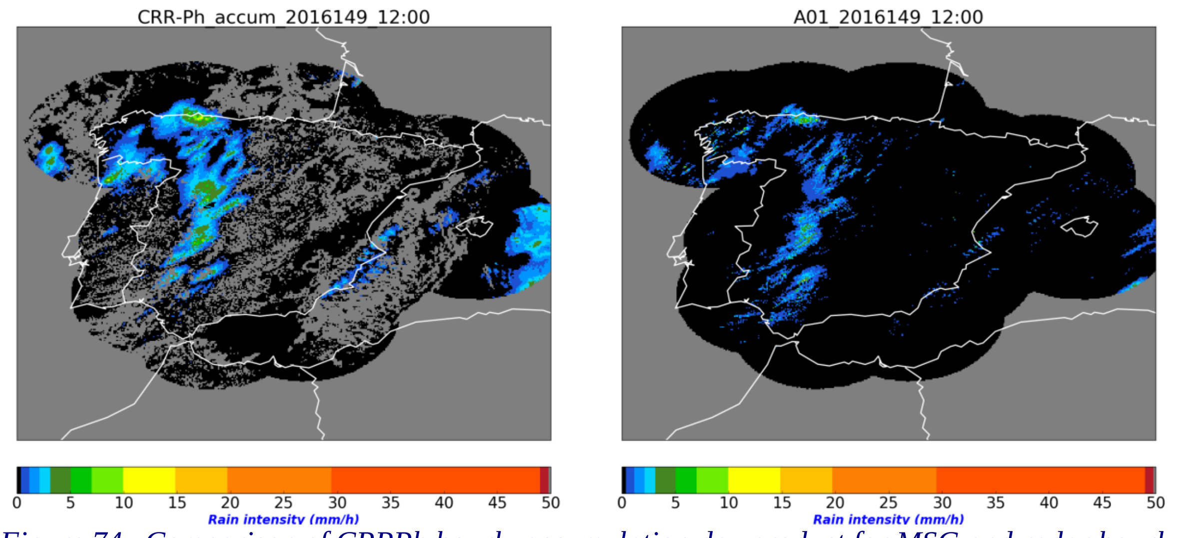

Figure 74. Comparison of CRRPh hourly accumulation day product for MSG and radar hourly accumulation on 28th May 2016 at 12:00UTC

Since the hourly accumulation is based on the CRRPh output for 4 consecutive slots, it has a similar performance compared with the instantaneous rain rates. This is an example of an hourly accumulation at day time. There is a general visual agreement in both images. Near the Balearic Islands the precipitating area is overestimated.

5.1.1.2 MTG DAY

A pair of images are shown to subjectively validate the CRRPh day product: The image on the right side corresponds with the OPERA radar rainfall rate (RFR) and the image on the left side corresponds with the rain rates of the CRRPh product.

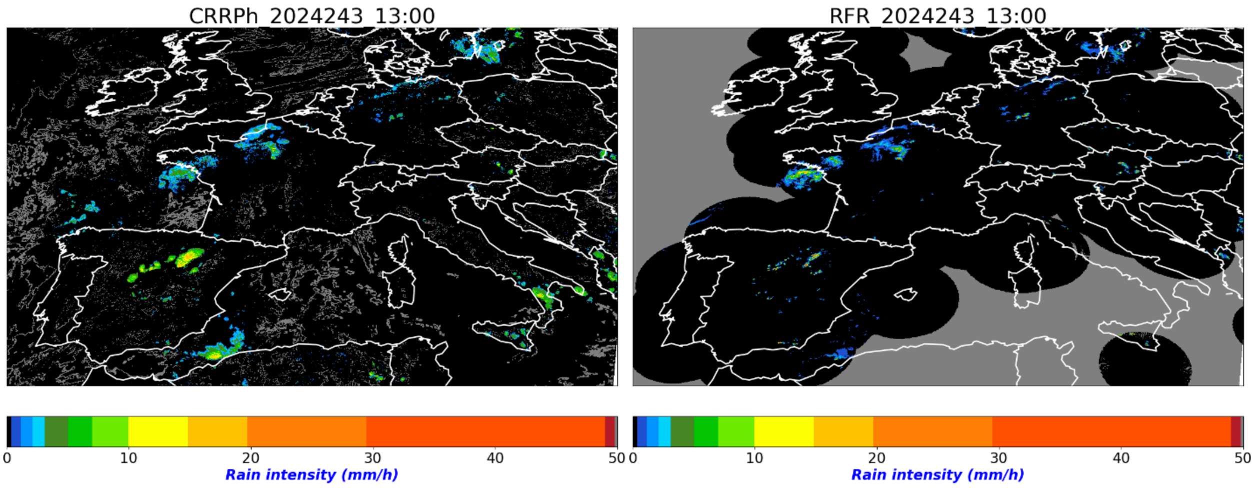

Figure 75. Comparison of CRRPh day produc for MTG and OPERA radar rainfall rate on 30th August 2024 at 13:00UTC

In this first example it can be noticed that developing precipitating convective cores are developpping in the Iberian Peninsula. CRRPh detects those convective cores, along with others in Germany.

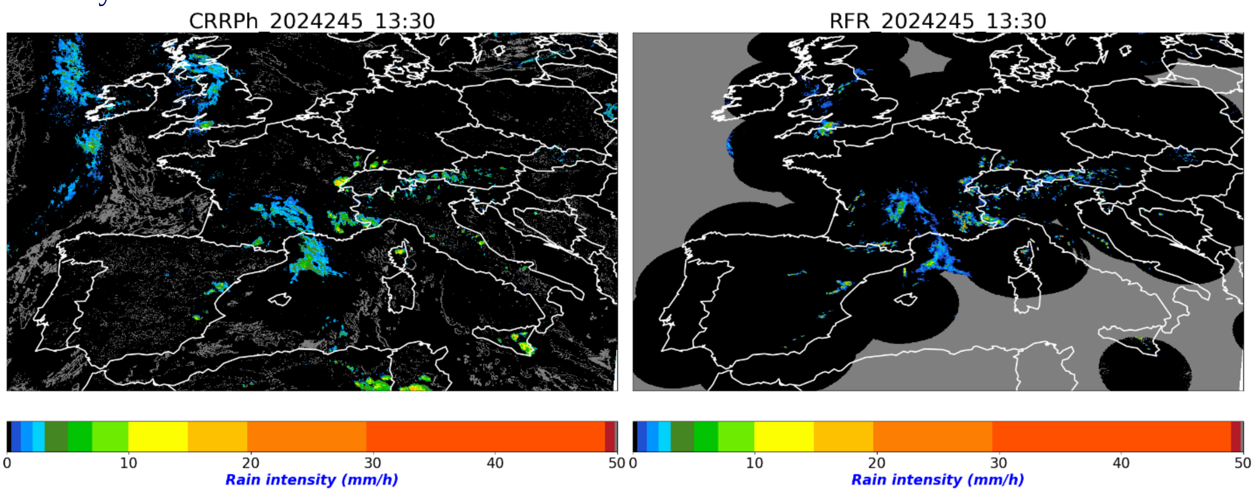

Figure 76. Comparison of CRRPh day product for MTG and radar rainfall rate on 1th September 2024 at 13:30UTC

In this other example precipitation pattern over France and Great Britain is reproduced. Convection over the Iberian Peninsula and the Alps is being triggered. CRRPh is able to detect first stages of convection, however it overestimates the rain rates associates to convection.

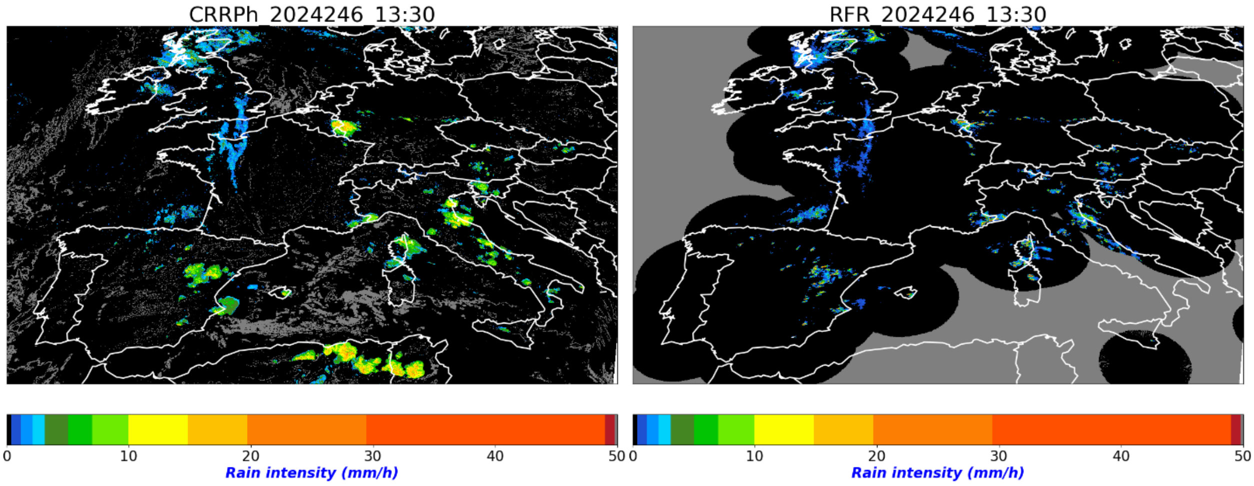

Figure 77. Comparison of CRRPh day product for MTG and OPERA radar rainfall rate on 2nd September 2024 at 13:30UTC

In Figure 32 there is a mixture of precipitation patterns. There is a front moving from Great Britain and France that also have influence in the north part of Spain. That stratiform rain is well detected by the product. Convection over Spain and Italy is also evident. CRRPh convective performance is also good in this areas. CRRPh tends to overestimate the precipitation area whenever the anvil associated Cumulonimbus is developed.

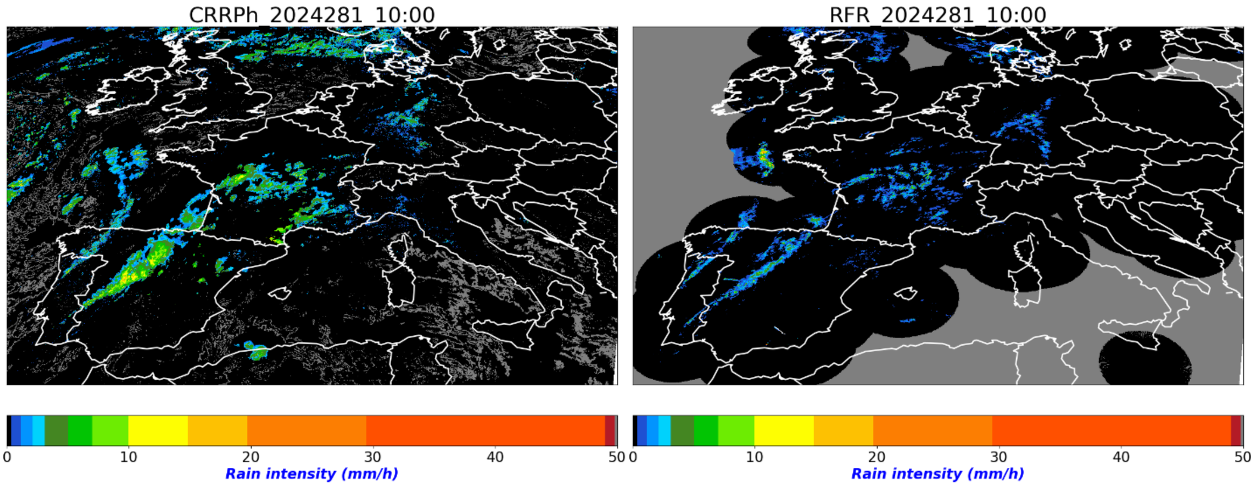

Figure 78. Comparison of CRRPh day product for MTG and OPERA radar rainfall rate on 7th October 2024 at 10:00UTC

An autumn example is shown in Figure 33. A cold front with convection associated is passing over Spain. A combination of convective and stratiform rain is shown.

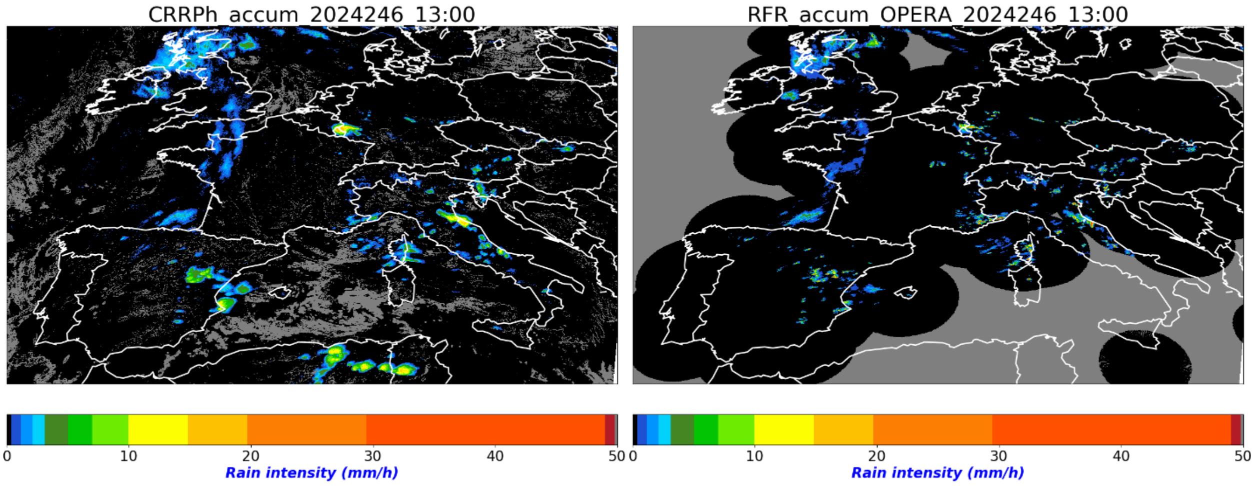

Figure 79. Comparison of CRRPh hourly accumulation day product for MTG and OPERA radar hourly accumulation on 2nd September 2024 at 13:00UTC

Since the hourly accumulation is based on the CRRPh output for 4 consecutive slots, it has a similar performance compared with the instantaneous rain rates. This is an example of an hourly accumulation at day time. There is a general visual agreement in both images.

5.1.2 NIGHT

5.1.2.1 MSG NIGHT

With the aim of visually validate the CRRPh night product two images are plotted. The one on the right side corresponds with the reflectivity of the radar (PPI image) and the image on the left side corresponds with the rain rates of the CRRPh product.

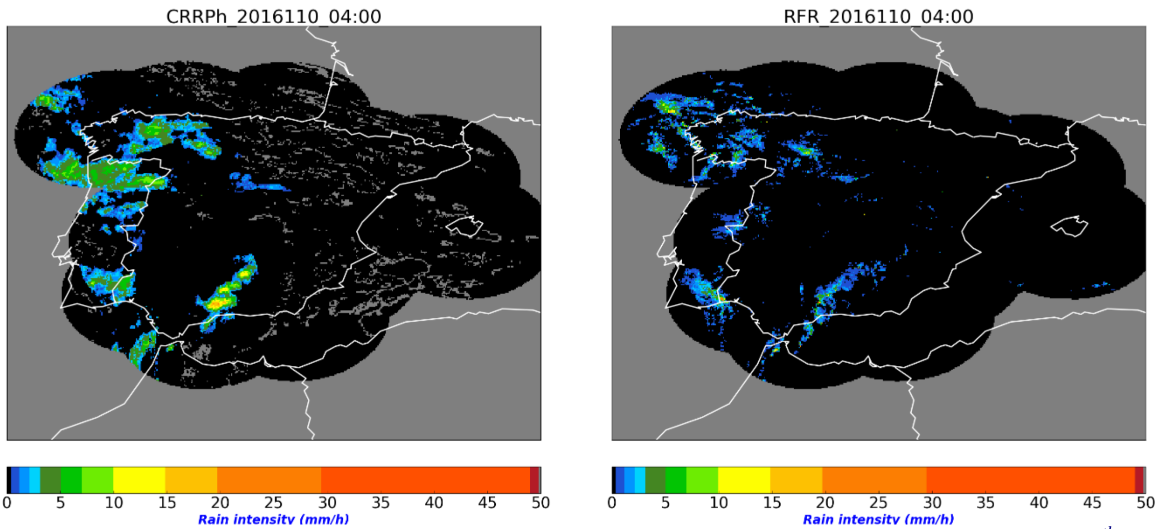

Figure 80. Comparison of CRRPh day product for MSG and the Spanish radar composite on 19th April 2016 at 04:00UTC

In this first night example it can be noticed a reasonable good correspondence between both images. Rain intensities assignation is not so good compared with day time.

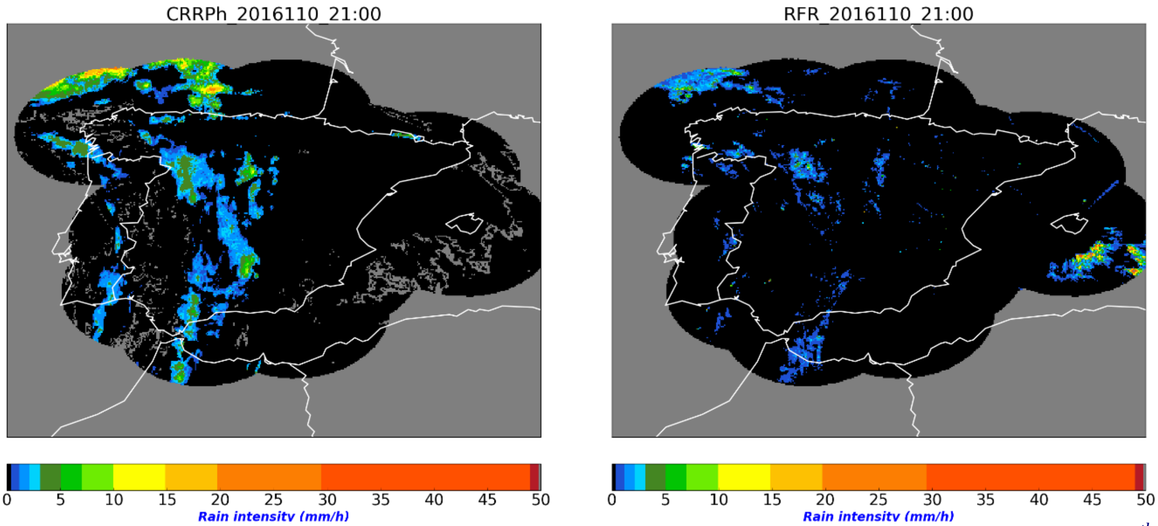

Figure 81. Comparison of CRRPh day product for MSG and the Spanish radar composite on 19th April 2016 at 21:00UTC

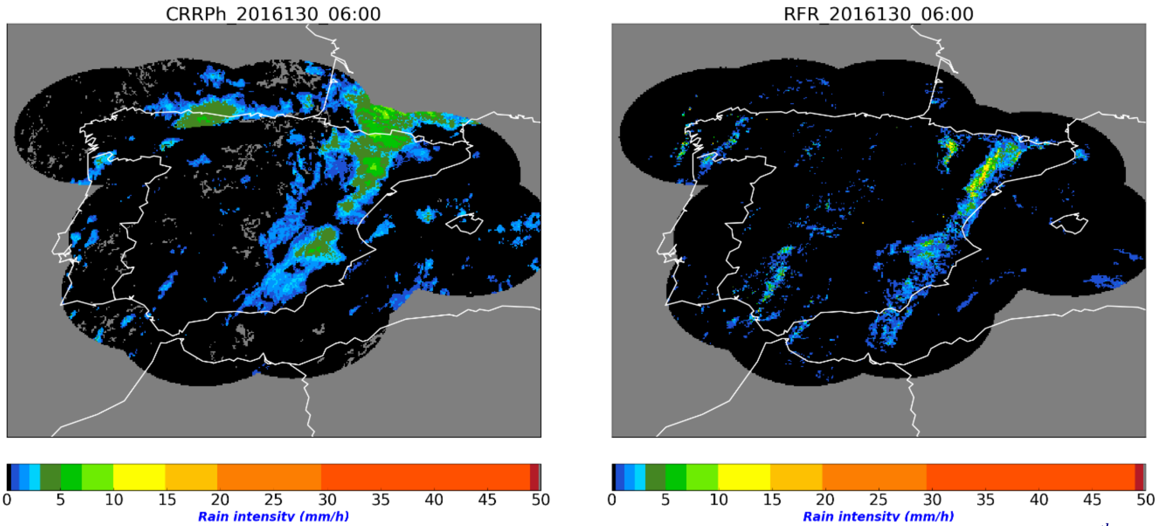

Figure 82. Comparison of CRRPh day product for MSG and the Spanish radar composite on 9th May 2016 at 06:00UTC

Figures 81 and 82 show how the product detect rainy areas at night. The extension of those areas are in general wider than at day time. The product tends to extent the night precipitation areas and introduces more False Alarm proportion. In Figure 81 there is an active precipitation area near the Balearic Islands not detected by the product. Like PCPh, the detail and accuracy of CRRPh night version reduces compared with the day algorithm because visible channels and cloud microphysics are not available. Although a simulation of these channels is done and used in the algorithm, this simulations are not perfect.

More information about CRRPh day and night algorithm can be found in the "Algorithm Theoretical Basis Document for the Precipitation Product Processors of the NWC/GEO "*[RD 4]*.

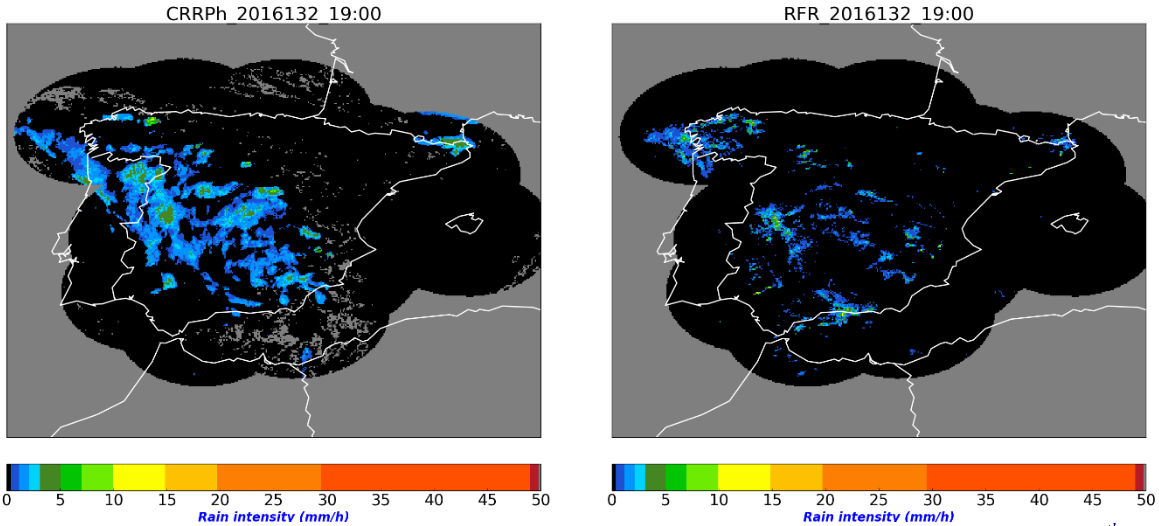

Figure 83. Comparison of CRRPh day product for MSG and the Spanish radar composite on 11th May 2016 at 19:00UTC

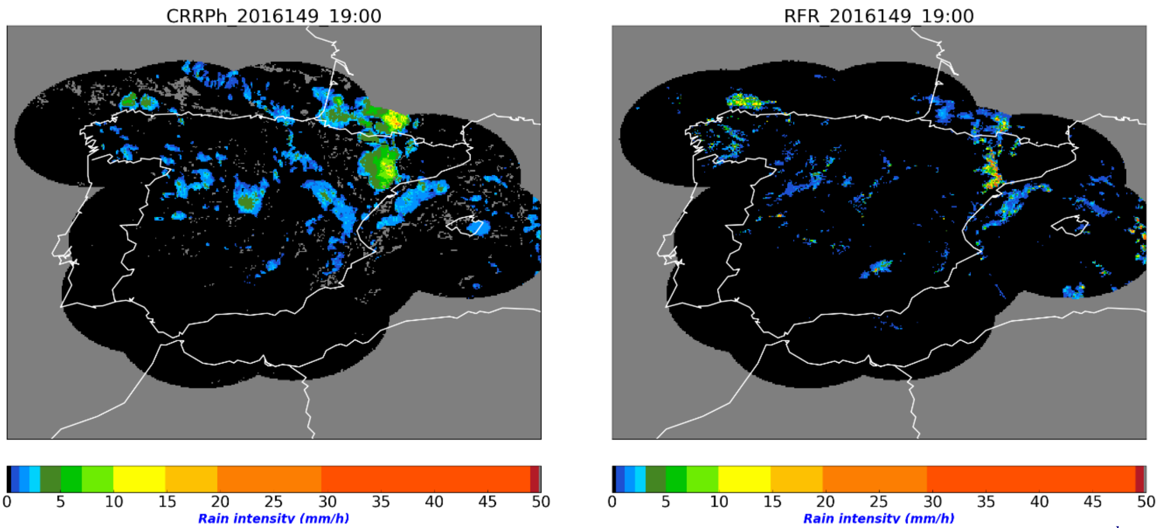

Figure 84. Comparison of CRRPh day product for MSG and the Spanish radar composite on 28th May 2016 at 19:00UTC

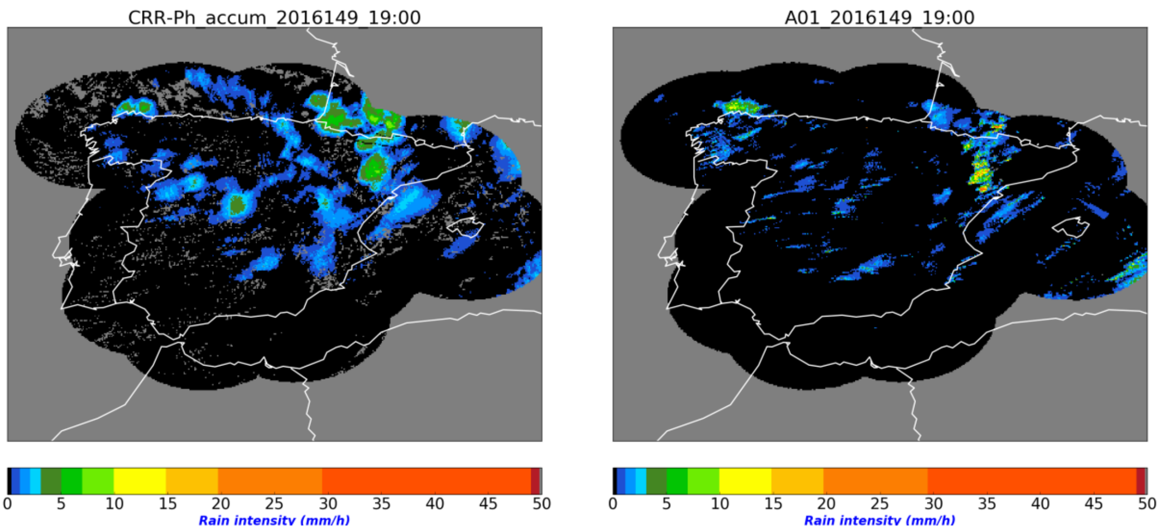

Figure 85 . Comparison of CRRPh hourly accumulation night product for MSG and radar hourly accumulation on 28th May 2016 at 19:00UTC

Figures 83 and 84 show a good performance of the night product. Not only is the product able to detect the bigger and with higher rain rates convective nuclei but also a big quantity of the smaller ones.
Figure 85 is an example of the CRRPh hourly accumulations.

5.1.2.2 MTG NIGHT

With the aim of visually validate the CRRPh night product two images are plotted. The one on the right side corresponds with the radar reflectivity of the OPERA composite and the image on the left side corresponds with the rain rates of the CRRPh product.

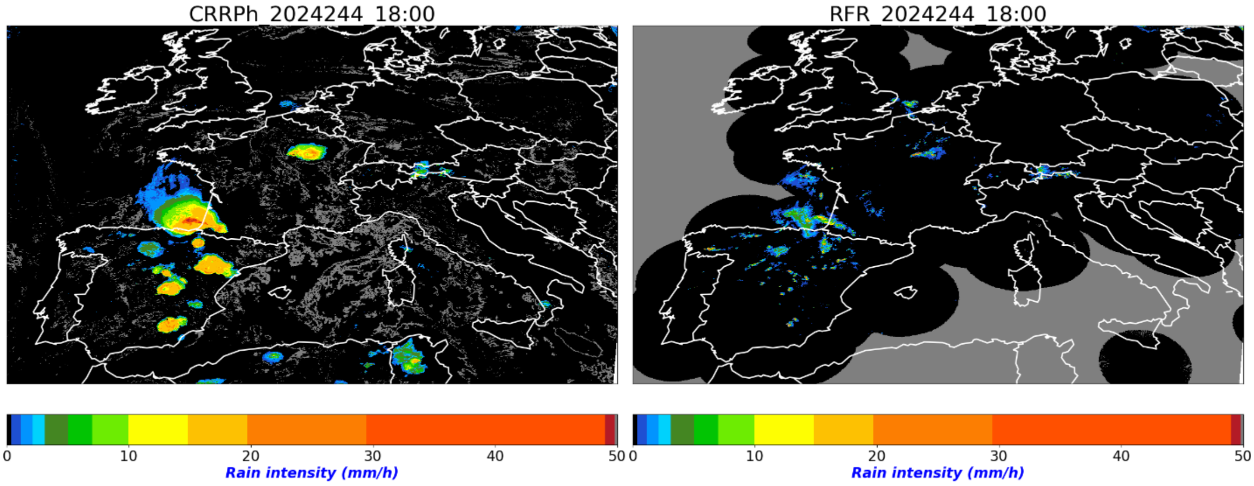

Figure 86. Comparison of CRRPh day product for MTG and the OPERA radar rain rate composite on 31th August 2024 at 18:00UTC

In this example of CRRPh night performance it can be noticed an overestimation of the precipitation area. There are many convective cells over Spain and some of them are not detetected and others are overestimated. It is at night when is more evident the overestimation of the precipitation area whenever the cirrus associated at convective clouds spreads. Rain intensities assignation is not so good compared with day time.

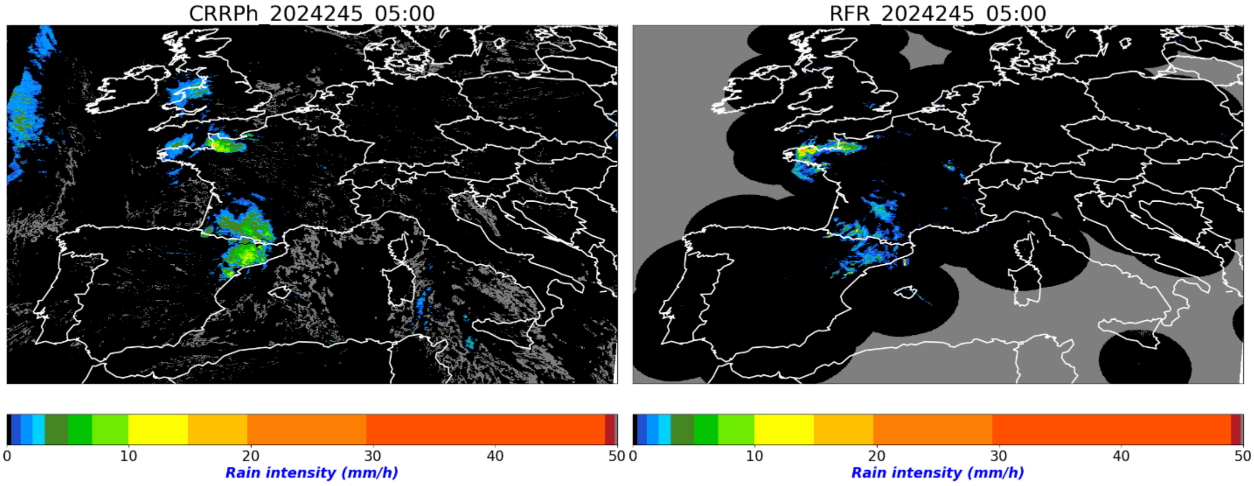

Figure 87. Comparison of CRRPh day product for MTG and the OPERA radar rain rate composite on 1th September 2024 at 05:00UTC

Figure 87 is another example of CRRPh night performance.

The extension of the precipitation areas are in general wider than at day time. The product tends to extent the night precipitation areas and introduces more False Alarm proportion. In Figure 36 there is an active precipitation area at the northest of France that hardly is detected by the product. Like PCPh, the detail and accuracy of CRRPh night version reduces compared with the day algorithm because visible channels and cloud microphysics are not available. Although a simulation of these channels is done and used in the algorithm, this simulations are not perfect.

More information about CRRPh day and night algorithm can be found in the "Algorithm Theoretical Basis Document for the Precipitation Product Processors of the NWC/GEO "*[RD 4]*.

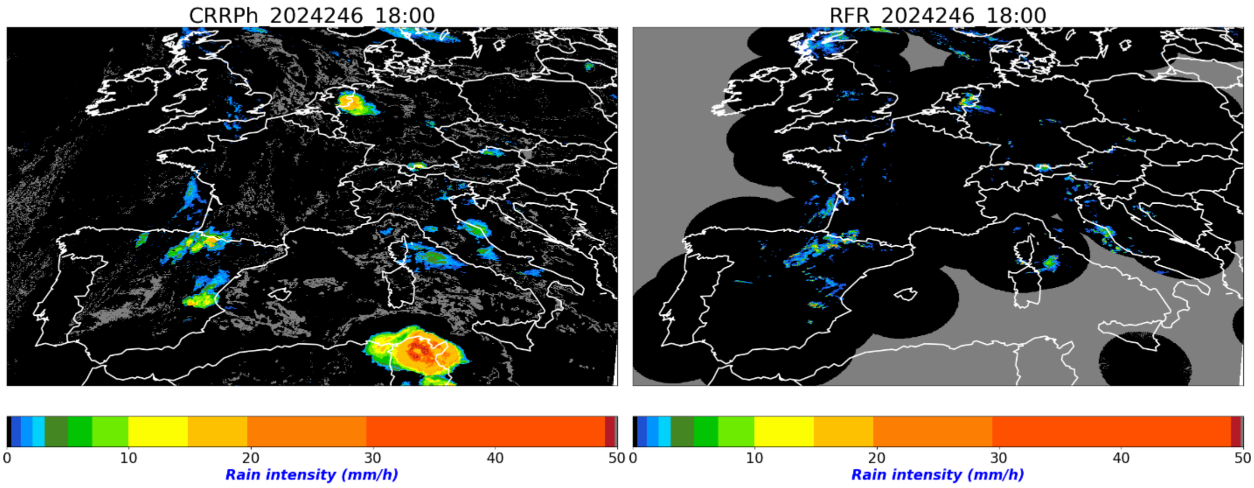

Figure 88. Comparison of CRRPh day product for MTG and the OPERA rain rate radar composite on 2th September 2024 at 18:00UTC

Good performance of CRRPh night algorithm is shown in this example. Several active convective cells are found in Spain, Italy and Germany. Strong points of the CRRPh product are shown here.

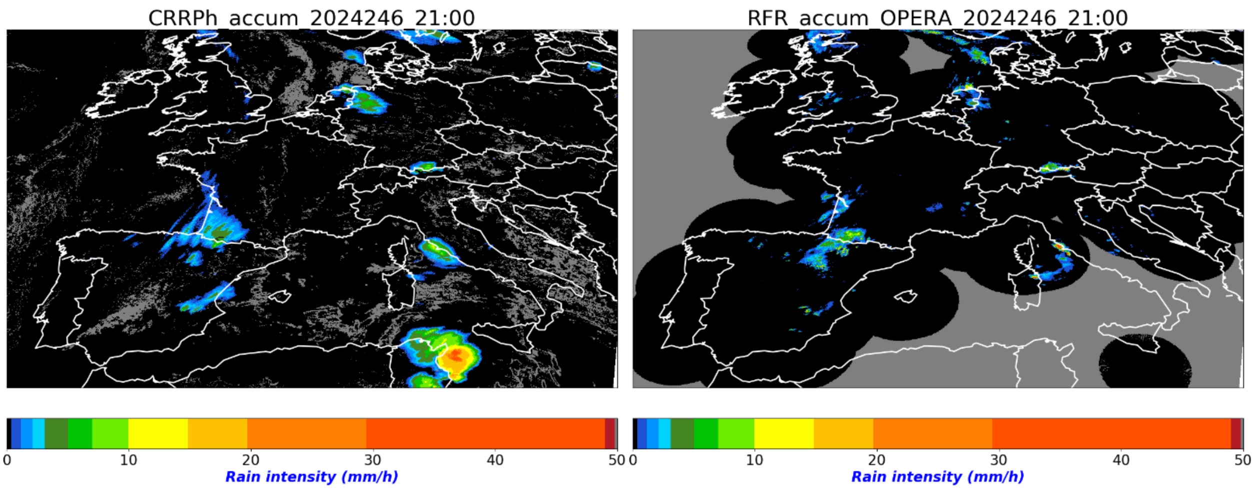

Figure 89 . Comparison of CRRPh hourly accumulation night product for MTG and OPERA radar hourly accumulation on 2th September 2024 at 21:00UTC

Figure 89 is an example of the CRRPh hourly accumulations. The same pattern that is found in the CRRPh algorithm is found in the hourly accumulations. There is a slight overestimation of the precipitation area that is traduced in FAR values.

5.2 OBJECTIVE VALIDATION FOR CONVECTIVE RAINFALL RATE FROM CLOUD PHYSICAL PROPERTIES (CRRPH)

5.2.1 Validation Procedure

Section 4.2.1 also applies to this section.

Validation procces has been done over the Iberian Peninsula for MSG and over the OPERA region for MTG.

MSG:
As far as the hourly accumulations is concerned, the validation has been done against the OPERA radar hourly accumulations. In this case a day-night distinction has also ben taken into account, validating only pixels of the same category.

Despite the fact the product has been calibrated in the Iberian Península only in convective events, it has also been been generated in non-convective situations. However, CRRPh requirements included in the "NWCSAF Product Requirements Document" [AD.4] refer exclusively to convective areas, since the main goal for this product is to detect convection.

Operational Programme for the exchange of weather radar information (OPERA) provides RFR in the lowest radar level and maximum column dBZ parameters. (It does not include Echotop).
As for validating in OPERA region for MSG, in this validation report a threshold of dBz = 40 in the vertical column was chosen. Additionally, a threshold of RFR = 3 mm/h was used to ensure that moderate rainfall was present on surface level in order to compare with the satellite derived surface precipitation. When a pixel was classified as convective, a box of 25x25 pixels centred in that pixel was chosen

MTG:
Convective areas have been built up selecting 25x25 boxes around those pixels that met two criteria at the same time: column maximum reflectivity > 40 dBz and surface rain intensity > 10 mm/h.

5.2.2 Instantaneous Rain Rates

5.2.2.1 CATEGORICAL VALIDATION

In order to compute the categorical scores, two thresholds have been established, one for the CRRPh intensity and another one for the rainy pixels of the radar.
The CRRPh intensity threshold for an instantaneous rain rate is fixed to 0.2 mm/h or higher.
The rainy pixels from the radar are fixed to at least 0.2 mm/h.

.

5.2.2.1.1 DAY

MSG - Convective areas over the Iberian Península

N	POD (%)	FAR (%)	CSI (%)	PC (%)
1386323	78	27	60	77

Table 27. Categorical scores for CRRPh intensity day algorithm in convective areas for MSG

MSG - All Areas_over the Iberian Península

N	POD (%)	FAR (%)	CSI (%)	PC (%)
4208125	71	47	43	88

Table 28. Categorical scores for CRRPh intensity day algorithm in all areas for MSG

MSG - Convective areas over OPERA_region (Europe)

N	POD (%)	FAR (%)	CSI (%)	PC (%)
3600322	65	25	53	76

Table 29. Categorical scores for CRRPh day algorithm in convective areas over OPERA region for MSG

MTG - Convective areas over OPERA_region (Europe)

N	POD (%)	FAR (%)	CSI (%)	PC (%)
13931055	76	19	65	81

Table 30. Categorical scores for CRRPh day algorithm in convective areas over OPERA region for MTG

5.2.2.1.2 NIGHT

MSG - Convective areas over the Iberian Península

N	POD (%)	FAR (%)	CSI (%)	PC (%)
4051369	71	34	52	67

Table 31. Categorical scores for CRRPh intensity night algorithm in convective areas for MSG

MSG - All Areas over the Iberian Península

N	POD (%)	FAR (%)	CSI (%)	PC (%)
15403702	56	66	27	85

Table 32. Categorical scores for CRRPh intensity night algorithm in all areas for MSG

MSG - Convective areas over OPERA region (Europe)

N	POD (%)	FAR (%)	CSI (%)	PC (%)
7264709	50	34	39	66

Table 33. Categorical scores for CRRPh night algorithm in convective areas over OPERA region for MSG.

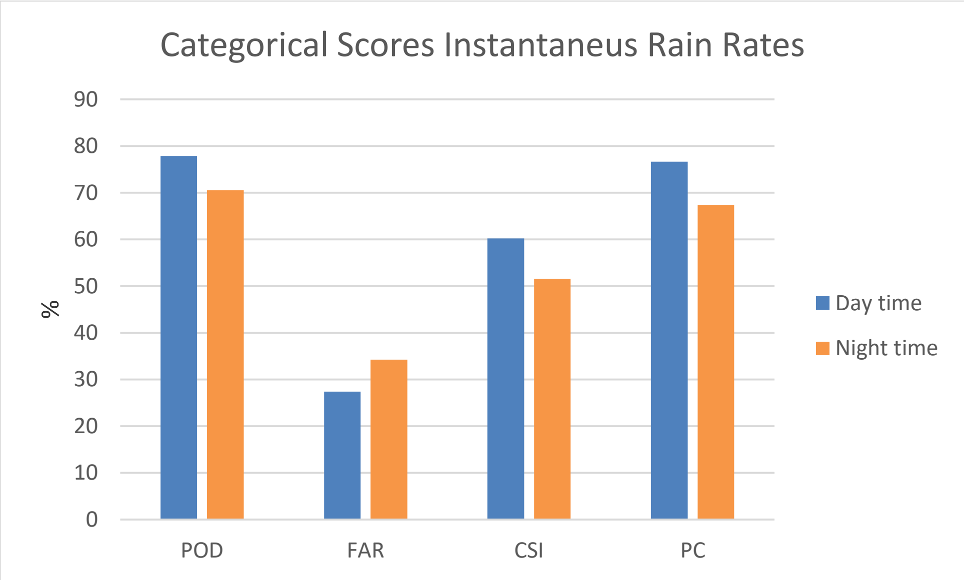

Figure 90. Categorical scores for CRRPh instantaneous rain rates in convective areas over the Iberian Península for MSG.

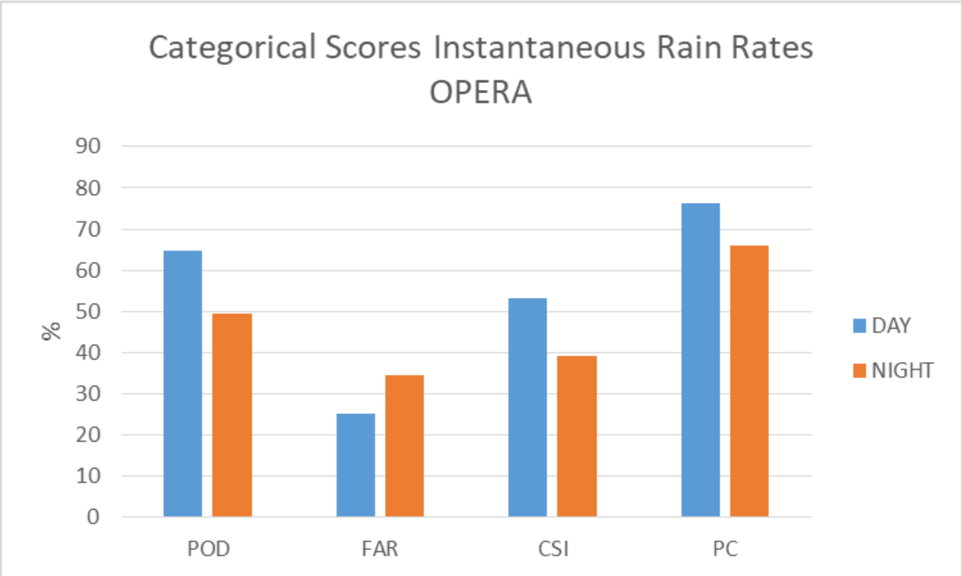

Figure 91. Categorical scores for CRRPh instantaneous rain rates in convective areas over OPERA region for MSG

MTG - Convective areas over OPERA region (Europe)

N	POD (%)	FAR (%)	CSI (%)	PC (%)
23329017	59	21	51	70

Table 34. Categorical scores for CRRPh night algorithm in convective areas over OPERA region for MTG.

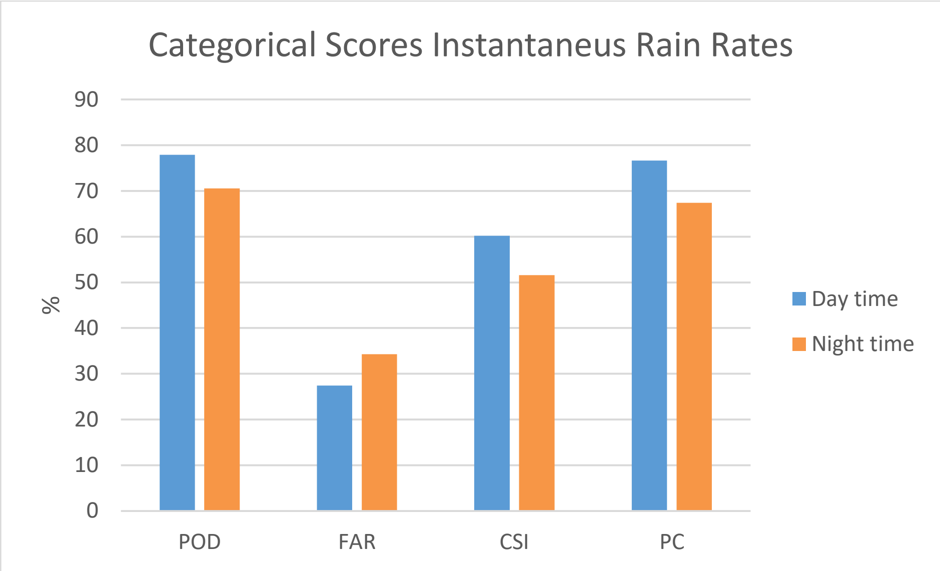

Figure 92. Categorical scores for CRRPh instantaneous rain rates in convective areas over OPERA region for MTG

5.2.3 Hourly Accumulations

With the aim of computing the categorical scores for the hourly accumulations, two thresholds were established: one for the CRRPh and another one for the rainy pixels of the radar.
The CRRPh threshold is fixed at 0.2 mm/h.
The threshold for the rainy pixels from the radar is fixed at 0.2 mm/h.

Before calculating the POD and FAR scores, correct negatives (see ANNEX 1: VERIFICATION METRIC section) were filtered because they represent a large number of the data population, they reduce the computing speed and they are not involved in the categorical scores formula of the POD and the FAR.

MSG DAY

N	POD (%)	FAR (%)	CSI (%)	PC (%)
265782	83	30	61	76

Table 35. Categorical scores for CRRPh hourly accumulation day algorithm in convective areas for MSG

N	POD (%)	FAR (%)	CSI (%)	PC (%)
2198129	77	52	42	85

Table 36. Categorical scores for CRRPh hourly accumulation day algorithm in all areas for MSG

MTG DAY

N	POD (%)	FAR (%)	CSI (%)	PC (%)
4329882	80	21	66	67

Table 37. Categorical scores for CRRPh hourly accumulation day algorithm in convective areas for MTG

MSG NIGHT

N	POD (%)	FAR (%)	CSI (%)	PC (%)
885197	75	36	52	66

Table 38. Categorical scores for CRRPh hourly accumulation night algorithm in convective areas for MSG

N	POD (%)	FAR (%)	CSI (%)	PC (%)
8815013	61	69	26	82

Table 39. Categorical scores for CRRPh hourly accumulation night algorithm in all areas for MSG

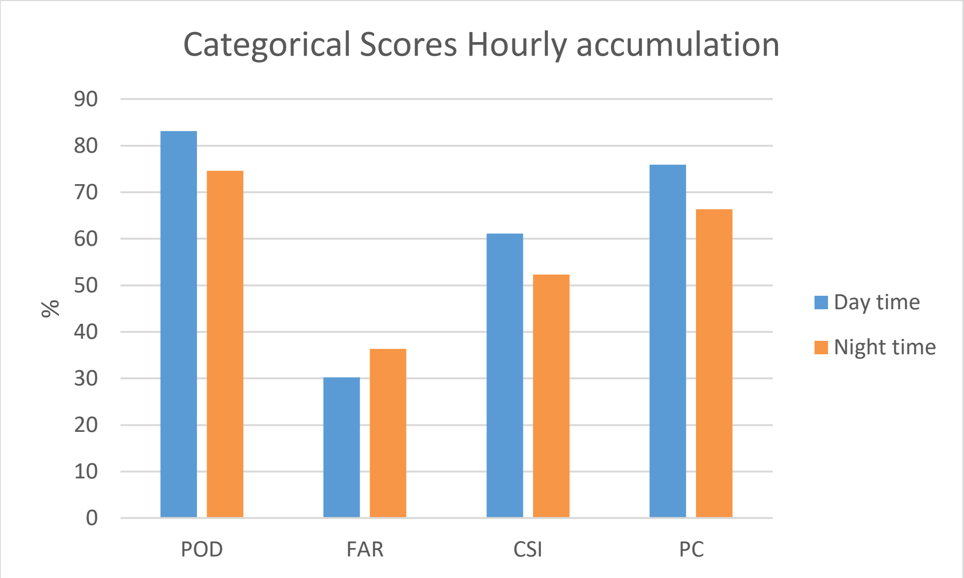

Figure 93. Categorical scores for CRRPh hourly accumulations in convective areas for MSG

MTG NIGHT

N	POD (%)	FAR (%)	CSI (%)	PC (%)
7730376	66	26	53	54

Table 40. Categorical scores for CRRPh hourly accumulation night algorithm in convective areas for MTG.

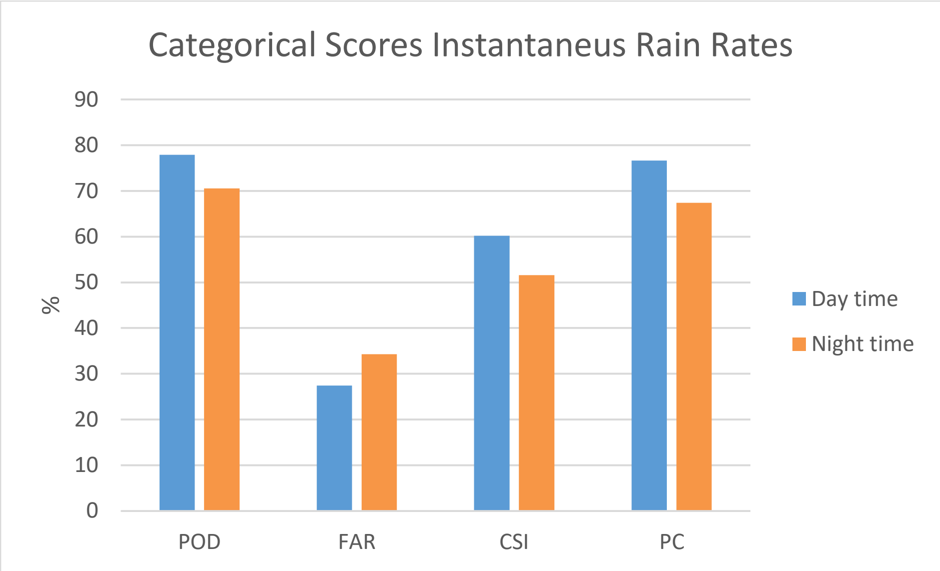

Figure 94. Categorical scores for CRRPh hourly accumulations in convective areas for MTG

Hourly accumulation results shown in Figure 94 are consistent with those thrown by instantaneous rain rates. PC values are lower than instantaneous ones because of the exclusion of correct negatives.

Higher POD, CSI and PC and lower FAR of day time accumulations compared with night values prove a better performance of day CRRPh algorithm.

5.2.4 Conclusions

Validation results for the CRRPh are going to be compared with those requirements included in the "NWCSAF Product Requirements Document" [AD.4] for both the CRRPh intensity and the CRRPh hourly accumulation. The commitment for the product is to reach the requirement in the convective areas. An additional table with the performance in OPERA (Europe) region is included.

5.2.4.1 MSG

CRRPh Algorithm	Threshold Accuracy POD (%)	Target Accuracy POD (%)	Optimal Accuracy POD (%)	POD (%)
Day time	>50	>75	>90	78
Night time	>35	>47	>80	71

Table 41. Comparison of CRRPh values against POD scores defined in the NWCSAF Product Requirement table for MSG over the Iberian Peninsula

CRRPh Algorithm	Threshold Accuracy FAR (%)	Target Accuracy FAR (%)	Optimal Accuracy FAR (%)	FAR (%)
Day time	<65	<50	<45	27
Night time	<70	<60	<50	34

Table 42. Comparison of CRRPh values against FAR scores defined in the NWCSAF Product Requirement table for MSG over the Iberian Peninsula

CRRPh Hourly accumulations	Threshold Accuracy POD (%)	**Target Accuracy POD (%)**	Optimal Accuracy POD (%)	POD (%)
Day time	>60	>80	>95	83
Night time	>37	>50	>85	75

Table 43. Comparison of CRRPh hourly accumulations FAR scores defined in the NWCSAF Product Requirement table for MSG over the Iberian Peninsula

CRRPh Hourly accumulations	Threshold Accuracy FAR (%)	**Target Accuracy FAR (%)**	Optimal Accuracy FAR (%)	FAR (%)
Day time	<60	<55	<45	30
Night time	<70	<60	<50	36

Table 44. Comparison of CRRPh hourly accumulations FAR scores defined in the NWCSAF Product Requirement table for MSG over the Iberian Peninsula

CRRPh Algorithm	Threshold Accuracy POD (%)	**Target Accuracy POD (%)**	Optimal Accuracy POD (%)	POD (%)
Day time	>50	>75	>90	65
Night time	>35	>47	>80	50

Table 45. Comparison of CRRPh values against POD scores defined in the NWCSAF Product Requirement table over OPERA region for MSG

CRRPh Algorithm	Threshold Accuracy FAR (%)	**Target Accuracy FAR (%)**	Optimal Accuracy FAR (%)	FAR (%)
Day time	<65	<50	<45	25
Night time	<70	<60	<50	34

Table 46. Comparison of CRRPh values against FAR scores defined in the NWCSAF Product Requirement table over OPERA region for MSG

With respects to the instantaneous rain rates, POD and FAR scores are better in convective areas than in all areas and results are also better during day time than during night time.

Despite a general good behaviour of the CRRPh day product in convective areas there isn't a perfect spatial matching between radar pixels and the CRRPh product. A spatial displacement between radar pixels and CRRPh pixels penalizes the product. It is known that in an objective validation made pixel by pixel, collocation problems between radar and satellite makes the double penalty problem visible.

According to the "NWCSAF Product Requirements Document" [AD 4], POD and FAR scores corresponding to the CRRPh instantaneous rate during day time and also at night time on convective areas are achieved .

Regarding the CRRPh hourly accumulation, it inherits the same strong and weak points from its precursor CRRPh instantaneous rain rate. Better results are obtained at day time than at night time and also are better in convective areas compared with all areas.

POD and FAR requirements are both fulfilled in convective areas for day and night time cases in the Iberian Peninsula. Good results are also obtained if the validation is extended to Europe (OPERA region).

Regarding the visual validation, it has visually checked that the orography may produce unrealistic shapes. These artefacts produced by mountains are steady and it appears in the same places so it can be easily detected. The stability correction finally depends on the NWP model. Hence, if the NWP model fails at detecting stable regions, black holes with unrealistic shapes inside precipitating areas may appear. The stability correction seems to be beneficial on average for the whole year and Europe extension.

According to the objective and subjective validations this product can be stated as operational.

5.2.4.2 MTG

CRRPh Algorithm	Threshold Accuracy POD (%)	**Target Accuracy POD (%)**	Optimal Accuracy POD (%)	POD (%)
Day time	>50	>75	>90	76
Night time	>35	>47	>80	59

Table 47. Comparison of CRRPh values against POD scores defined in the NWCSAF Product Requirement table for MTG

CRRPh Algorithm	Threshold Accuracy FAR (%)	**Target Accuracy FAR (%)**	Optimal Accuracy FAR (%)	FAR (%)
Day time	<65	<50	<45	19
Night time	<70	<60	<50	21

Table 48. Comparison of CRRPh values against FAR scores defined in the NWCSAF Product Requirement table for MTG

CRRPh Hourly accumulations	Threshold Accuracy POD (%)	**Target Accuracy POD (%)**	Optimal Accuracy POD (%)	POD (%)
Day time	>60	>80	>95	80
Night time	>37	>50	>85	66

Table 49. Comparison of CRRPh hourly accumulations FAR scores defined in the NWCSAF Product Requirement table for MTG

CRRPh Hourly accumulations	Threshold Accuracy FAR (%)	**Target Accuracy FAR (%)**	Optimal Accuracy FAR (%)	FAR (%)
Day time	<60	<55	<45	21
Night time	<70	<60	<50	26

Table 50. Comparison of CRRPh hourly accumulations FAR scores defined in the NWCSAF Product Requirement table for MTG PProduct Requirement table

Despite a general good behaviour of the CRRPh day product in convective areas there isn’t a perfect spatial matching between radar pixels and the CRRPh product. A spatial displacement between radar pixels and CRRPh pixels penalizes the product. It is known that in an objective validation made pixel by pixel, collocation problems between radar and satellite makes the double penalty problem visible.

According to the “NWCSAF Product Requirements Document” [AD 4], POD and FAR scores corresponding to the CRRPh instantaneous rate during day time and also at night time on convective areas meet “Target Accuracy” requirements .

Regarding the CRRPh hourly accumulation, it inherits the same strong and weak points from its precursor CRRPh instantaneous rain rate. Better results are obtained at day time than at night time.

POD and FAR requirements are both fulfilled in convective areas for day and night time cases over the OPERA region.

Despite the fact in the visual validation there are not shown artefacts, it is known that the orography may produce unrealistic shapes. These artefacts produced by mountains are steady and it appears in the same places so it can be easily detected and are due to the stability correction. The stability correction finally depends on the NWP model. Hence, if the NWP model fails at detecting stable regions, black holes with unrealistic shapes inside precipitating areas may appear. The stability correction seems to be beneficial on average for the whole year and Europe extension and it applies only at night time.

According to the objective and subjective validations this product can be stated operational.

Comparing CRRPh MSG and MTG results, there is a better performance of MTG version compared with MSG. Higher POD and lower FAR for day and night time are found in MTG version.

6. HIMAWARI DATA

Precipitation products have been computed in ASIA region for Himawari-8 satellite. In order to have a visual validation, some radar images have been depicted. The Japanese radar reflectivity composite imagery have been downloaded from the following website: " http://agora.ex.nii.ac.jp/digital-typhoon/archive/radar/intensity/". This website was accessed for the last time the 22th December 2021.

Two days have been represented: the 28th and 30th of August 2021 at 0Z UTC (09 Japan Standard Time). Despite the fact the whole image have been created with the intention of having day and night time algorithm at the same time in the same frame. It has been zoomed in Japan region where the radar images were available.

The following colour palette applies to the Japan Radar Echo images:

Radar Echo Intensity (Unit: Milimeters)

-0	0-1	1-2	2-4	4-8	8-12	12-16	16-24	24-32	32-40	40-48	48-56	56-64	64-80	80-

6.1 30TH AUGUST 2018

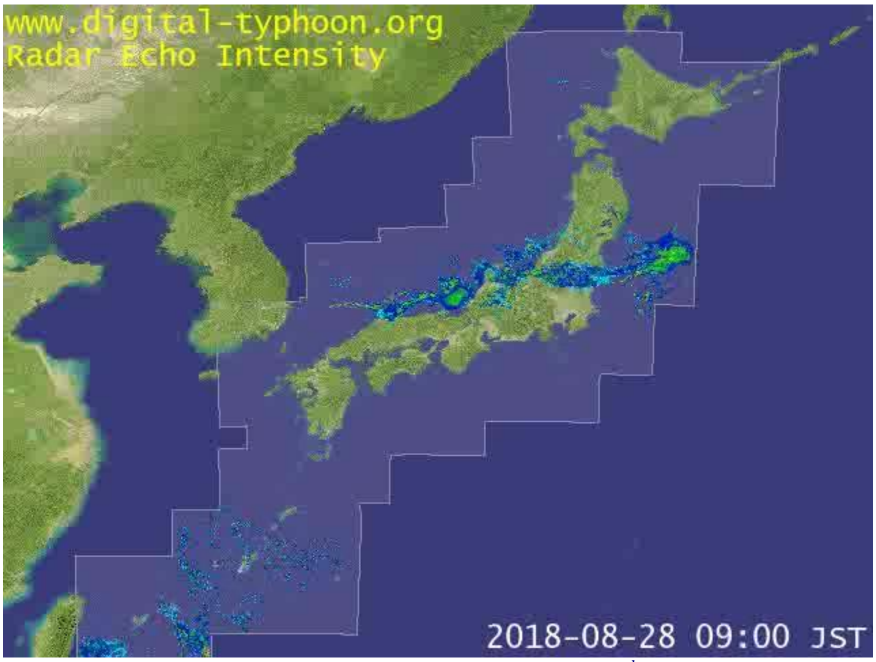

Figure 95. Composite weather radar echoes (mm/h) on 28th August 2018 at 00:00 UTC

According to Figure 57, the wider precipitating area was located in the centre of Japan. In that area there was convective nuclei which were detected by the CRRPh (see Figure 58). At the southwest Japan islands there was another precipitating area that was also depicted. Regarding PCPh (see Figure 59), all those areas were painted with very high probability of rain.

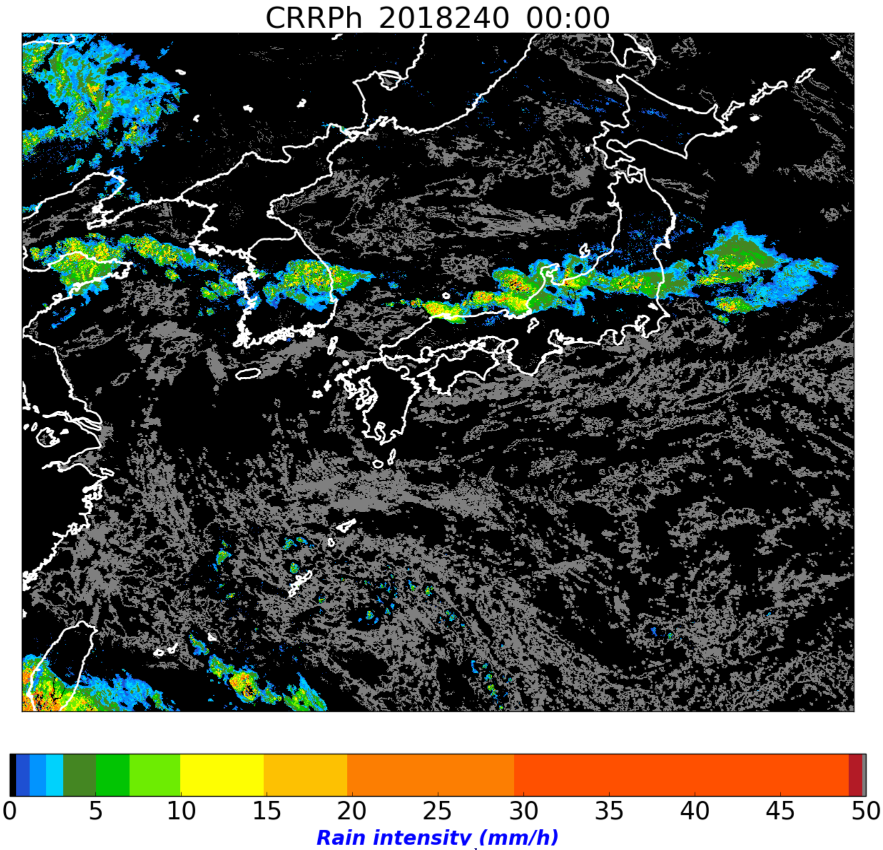

Figure 96.CRRPh product on 28th August 2018 at 00:00 UTC

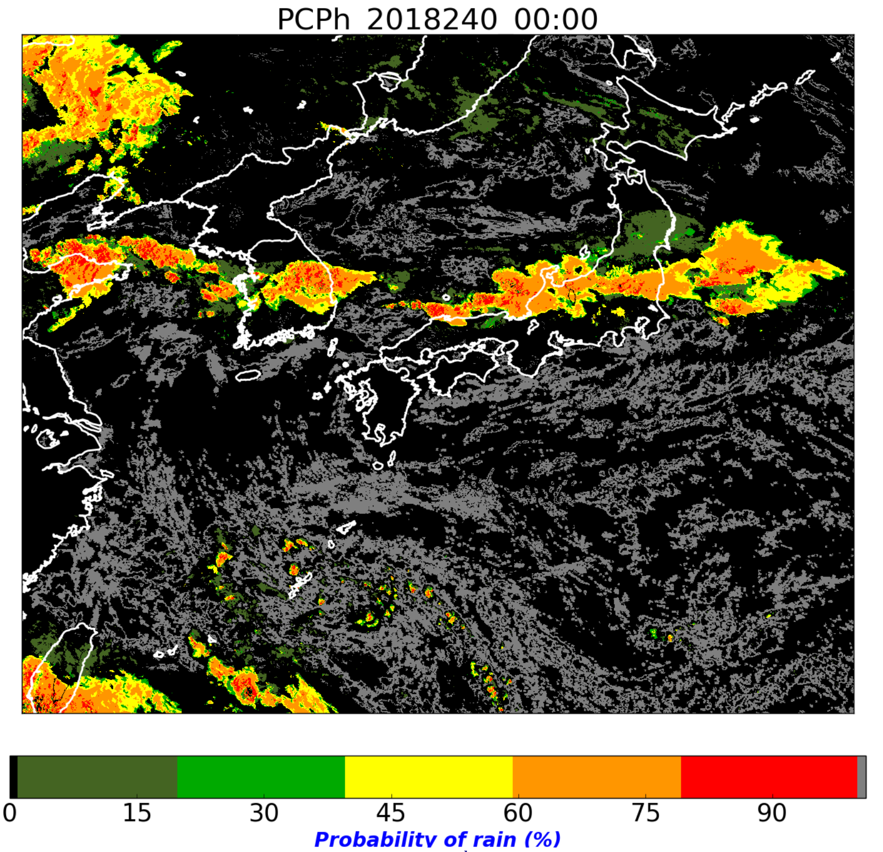

Figure 97. PCPh product on 28th August 2018 at 00:00 UTC

6.2 30TH AUGUST 2018

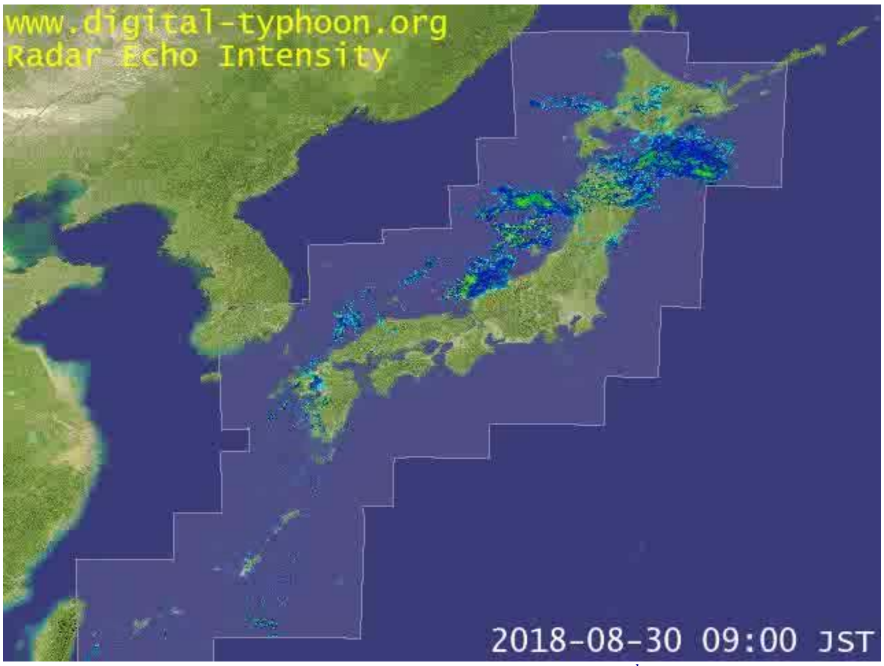

Figure 98. Composite weather radar echoes (mm/h) on 30th August 2018 at 00:00 UTC

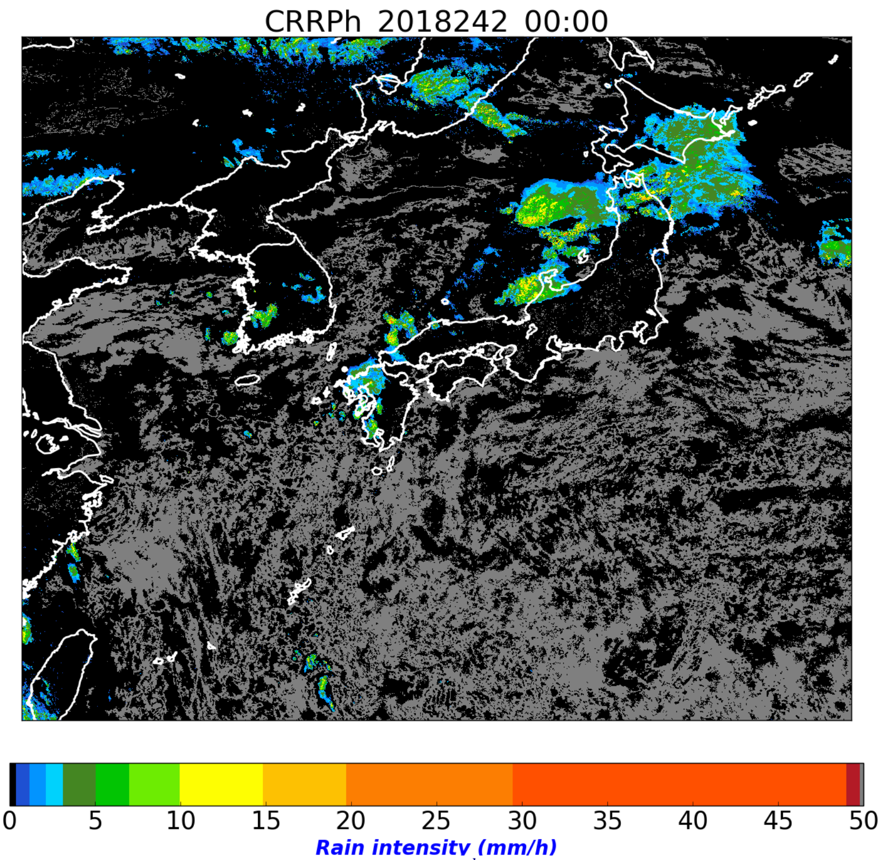

Figure 99.CRRPh product on 30th August 2018 at 00:00 UTC

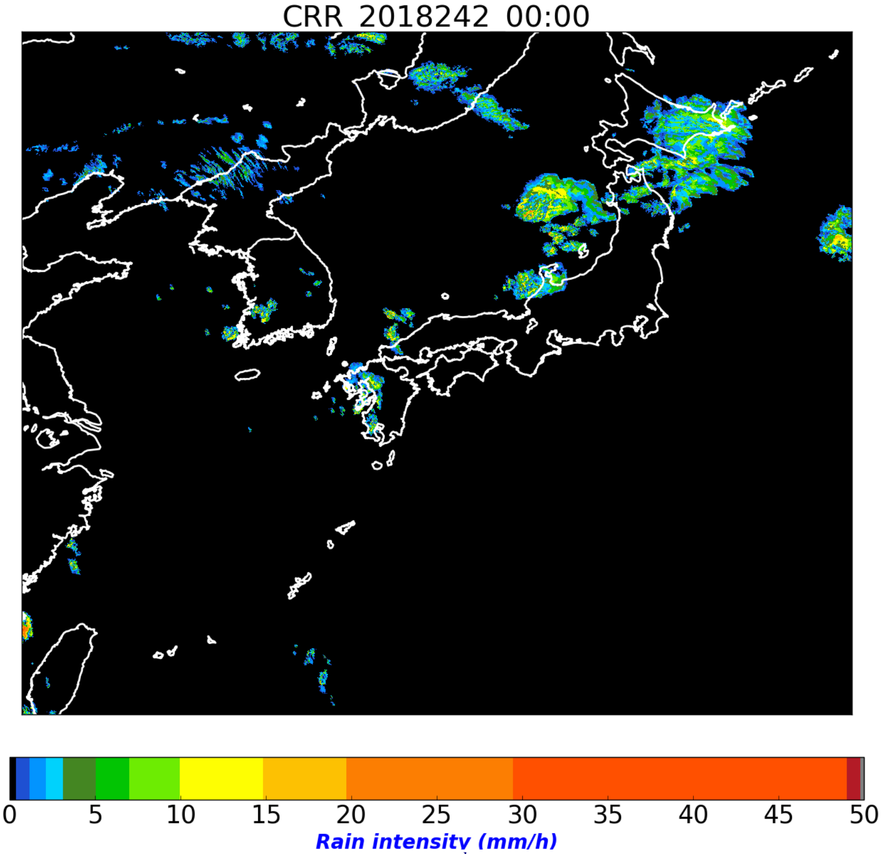

Figure 100.CRR product on 30th August 2018 at 00:00 UTC

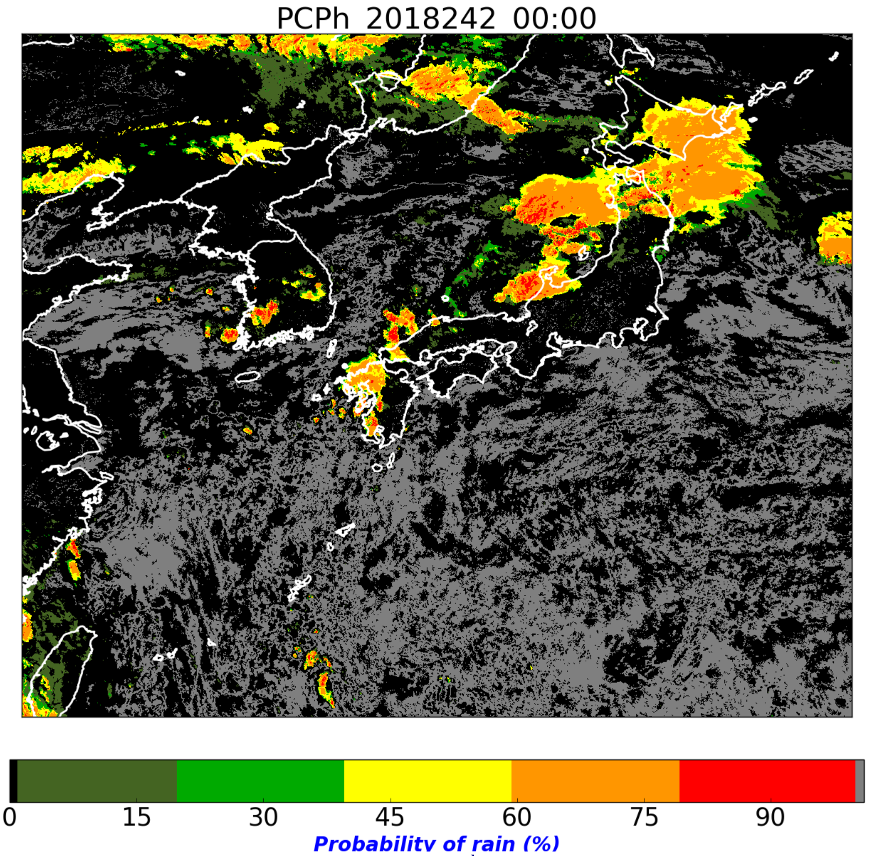

Figure 101.PCPh product on 30th August 2018 at 00:00 UTC

In this another event, there are several convective nuclei coming to southwest to the northeast of Japan island. This time an example of CRR is been introduced. Both CRRPh and CRR detect the same precipitating areas. However, it seems to have more detail the CRRPh version. PCPh reproduces the precipitating areas with high values of probability of rain.

7. GOES-16 DATA

CRR , PCPh and CRRPh have been computed over North America. A composite imagery of radar data have been downloaded from the following website https://www.ncei.noaa.gov/maps/radar/.
A visual validation between the precipitating products and the radar data (in dBz) have been done. GOES-16 satellite data, NWP models, CMIC and Cloud products have been necessary to generate the precipitating products.

Three days have been selected to validate the precipitating products: 7th July 2019 for checking day time algorithm and the 7th and 8th of May 2019 to test the night time performance.

The following colour palette applies to the United States of America Radar mosaic (dBz)

7.1 7TH JULY 2019

Figure 102. USA Radar mosaic (dBz) on 7th July 2019 at 20:40 UTC

According to Figure 64, on this first date, there were many convective cells all over the country. The more developed ones were located on the east and little growing thunderstorms can be found on the west. PCPh on Figure 65 represented well these precipitating areas, giving higher probability of rain to the ones on the east where were placed the higher rain rates.
Both CRR (Figure 67) and CRRPh (Figure 66) detected many of the convective nuclei on the west with similar rain intensity. However, when it comes to the little cells on the east part of the country, it seems the CRRPh detect a little bit more and with higher intensity.

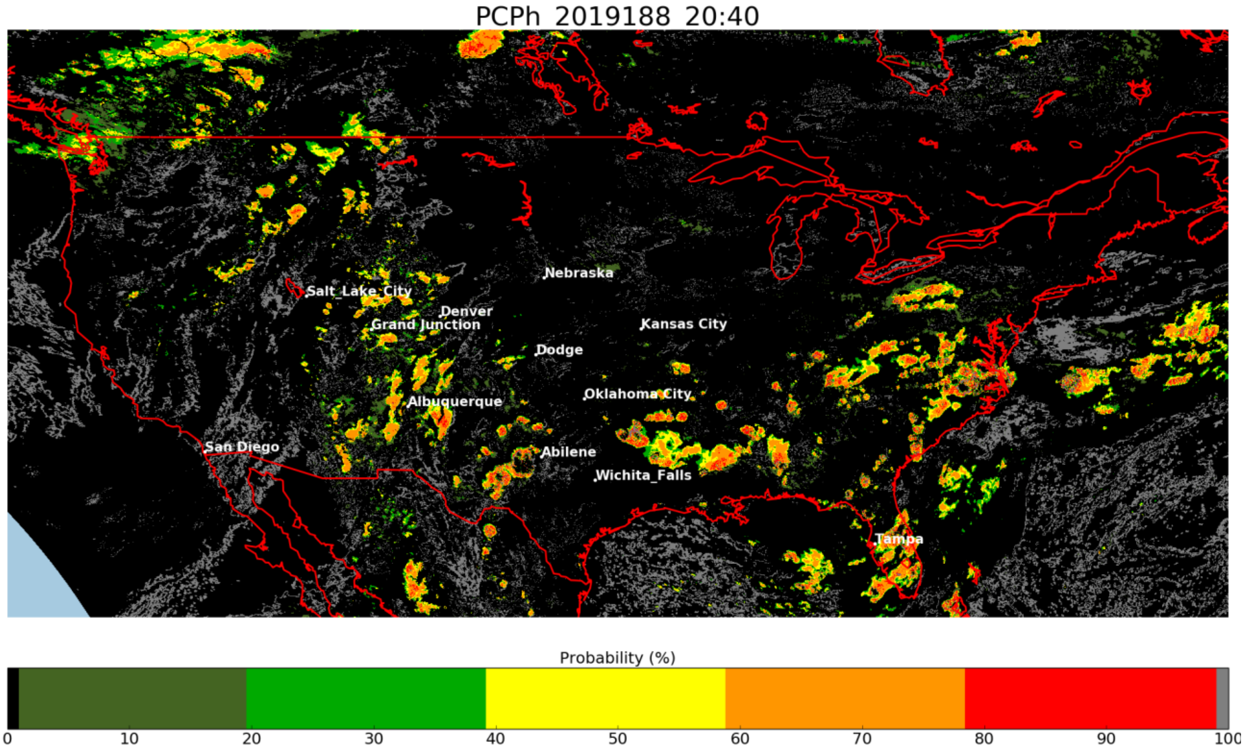

Figure 103. PCPh product on 7th July 2019 at 20:40 UTC over USA.

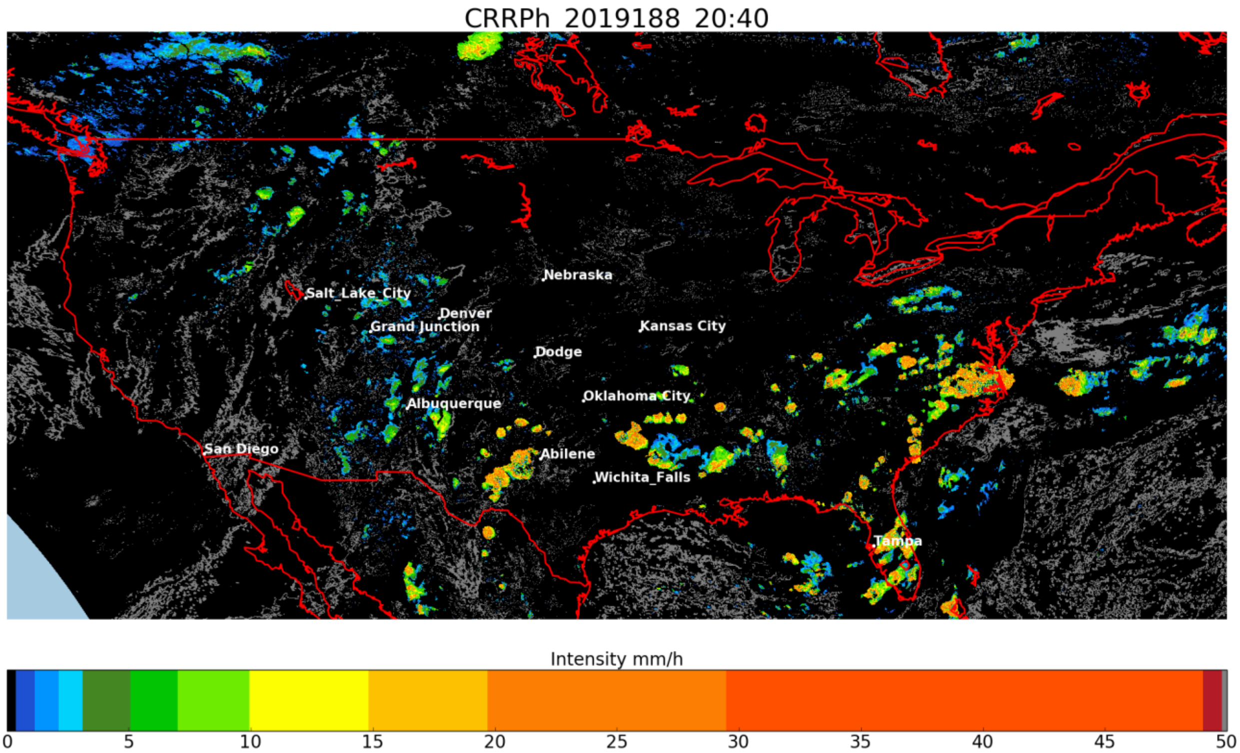

Figure 104. CRRPh product on 7th July 2019 at 20:40 UTC over USA.

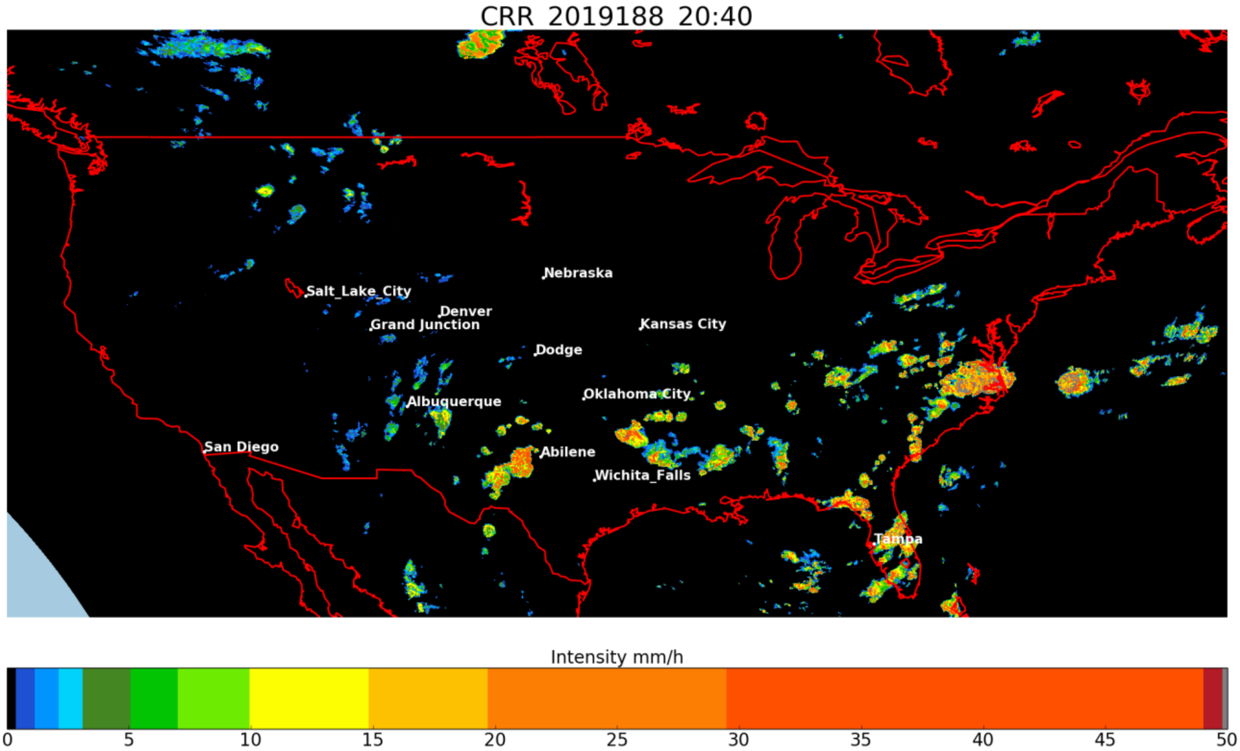

Figure 105. CRR product on 7th July 2019 at 20:40 UTC over USA.

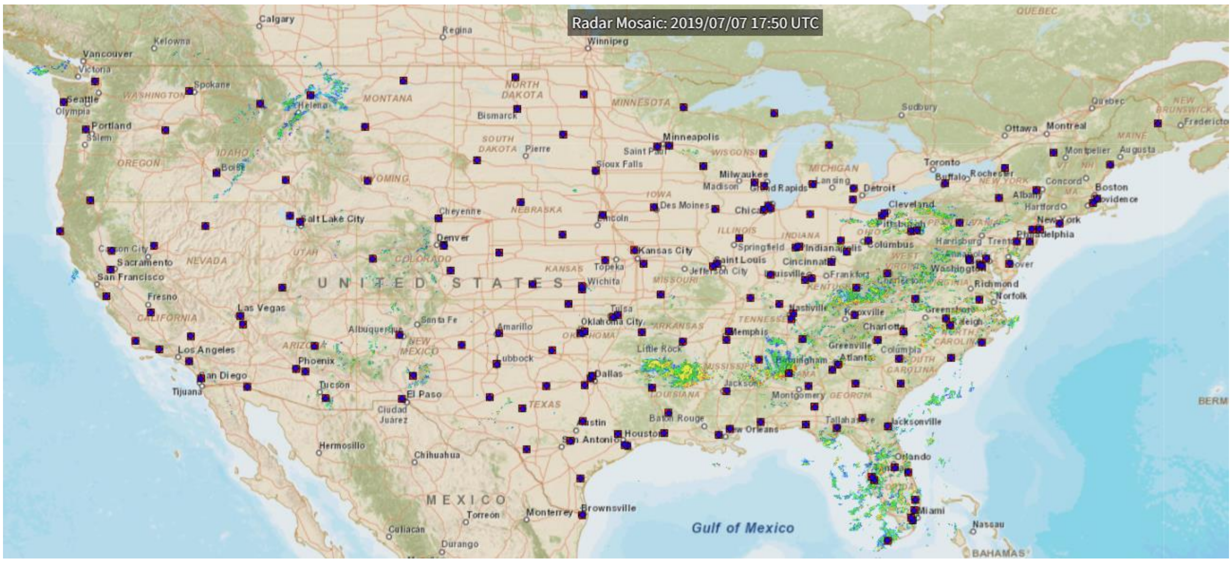

Figure 106. USA Radar mosaic (dBz) on 7th July 2019 at 17:50 UTC

Three hours before, there is still convective activity on the east. If we zoom in on this east area, many convective nuclei were active from Miami to Cleveland. CRR (Figure 72) and CRRPh (Figure 71) again reproduced with detail the situation, with a little bit more accuracy from the CRRPh. PCPh (Figure 69) had again a good performance .

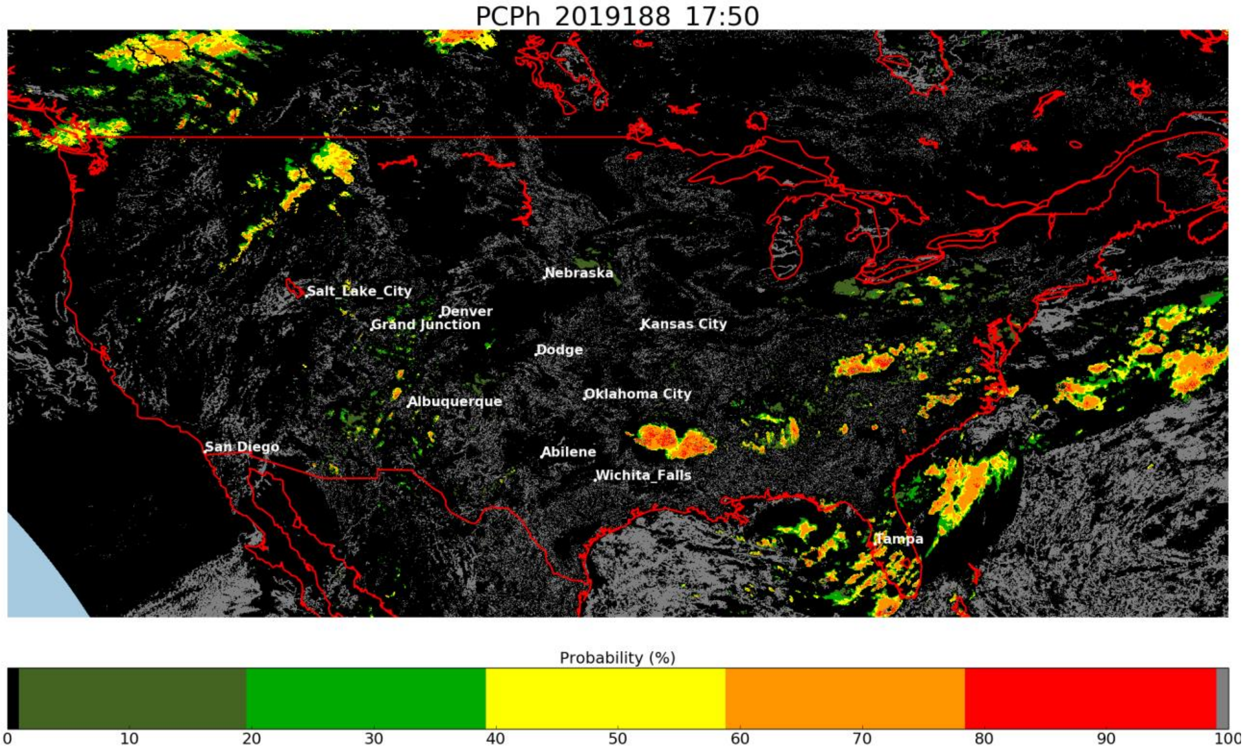

Figure 107. PCPh product on 7th July 2019 at 17:50 UTC over USA.

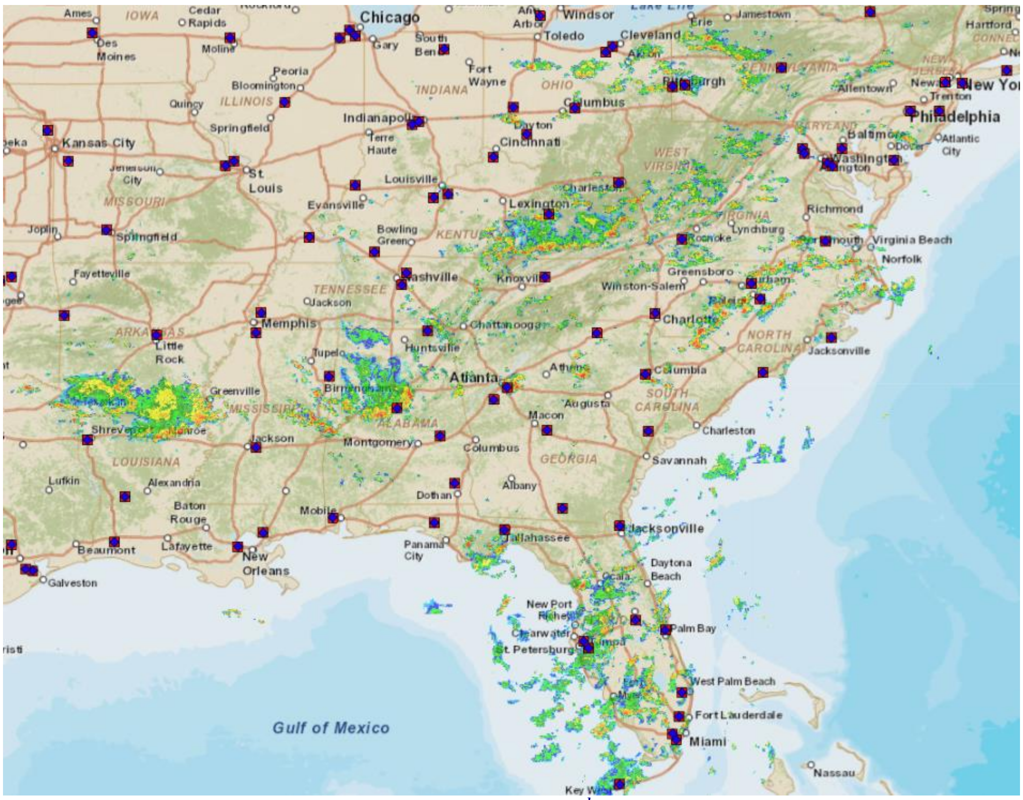

Figure 108. Radar mosaic (dBz) on 6th July 2018 at 00:00 UTC.

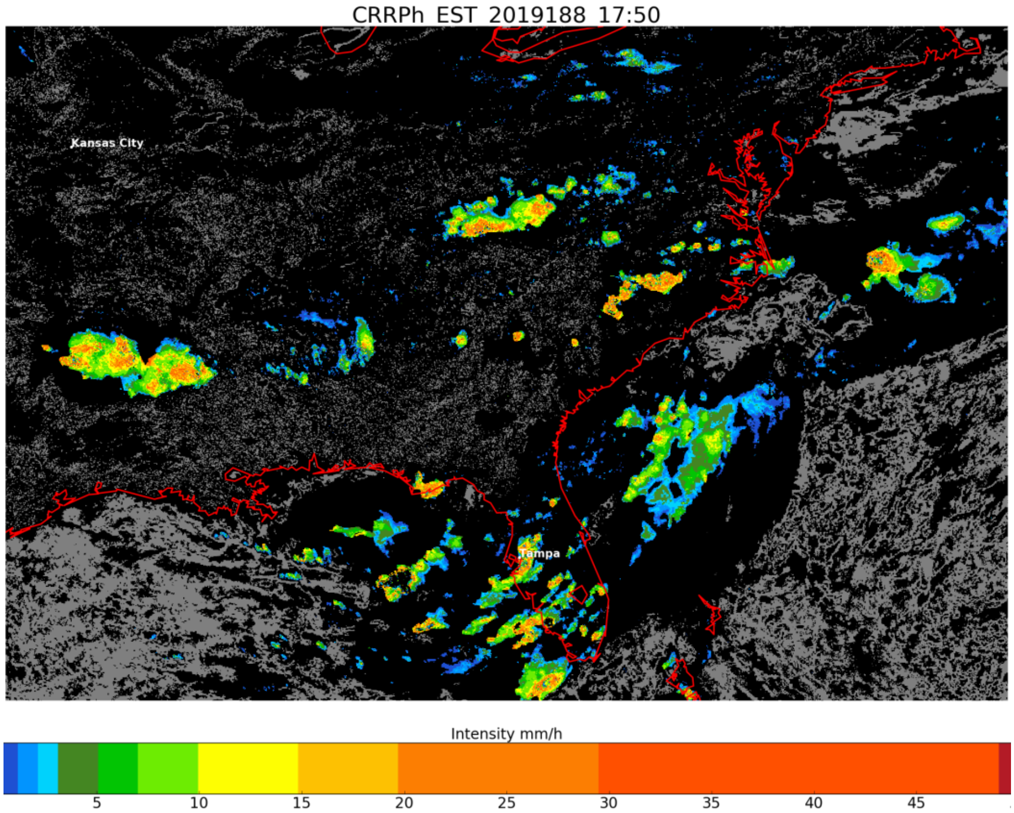

Figure 109. CRRPh product on 7th July 2019 at 17:50 UTC over USA.

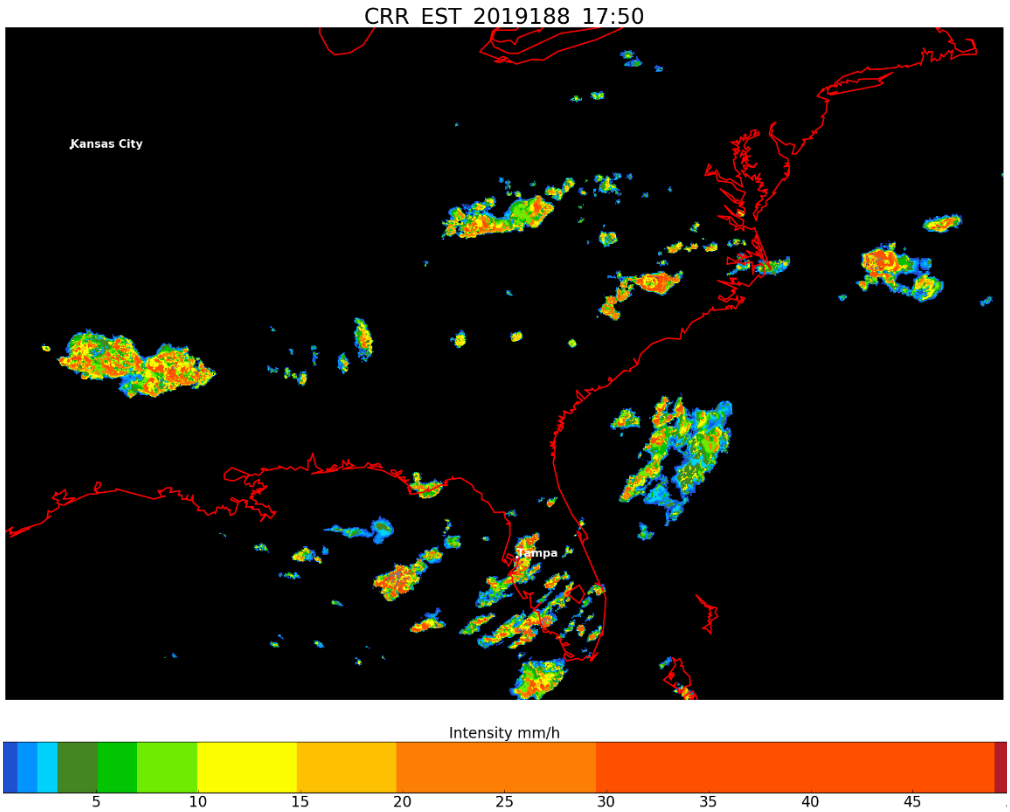

Figure 110. CRR product on 7th July 2019 at 17:50 UTC over USA.

7.2 7TH JULY 2019

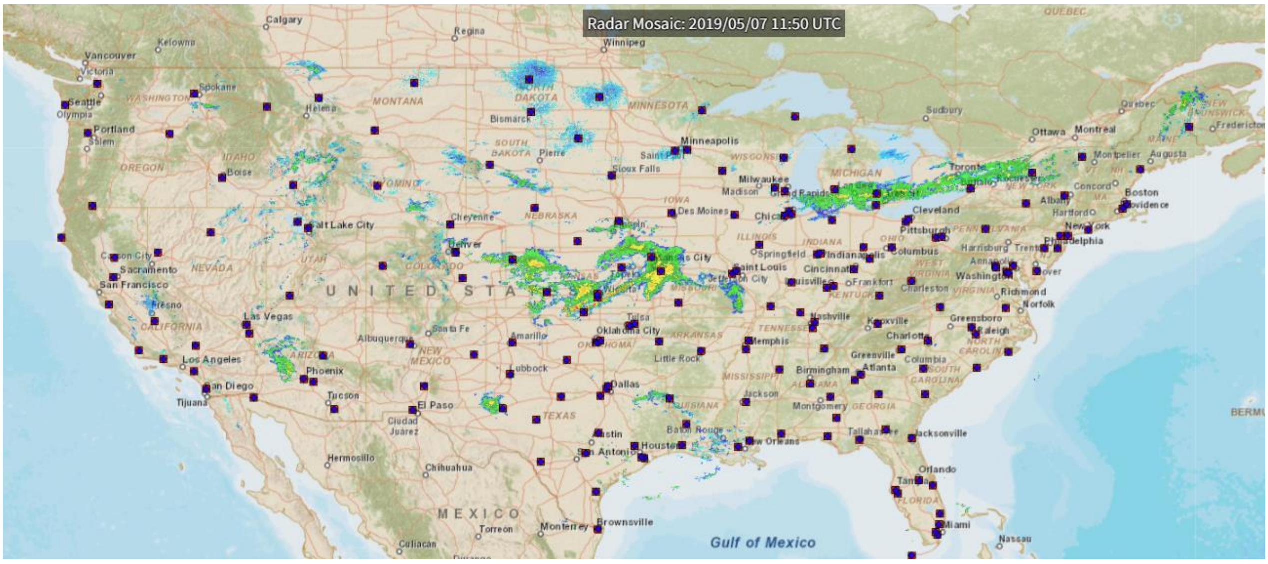

Figure 111. USA Radar mosaic (dBz) on 7th May 2019 at 11:50 UTC

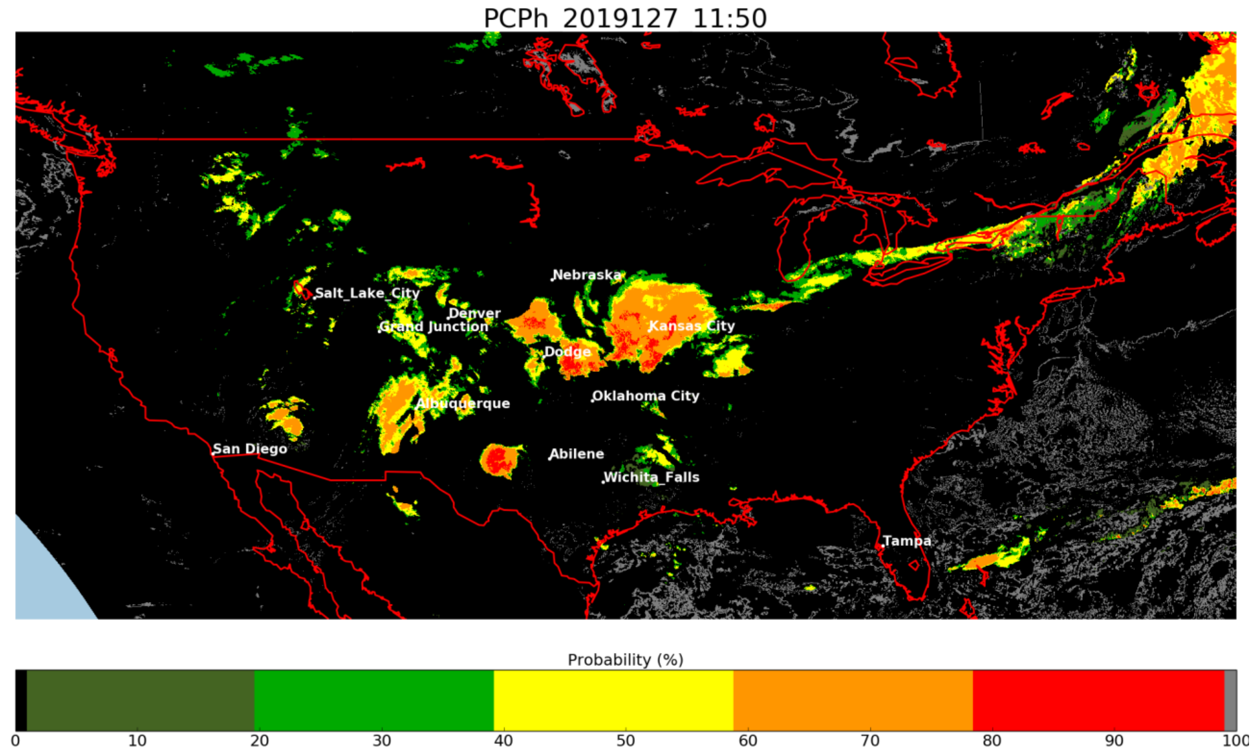

Figure 112. PCPh product on 7th May 2019 at 11:50 UTC

This is an example of a severe weather event. During this day took place strong storms with hail and some tornados associated to them. In the centre of the image there is large area with several thunderstorms taking place. PCPh detected quite well all the precipitating areas. CRR was able to depict the biggest ones. CRRPh represented more rainy areas at the east and a line of precipitation in the Great Lakes Region.

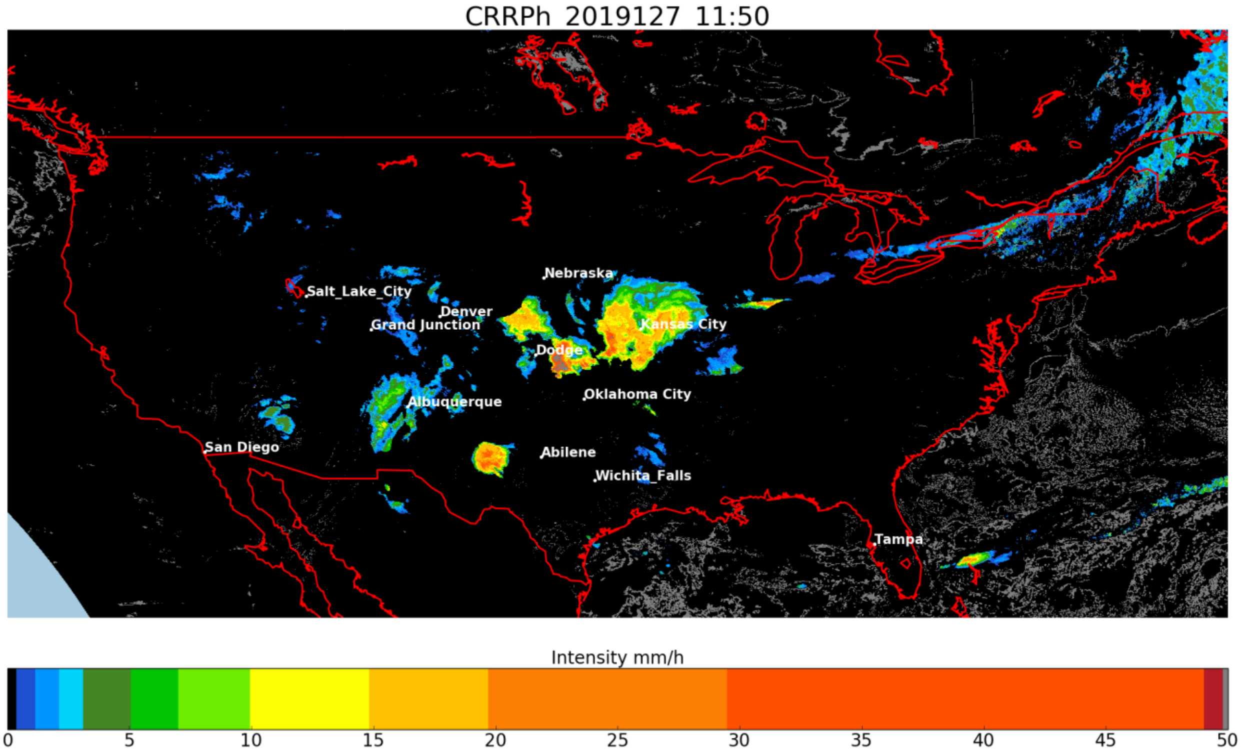

Figure 113. CRRPh product on 7th May 2019 at 11:50 UTC

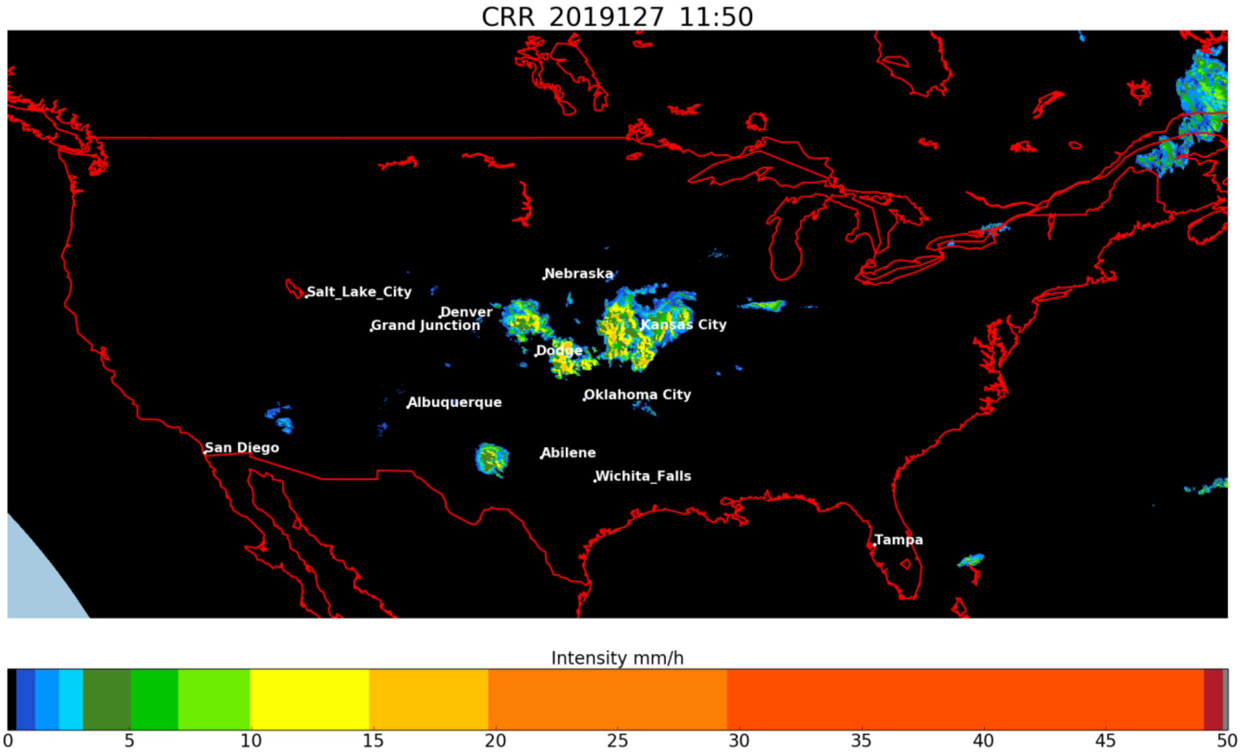

Figure 114. CRR product on 7th May 2019 at 11:50 UTC

7.3 8TH MAY 2019

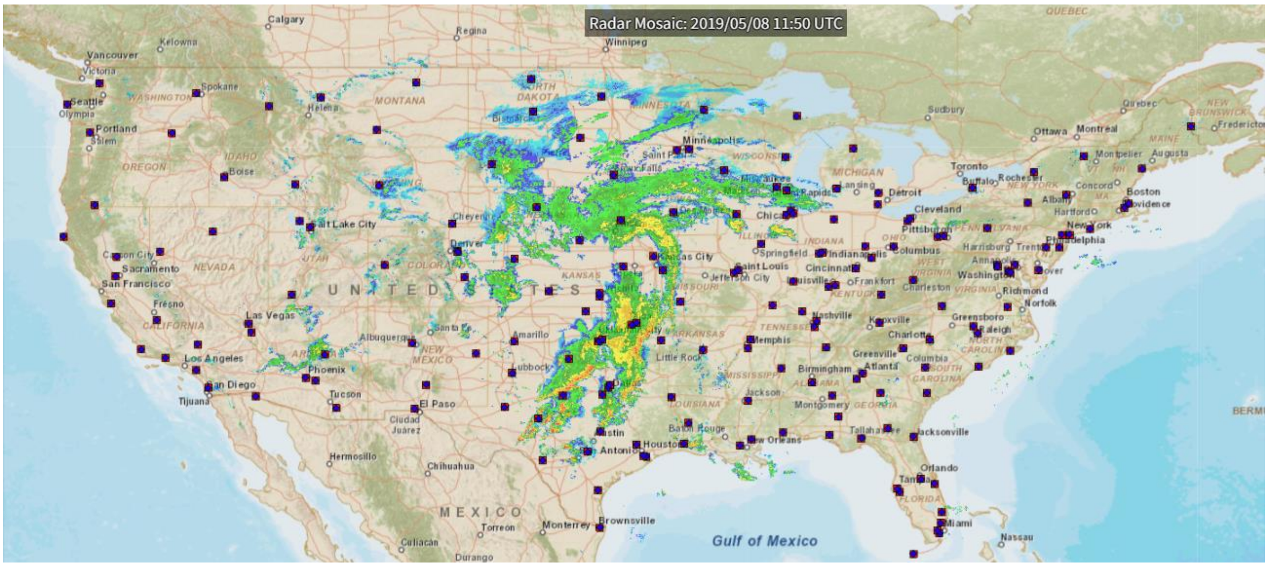

Figure 115. USA Radar mosaic (dBz) on 8th May 2019 at 11:50 UTC

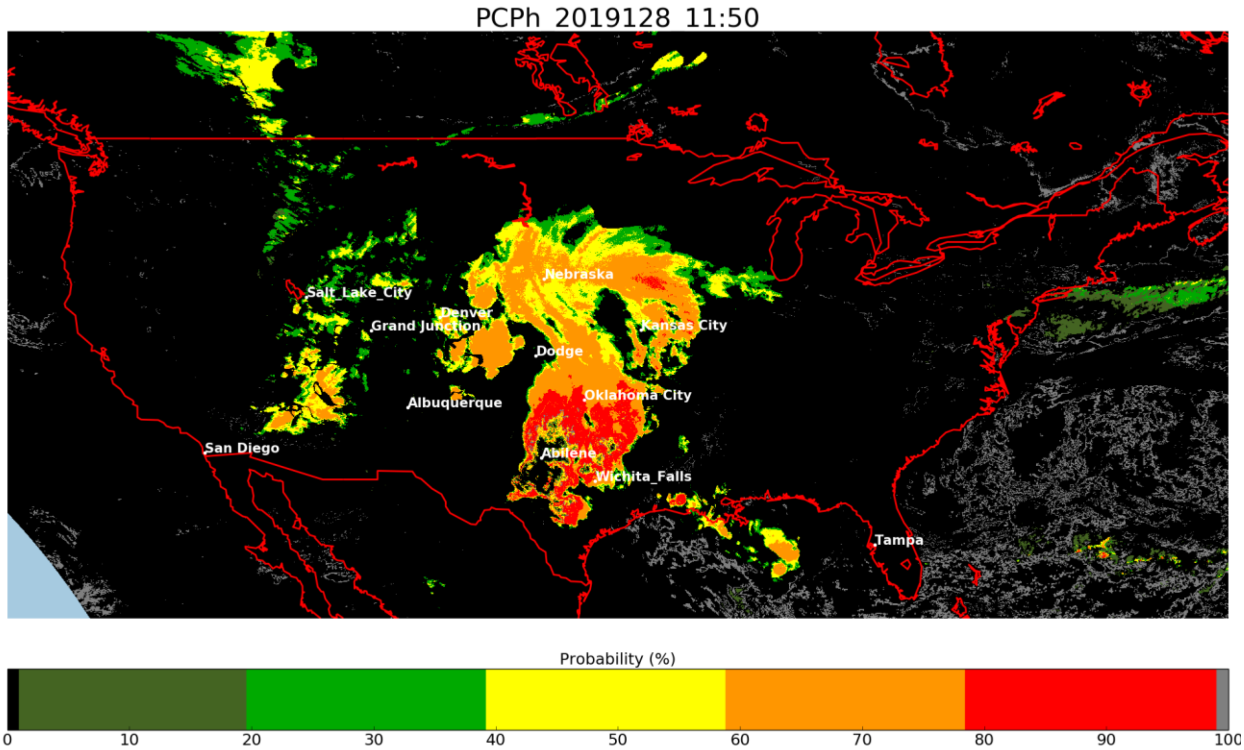

Figure 116. PCPh product on 8th May 2019 at 11:50 UTC

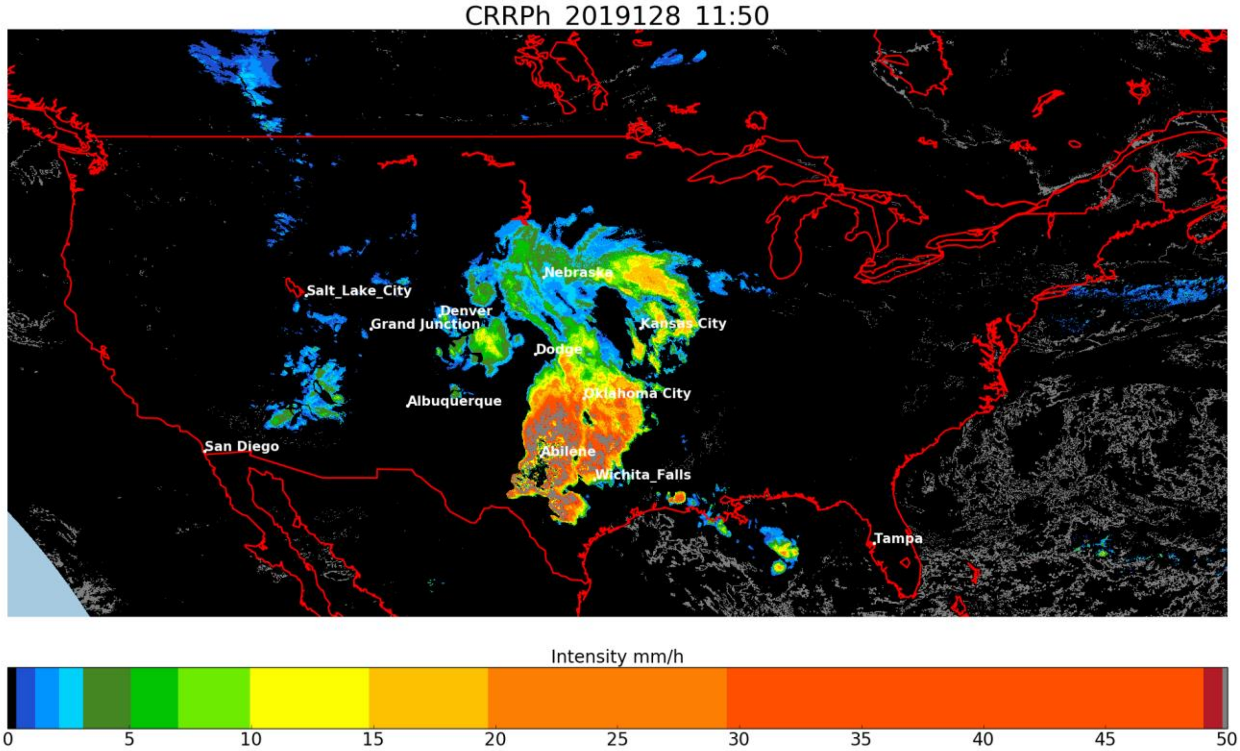

Figure 117. CRRPh product on 8th May 2019 at 11:50 UTC

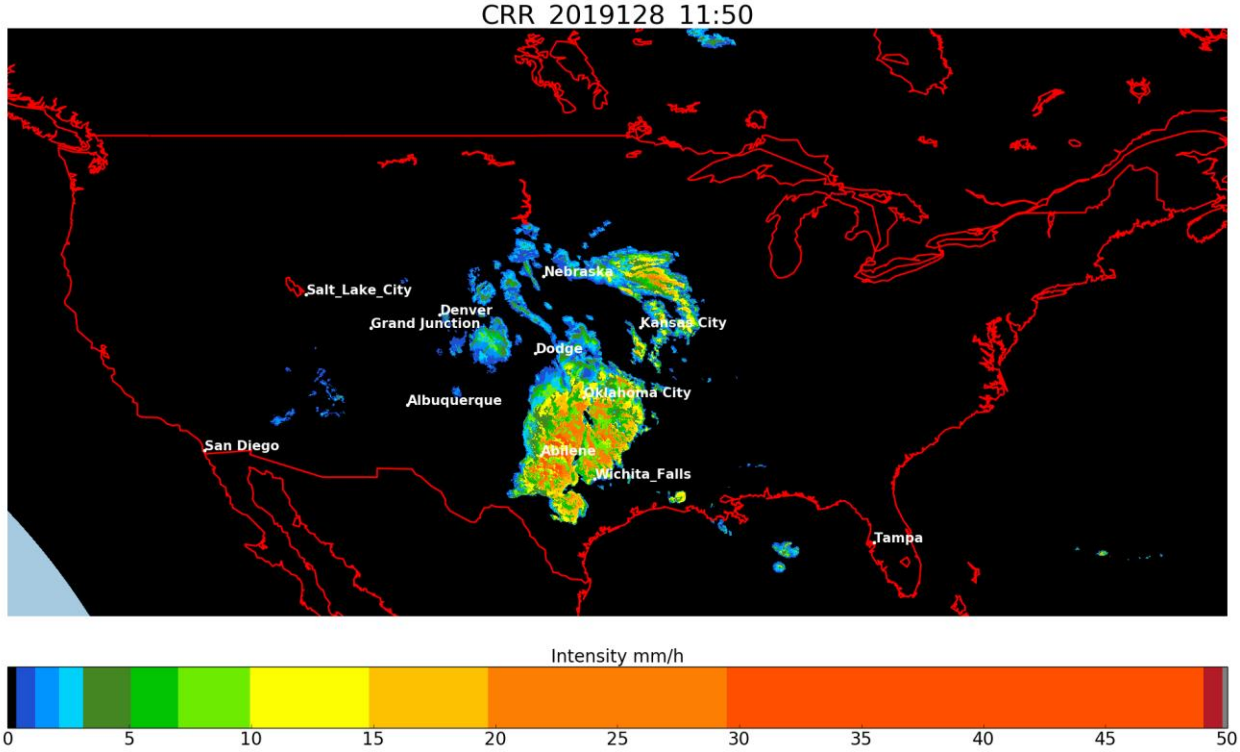

Figure 118. CRR product on 8th May 2019 at 11:50 UTC

During this last event, the same precipitating pattern is reproduced. A huge precipitating area in the centre of the image can be seen. The USA Radar mosaic (dBz) (Figure 77) shows heavy rain in the middle of the country. Both CRR and CRRPh detect it. CRRPh assigns more intensity of rain to the big convective nuclei placed at the centre and south of the image, and it also depicts a larger precipitating area at the north and east.

In general, the three precipitating products show a good behaviour, being more accurate the day algorithm. At night CRRPh detects more active convective nuclei and a larger precipitating area. The bigger convective cells are well reproduced by both of them: CRR and CRRPh. PCPh shows also a better performance at day time and a reasonable good behaviour at night time.

8. ANNEX 1: VERIFICATION METRIC

CATEGORICAL STATISTICS

The following scores derived from Table 51, have been calculated:

- False Alarm Ratio:

$$FAR = \frac{false\_alarms}{hits + false\_alarms}$$

Measures the fraction of estimated events that were actually not events.

- Probability of Detection:

$$POD = \frac{hits}{hits + misses}$$

Measures the fraction of observed events that were correctly estimated.

- Critical Success Index:

$$CSI = \frac{hits}{hits + misses + false\_alarms}$$

Measures the fraction of observed and/or estimated events that were correctly diagnosed.

- Percentage of Corrects:

$$PC = \frac{hits + correct\_negatives}{hits + misses + false\_alarms + correct\_negatives}$$

Is the percentage of correct estimations.

		Estimated (CRRPh, PCPh) occurred[1]	Estimated (CRRPh, PCPh) no occurred
Observed (Radar)	occurred*	hits	misses
	no occurred	false alarms	correct negatives

Table 51. Contingency table convention

9. REFERENCES

[1] *Occurred means values higher than or equal to 0.2 mm/h for instantaneous rates and higher than or equal to 0.2 mm for hourly and daily accumulations.*

Vicente, G.A., Scofield, R.A. and Menzel W.P. 1998: The Operational GOES Infrared Rainfall Estimation Technique, Bull. American Meteorological Society, Vol. 79, No. 9, pp. 1883-1898.

Steiner M., Houze J.A. Jr., Yuter S.E.: Climatological characterization of three-dimensional storm structure from operational radar and rain gauge data. J. Appl. Meteor., 34, 1978-2007, DOI: https://doi.org/10.1175/1520-0450(1995)034<1978:CCOTDS>2.0.CO;2

Poelman D., Delobbe L.: Daily convective precipitation maps. EUMETNET OPERA. Work Package OD19, 2018

OPERA NIMBUS and ODYSSEY. Description of differences between NIMBUS and ODYSSEY composite production Bouilloud, L., Haase, G., Koutek, M., Leijnse, H., von Lerber, A., Meyer, V., Radojevic, M., and Stephan, K.

EUMETNET OPERA NIMBUS. Product Datasheet on Instantaneous surface rain rate (in mm/h) and 1h rainfall accumulation (in mm) composites (2 km; 15 min). Haase, G., Koutek, M., Lankamp, B., Leijnse, H., von Lerber, A., Meyer, V., and Stephan, K.

EUMETNET OPERA NIMBUS. Product Datasheet on Quality controlled volume radar data. Haase, G., Koutek, M., Lankamp, B., Leijnse, H., von Lerber, A., Meyer, V., and Stephan, K.